NASA CONTRACTOR REPORT

NASA CR-2647

A STUDY OF SOME EFFECTS OF VERTICAL SHEAR ON THUNDERSTORMS

James Connell

Prepared by
UNIVERSITY OF TENNESSEE SPACE INSTITUTE
Tullahoma, Tenn.
for George C. Marshall Space Flight Center

NATIONAL AERONAUTICS AND SPACE ADMINISTRATION • WASHINGTON, D. C. • JANUARY 1976

TECHNICAL F

1. REPORT NO.	2. GOVERNMENT ACCESSION NO.	3.
NASA CR-2647		

4. TITLE AND SUBTITLE	5. REPORT DATE
A Study of Some Effects of Vertical Shear on Thunderstorms	January 1976
	6. PERFORMING ORGANIZATION CODE M161
7. AUTHOR(S) James Connell	8. PERFORMING ORGANIZATION REPORT #
9. PERFORMING ORGANIZATION NAME AND ADDRESS University of Tennessee Space Institute Tullahoma, Tennessee	10. WORK UNIT NO.
	11. CONTRACT OR GRANT NO. NAS8-31197
12. SPONSORING AGENCY NAME AND ADDRESS National Aeronautics and Space Administration Washington, D. C. 20546	13. TYPE OF REPORT & PERIOD COVERED Contractor
	14. SPONSORING AGENCY CODE

15. SUPPLEMENTARY NOTES

Prepared under the technical direction of the Aerospace Environment Division, NASA, Marshall Space Flight Center

16. ABSTRACT

Evidence is presented for the existence of vortices and vortex pairs in thunderstorms. A preliminary parameterized model of the nonthermal generation of thunderstorm vortices derived from field observations of storms and laboratory observations of a jet in crossflow is reported, together with an explanation of how such a model might be used to guide analysis of mesoscale rawinsonde, radar, and satellite data toward an improved capability for prediction of thunderstorm motion and growth. Preliminary analyses of radar and satellite data from Atmospheric Variability Experiment IV are used with available rawinsonde data to develop a correlation between wind shears, instability, and thunderstorm motion and development. Specific studies are recommended for best development of concepts and utilization of data from Atmospheric Variability and Atmospheric Variability Severe Storms Experiments.

17. KEY WORDS	18. DISTRIBUTION STATEMENT
	Category 46

19. SECURITY CLASSIF. (of this report)	20. SECURITY CLASSIF. (of this page)	21. NO. OF PAGES	22. PRICE
Unclassified	Unclassified	105	$5.25

MSFC - Form 3292 (Rev December 197

For sale by the National Technical Information Service, Springfield, Virginia 22161

Table of Contents

List of Figures

Page

List of Tables

Chapter I.

Introduction

Thunderstorms are inadequately understood, but that they are essentially three dimensional and usually highly time dependent is becoming obvious (e.g.,Connell, 1973, 1975 a,b,c). One feature which is coming to light is the existence of pairs of counter-rotating vortices in the low-to-middle levels of the storm (e.g.,Connell, 1973, 1975, a,b,c; Schlesinger, 1975; Jessup, 1972; Lemon, 1974; Kropfli and Miller, 1975; and others).

It may be possible, with measured understanding of these vortices and their mechanisms, to partly explain a number of seemingly unrelated characteristics of thunderstorms such as left and right deviate motion, splitting, tornado development, location and motion, and updraft pairs and downdraft on single circulations at cloudbase. It may even be that differences in microphysics occur in different portions of the spiraling updrafts which seem to be organized, though not totally driven, by the non-thermal mechanism of the vortex pairs.

The object of the present report is fivefold.

(1) To assemble some of the evidence for existence of vortices and vortex pairs in thunderstorms.

(2) To report a preliminary parameterized model of the non-thermal generation of thunderstorm vortices derived from field observations of storms and laboratory observations of a jet in crossflow.

(3) To explain how such a model might be used to guide analysis of mesoscale rawinsonde, radar and satellite data toward an improved capability for prediction of thunderstorm motion and growth.

(4) To present preliminary analyses of radar and satellite data from the AVE IV* experiment which will be used with rawinsonde data, when available, to develop a correlation between wind shears, instability and thunderstorm motion and development.

(5) To recommend specific studies for best development of concepts and utilization of AVE* and AVSSE** data.

The report incorporates papers started prior to the NASA-MSFC contract by Dr. Connell but completed under it. There are also chapters reporting work done solely under the present contract. It is the author's purpose to make clear the rather exciting prospect that a non-thermal mechanism of airflow due to a cumulonimbus in a vertical shear of horizontal wind may lead to additional use of mesoscale data from satellites, rawinsondes and radars and to simplified three-dimensional modeling of thunderstorms.

---

* AVE: Atmospheric Variability Experiments I,II,III and IV have been undertaken by NASA-MSFC to improve understanding of mesoscale weather systems in parts of the eastern half of the U.S.

**AVSSE: Atmospheric Variability Severe Storms Experiments undertaken by NASA-MSFC and Goddard to study severe thunderstorms.

The next three chapters are comprised of three papers written by the author (Dr. Connell) concerning thunderstorm airflow. Chapter 2 sets the conceptual stage for interpretation of thunderstorm observations in terms of a non-thermodynamic forcing mechanism. Chapter 3 presents a case study of a hailstorm with right deviation, subcloud vortices and apparent splitting. Chapter 4 discusses the observations of a tornadic storm which contained cyclonic vortices on four scales.

References

Connell, J.R., 1973: Observed inflow-updraft structure related to thunderstorm precipitation and dynamics. 8th Conference on Severe Local Storms, American Meteor. Soc., Boston, 18-24. Unpublished manuscript.

_____, 1975a: A nonthermal mechanism for forcing cumulonimbus updrafts. Submitted to the J. App. Meteor.

_____, and L. Kimbrough, 1975: Subcloud vortices of a hailstorm. Preprints 9th Conf. on Severe Local Storms, American Meteor. Soc., Boston, 79-84.

_____, 1975c: Life cycle of a tornado with subscale superrotations, Preprints 9th Conf. on Severe Local Storms, American Meteor. Soc., Boston, 396-403.

Jessup, E.A., 1972: Interpretation of chaff trajectories near a severe thunderstorm. Mon. Wea. Rev., 100, 653-661.

Kropfli, R.A. and L.J. Miller, 1975: Thunderstorm flow pattern in three dimensions. Mon. Wea. Rev., 103, 1, 70-71.

Lemon, L.R., 1974: Thunderstorm wake vortex structure and aerodynamic origin. NOAA Tech. Memorandum ERL NSSL-71, National Severe Storms Laboratory, Norman, Oklahoma, 17-43.

Schlesinger, R.E., 1975: A three-dimensional numerical model of an isolated deep convective cloud: Preliminary results, J. Atmos. Sci., 32, 934-957.

Chapter II.

A non-thermal mechanism of thunderstorm development and motion

1. Introduction

Cumulonimbi must generate significant forces due to collisions between airflows having very different transports of momentum. Some such interactions have been discussed by Newton and Newton (1959), Fujita and Grandoso (1968), Fulks (1962), and Fankhauser (1971), among others. Recently observed cloud airflows appear to require a forcing mechanism not based upon buoyancy. Marwitz (1973) has shown that negatively buoyant updrafts in the WER were accelerating upward. The slope of wind in subcloud updrafts and the nature of near-lee horizontal circulations at cloud base have been reported by Connell (1973). Dual-doppler radar measurements of thunderstorm airflow provide especially valuable glimpses in three dimensions with exceptional resolution. The data by Kropfli and Miller (1975) show a near-lee lateral pair of contrarotating eddies, which is consistent with the model elaborated in the present communication.

2. Wake vortices and modified updrafts.

A wide range of observations of fluid flow around either solid or fluid-momentum obstacles suggests that pairs of contrarotating vortices often occur in the lee. Jessup (1972) reviewed some of the observations. Theoretical and flow-tunnel studies of a jet in a crossflow have elucidated features of the dynamics of stack plumes and jets from VTOL aircraft in crosswinds. See, for example, the series of papers in NASA (1969). Quantitative

information is available regarding scaling, mechanisms, velocity and pressure fields. A brief outline of some useful results is given below.

The main qualitative features of three-dimensional jets in a crossflow are as follows:

1) Elastic collision along the upwind surface of the jet spreads it laterally and forms contrarotating vortices and a wake in the lee.
2) Inelastic collision, or momentum mixing, bends the jet so that its axis turns downwind.
3) The contrarotating vortex pair induces mean flow in the wake region which corresponds to inflow-updraft.
4) Swirl,if forced upon the whole jet, enhances the lee vortex which is rotating in the same sense as the whole jet and inhibits the other lee vortex.

In most respects, replacement of a solid cylinder in a crossflow by a fluid jet whose initial direction is parallel to the axis of the solid and whose orifice is identical in shape to the cross section of the solid results in more pronounced effects. The wake is wider, the vorticity of the lee eddies is greater, the pressure defect is larger and the wake vortices may be very close to the upstream edge. The position of the vortices is a function of the ratio of the updraft speed to the wind speed, W/U, and the crosswind aspect ratio of the jet cross section.

A stationary vortex pair may remain with the jet for Reynolds numbers up to 2500. Von Karman vortex streets form for Reynolds numbers between 2500 and 5000. For larger Reynolds numbers up to at least 500,000, irregular vortex streets exist (see Butkewicz, 1970).

3. Scaling

Wind and water tunnel studies indicate that Reynolds number similarity holds for jets in crossflows (Keffer, 1969). The pressure is scaled using the nondimensional pressure coefficient, C_p, and is a function of the velocity ratio, W/U. The shape of the bent axis of the jet scales with the diameter of the jet orifice. Linear coordinates are stretched by the velocity ratio squared as shown in the equation with the plot of jet axis shape in Figure 1, adapted from Margason (1969). The shape of the axis could be readily modified to account for buoyancy (McAllister, 1968).

Application of Reynolds number similarity using molecular viscosity would lead to the conclusion that only irregular vortex streets may be shed by thunderstorms. However, turbulence is a much more significant momentum mixer at thunderstorm scales than is random molecular motion. A turbulence Reynolds number using typical eddy viscosities measured in and around cumulonimbi (Aleksandrov, Silayeva and Shmeter, 1967) may have magnitudes as indicated below.

$$Re_t = \frac{20 \times 10^4}{20 \text{ to } 100} \text{ MKS} = 10^4 \text{ to } 2 \times 10^3.$$

The Reynolds number for a jet in a crossflow studied in the wind tunnel by Jordinson (1956) is about 3×10^4.

4. Comparison of a scaled-up jet in a crossflow with a cumulonimbus.

Jordinson (1956) measured total pressures in the flow field of the jet of air represented by the diagrams in Figures 2, 3, and 4. The pressures are plotted as isopleths of the pressure coefficient, C_P. Using cumulonimbus wind speeds, the scaled static pressure defect in the lee vortices may be estimated using the following relations.

$$C_P = (P_j - P_w)/(P_{jo} - P_w), \text{ where}$$

$$P_j = P_o + \Delta P + \tfrac{1}{2}\rho U^2$$

$$P_w = P_o + \tfrac{1}{2}\rho U^2$$

$$P_{jo} = P_o + \tfrac{1}{2}\rho W_o^2,$$

P_o = static ambient environment pressure,
U = wind speed relative to the cloud (say, 10 m s^{-1}),
W = updraft speed (say, 10 m s^{-1}), and
W_o = updraft speed at the updraft base.

Assuming a velocity ratio of one and the central vortex pressure coefficient measured by Jordinson for the velocity ratio closest to one, the static pressure deficit is found to be approximately $\Delta P = 0.1$ mb. The trend of the data suggests that for extrapolation to $W/U = 1$ the pressure deficit will be considerably larger, perhaps 1 to 5 mb. The pressure deficit required to support the

cyclonic circulation shown in Figure 1 in Kropfli and Miller (1975) may be estimated using the cyclostropic relation. The calculation gives a value of $\Delta P = -0.2$ mb. The value of W/U is about two. The cyclonic circulation below cloud base for a hailstorm as measured by Connell (1973) is shown in Figure 5. A $\Delta P = -2$ mb is required to support that circulation.

The vorticity for the latter vortex was about 10×10^{-3} s^{-1}. The vorticity in the cyclonic member in the measurements by Kropfli and Miller was about 4×10^{-3} s^{-1}. Margason and Fearn (1969) measured the vorticity of the wake vortices of a jet in a crossflow to be about twice the value due to potential flow around a solid cylinder having the same diameter as the orifice of the jet. The exact conditions of the crossflow were not specified. The data scaled to the thunderstorm vortex diameter of four kilometers implies a vorticity of 30×10^{-3} s^{-1}.

The evidence is strongly suggestive that a properly formed jet in a crossflow could be a useful physical model of certain processes for a cumulonimbus in a vertical shear of the horizontal wind. Unlike the jet in the laboratory, a cumulonimbus must derive its updraft velocity from buoyancy as well as from the non-thermodynamic process of momentum deflection. In the next section the concept of the non-thermal mechanism as a controlling influence on the buoyancy force is briefly explored.

5. A mechanism for modifying motion and intensity.

An updraft collides with the wind from the environment in the upwind edge of the cloud and the interaction produces a pair of leeside, lateral, contrarotating vortices oriented somewhat symmetrically with respect to the vector of the environmental wind relative to the updraft wind. For certain achievable Reynolds numbers the vortices will be nearly stationary with respect to the cloud. They will be most intense at the height at which the bending forces on the updraft are strongest (Platten and Keffer, 1968). It seems that this region usually would be in the first few kilometers above cloud base where the inflow-updraft first collides with the environment wind. Figure 6 contains an adaption of the doppler-derived winds in a thunderstorm presented in two of the figures by Kropfli and Miller (1975). The updraft bending and the leeside, lateral, contrarotating vortex pair are quite apparent in the zone of collision.

A hypothetical airflow configuration for a cumulonimbus is shown in Figure 7. Figure 7a is a side view from the south and Figure b is a top view showing the inflow passing under the right lee vortex low pressure center. There would be a tendency for this inflow toward the updraft region to be lifted in the front right quadrant of the storm more than in the other quadrants. If the inflow were from the left, then it would be enhanced by the left vortex. Thus a tendency toward left or right deviation of the development of new cloud cells would be affected by the lateral contrarotating vortices and the low-

level inflow from the left or right of the direction of the wind in the cloud layer.

If the Reynolds number should increase to above about 2500, then regular or irregular streets of vortices would be generated. These vortices could cause storm splitting or generation of additional separate clouds. Laboratory experiments with jets in crossflows have shown streets of axially elongated vortices whose cores are suggestive of tornado vortices (McAllister, 1968).

Another situation of interest is crossflow when the whole cumulonimbus is rotating. The author has performed some tracer experiments with a swirling jet in a crossflow. A modest cyclonic swirl enhanced the right lee vortex and diminished the left lee vortex. This effect might lead to a correct explanation of why radar echoes often show the right-hand lee vortex but not its anticyclonic left counterpart (Lemon, 1974).

6. A concluding remark.

The effect of non-thermal forcing of a cumulonimbus in a crossflow is surely imbedded with other effects. Thus very specific conditions and measurements may be required to test the hypothesis in the field. On the other hand, simulations in the wind tunnel using correct vector wind shear relationships and velocity ratios could be of value for understanding real cumulonimbi. If valid scaling of wind tunnel results could be done, then a simpler numerical scheme for three-dimensional modeling of some thunderstorms could result.

FIGURES

LEGENDS

Figure 1. Non-dimensionalized shape of the axis of a round jet in a uniform crossflow as a function of initial angle of the jet. (Adapted from Margason and Fearn, 1969). Z = vertical distance from orifice, X is downwind distance and, D is the diameter of the orifice.

Figure 2. Streamlines in the vertical plane of symmetry of a round jet in a crossflow for W/U = 6 (Jordinson, 1956).

Figure 3. Total pressure coefficient isopleths in the vertical plane of symmetry of a round jet in a crossflow for W/U = 6 (Jordinson, 1956).

Figure 4. Total pressure coefficent isopleths in a cross section plane at Ż/D =2 for a round jet in a crossflow with W/U = 4 (Jordinson, 1956).

Figure 5. Cyclonic circulation at cloud base of a hailstorm. Light solid lines are streamlines. Dashed lines are isotachs of horizontal wind labeled in knots (adapted from Connell, 1973).

Figure 6. Schematic airflow in a thunderstorm based upon an extrapolation of the dual-doppler data presented by Kropfli and Miller (1975). (a) Side view showing strong collision zone by heavy dashed line. (b) Top view of the vortex pair at about the height of the heavy dashed line in (a).

Figure 7. Side and top views of a model cumulonimbus updraft in a crossflow which generates low-pressure leeside lateral vortices. The low level inflow is shown passing under the right vortex. The plus and minus signs denote pressure excess and deficiency regions respectively.

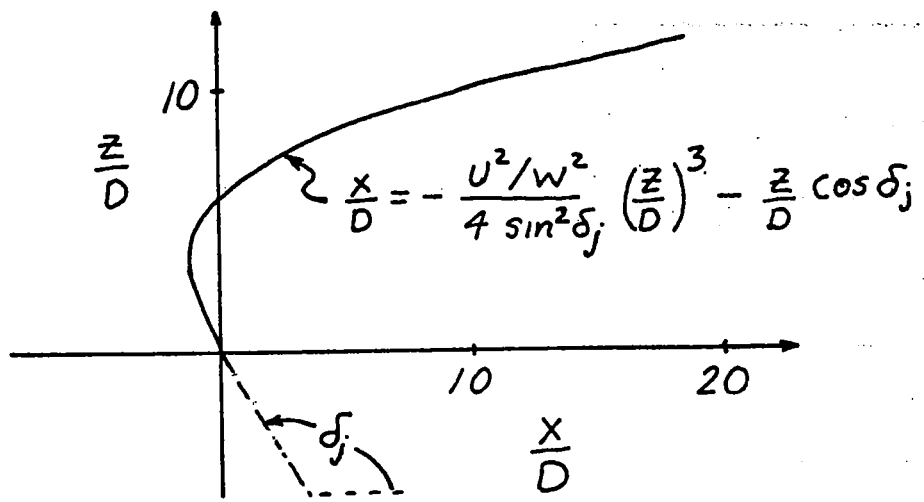
10
$\frac{z}{D}$
$\frac{x}{D} = -\frac{U^2/W^2}{4\sin^2\delta_j}\left(\frac{z}{D}\right)^3 - \frac{z}{D}\cos\delta_j$
10
20
$\frac{x}{D}$
δ_j

Figure 1

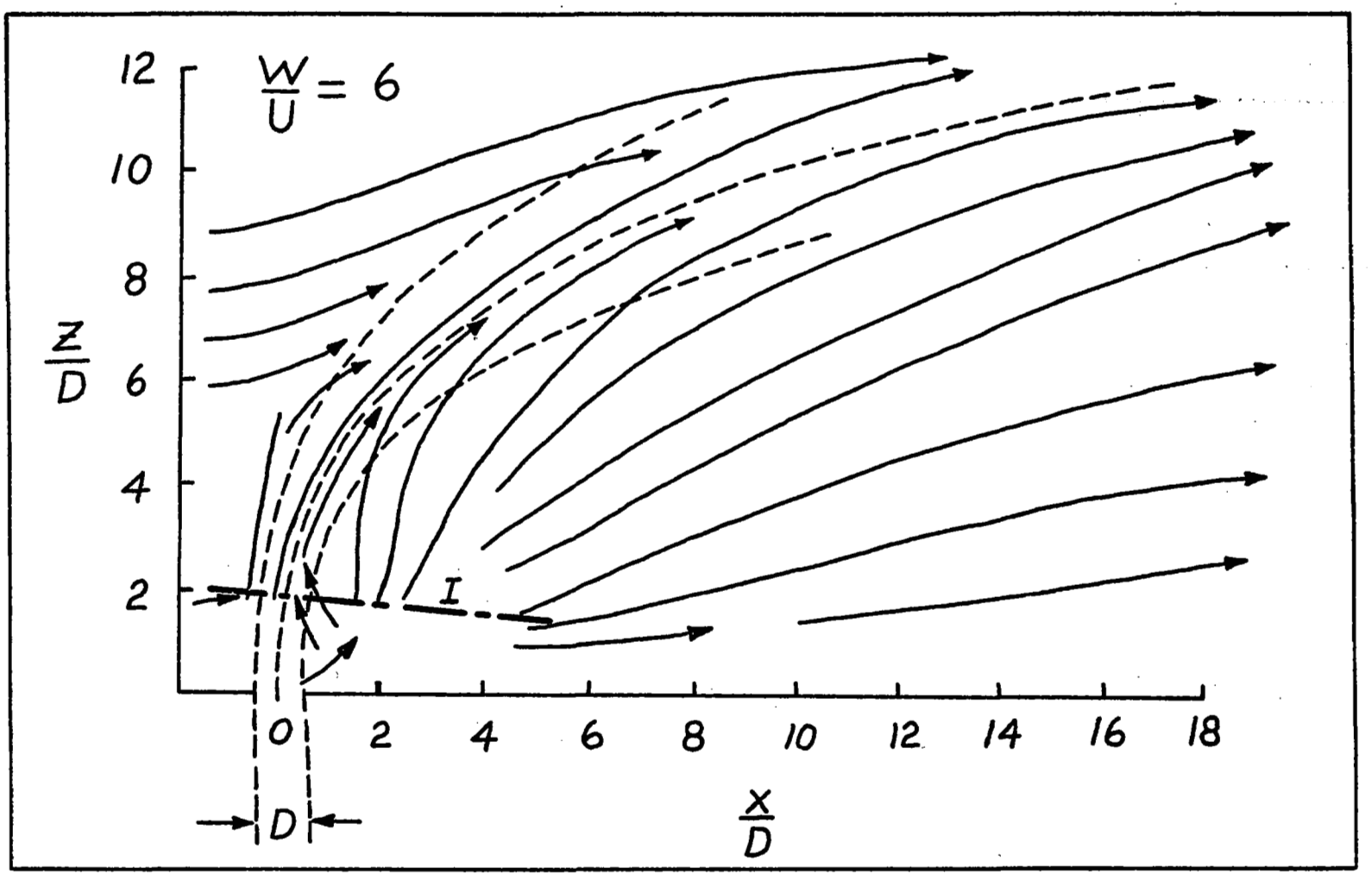

Figure 2

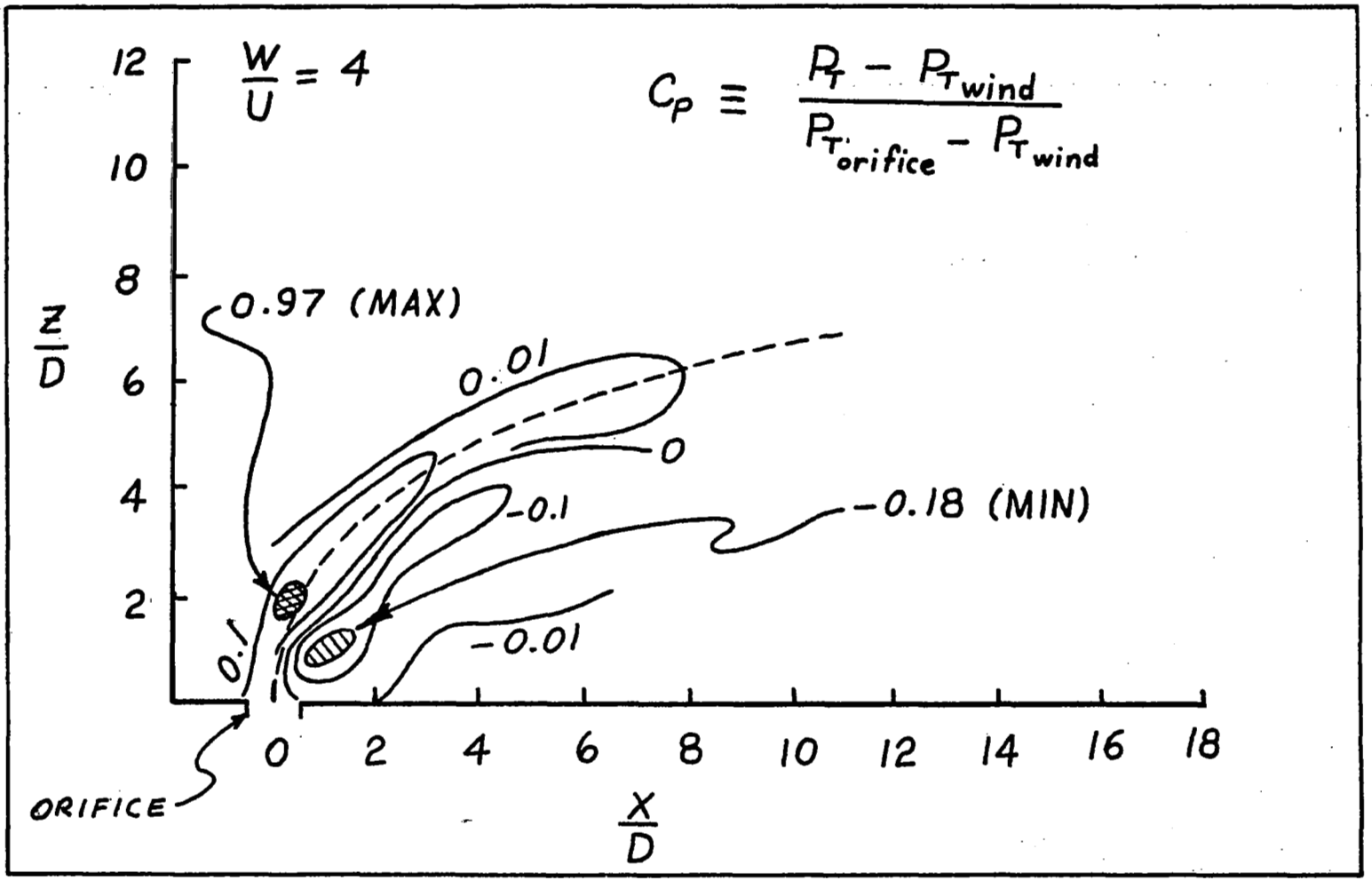
W/U = 4
$C_p \equiv \frac{P_T - P_{T_{wind}}}{P_{T_{orifice}} - P_{T_{wind}}}$
Z/D
X/D
0.97 (MAX)
0.01
0
-0.1
-0.18 (MIN)
-0.01
0.1
ORIFICE
12
10
8
6
4
2
0
2
4
6
8
10
12
14
16
18

Figure 3

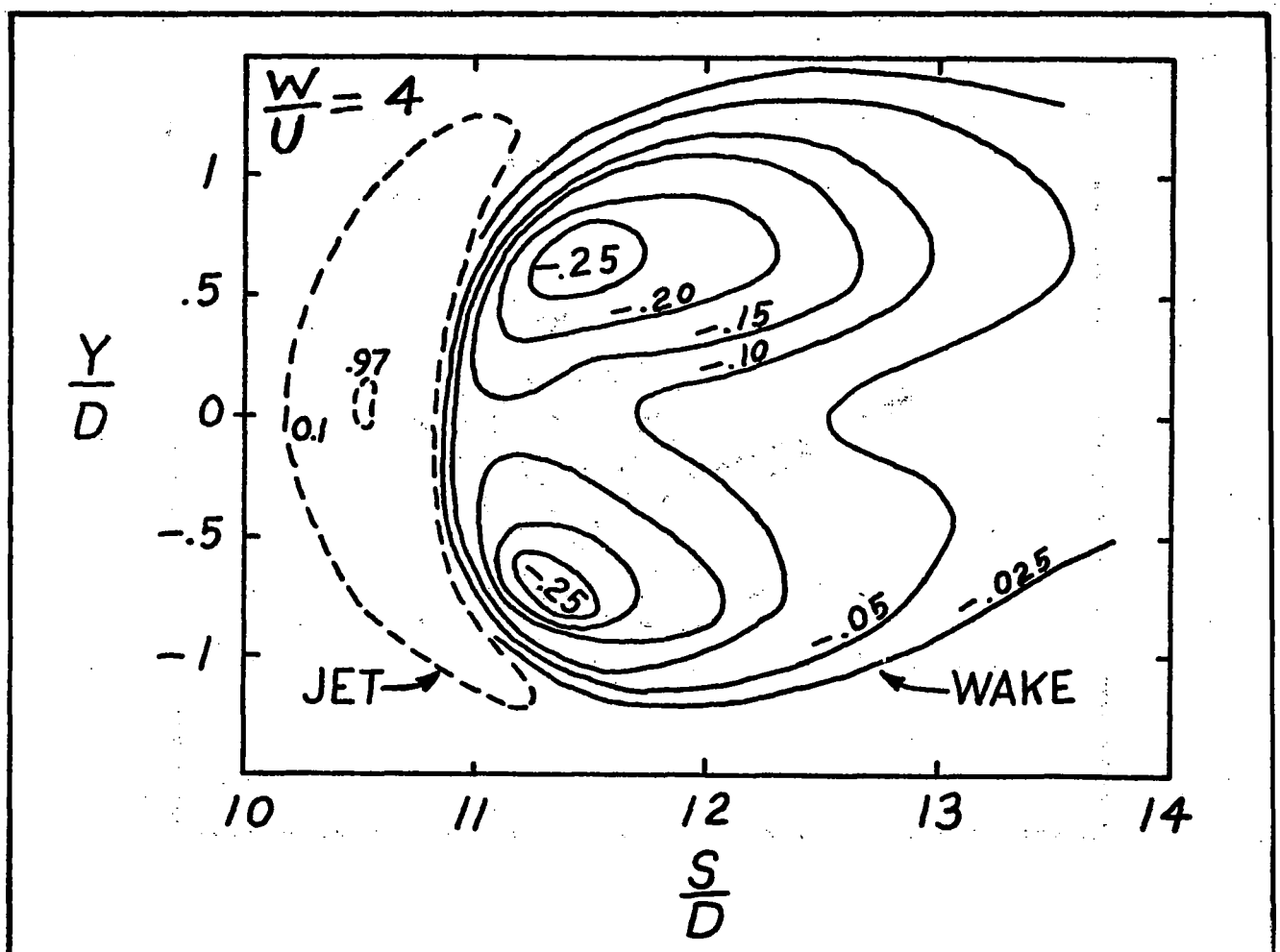

Figure 4

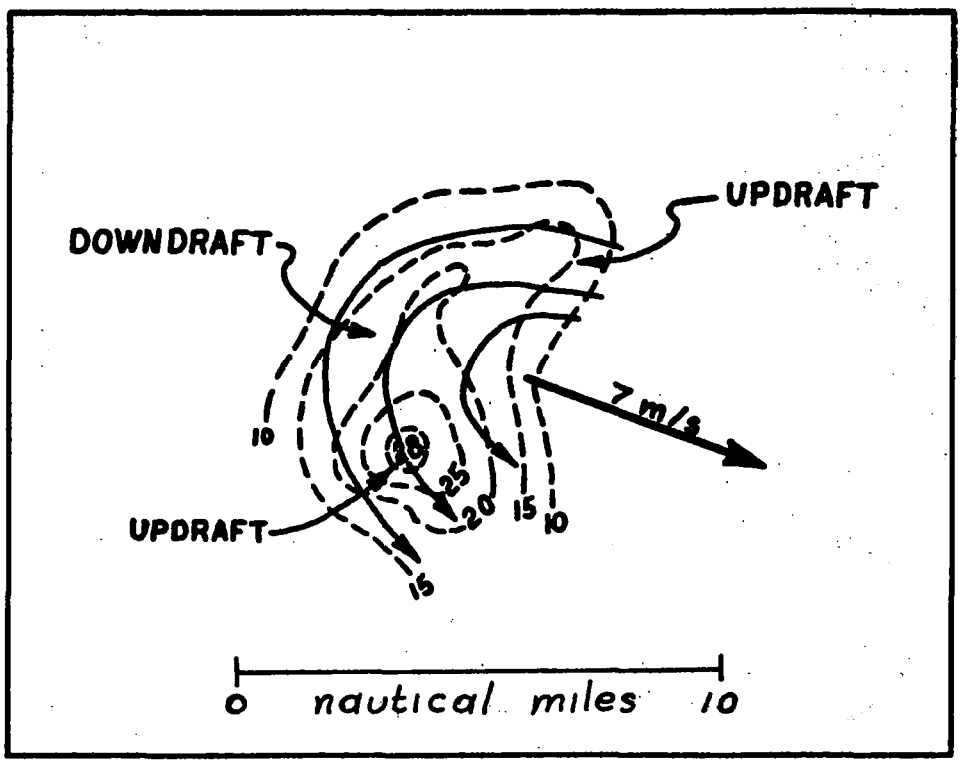
DOWNDRAFT
UPDRAFT
7 m/s
10
25
20
15
10
UPDRAFT
15
0 nautical miles 10

Figure 5

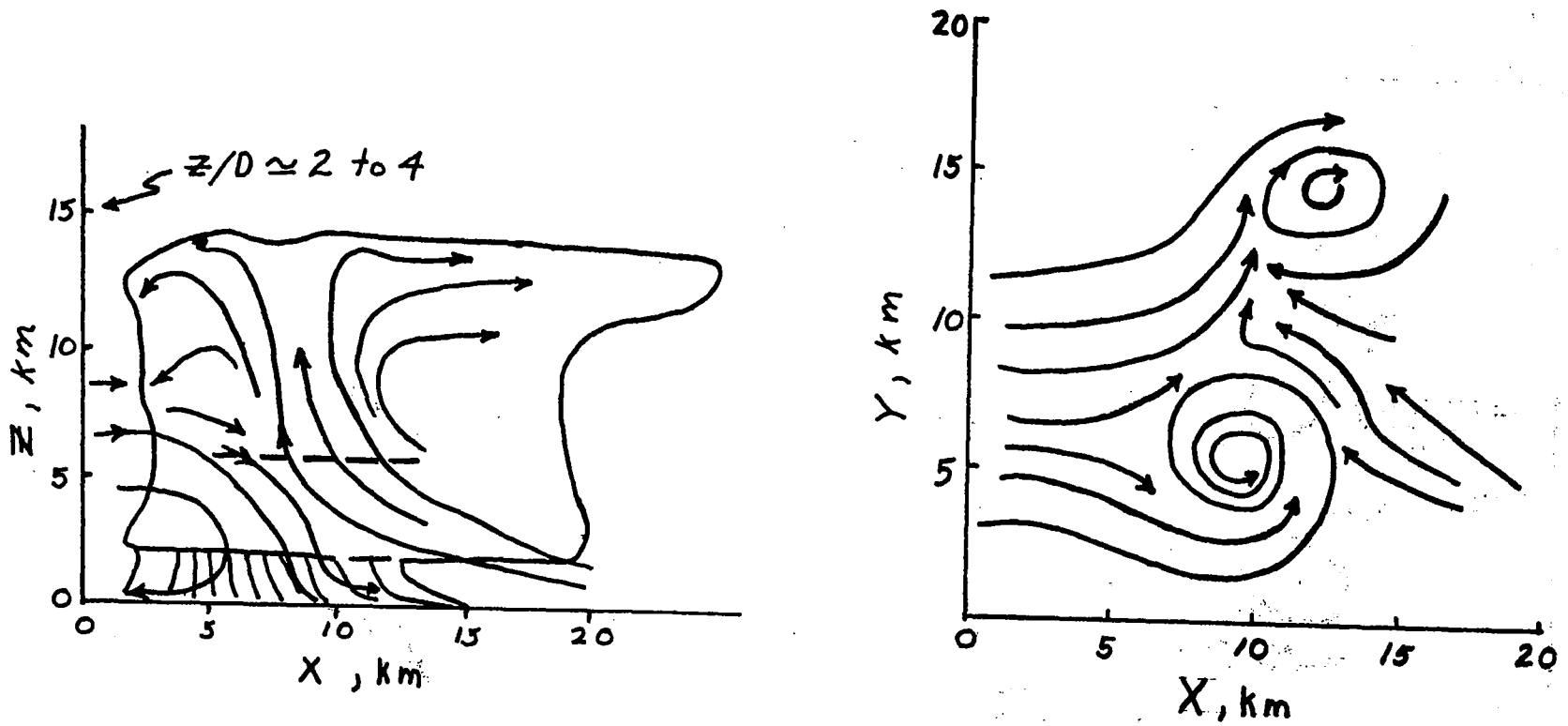

Figure 6

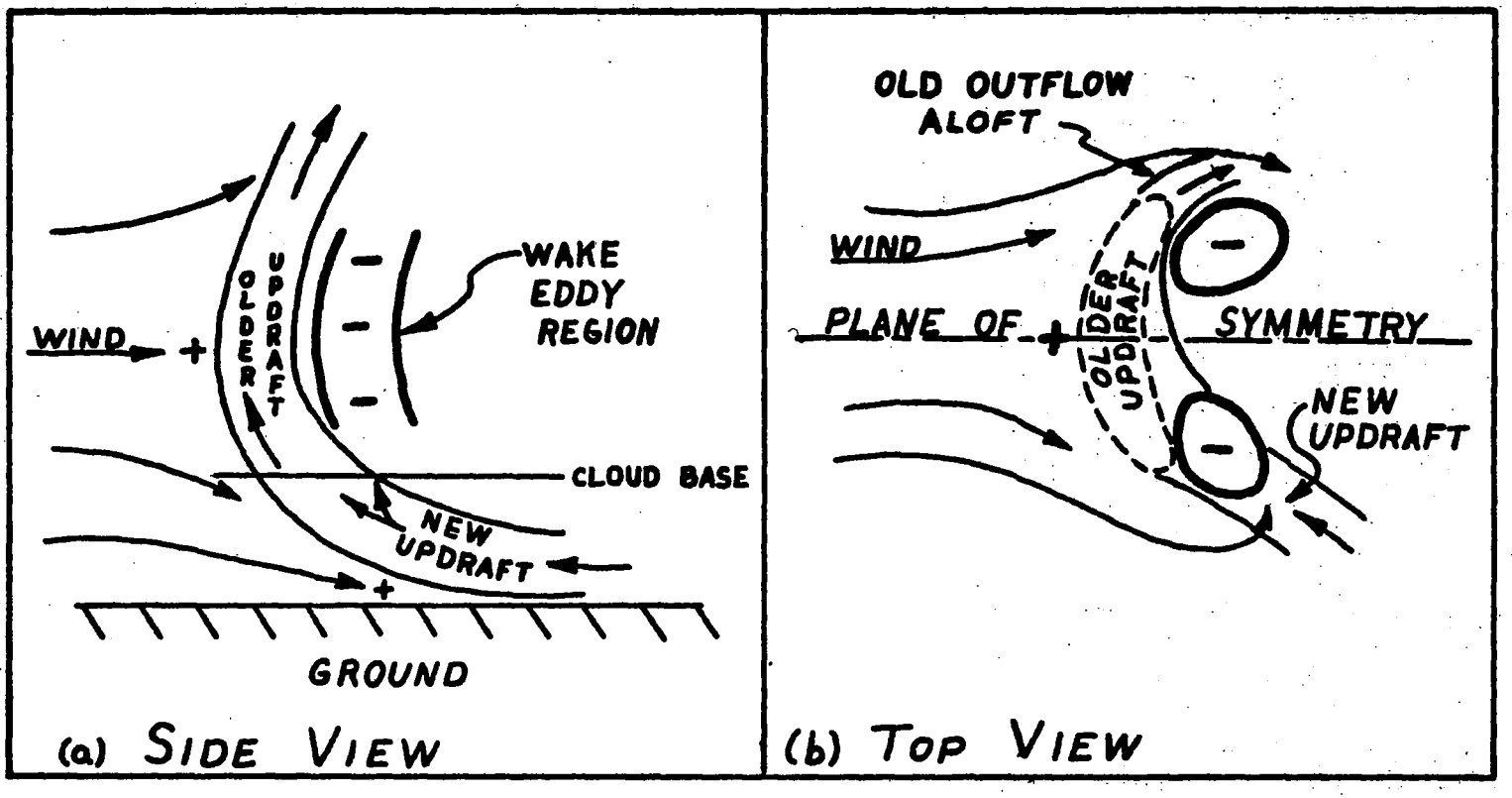
WIND
+
OLDER UPDRAFT
WAKE EDDY REGION
CLOUD BASE
NEW UPDRAFT
GROUND
(a) SIDE VIEW
OLD OUTFLOW ALOFT
WIND
PLANE OF SYMMETRY
OLDER UPDRAFT
NEW UPDRAFT
(b) TOP VIEW

Figure 7

REFERENCES

Aleksandrov, V.S., V.I. Silayeva and S.M. Shmeter, 1967: Atmospheric turbulence in and near cumulonimbus clouds. Central Aerological Observatory, Trudy, 78, 32-49.

Butkewicz, P.J., 1970: An investigation of the vortex wake and induced entrainment for a jet in low Reynolds number crossflow. Ph.D. Dissertation, University of Tennessee, Tullahoma, Tennessee, August, 1970.

Connell, James R., 1973: Observed inflow-updraft structure related to thunderstorm precipitation and dynamics. 8th Conference on Severe Local Storms, American Meteor. Soc., Boston, 18-24. Unpublished manuscript.

Frankhauser, J.C., 1971: Thunderstorm-environment interactions determined from aircraft and radar observations. Mon. Wea. Rev., 99, 171-192.

Fujita, T. and H. Grandoso, 1968: Split of a thunderstorm into anti-cyclonic and cyclonic storms and their motion as determined from numerical model experiments. J. Atmos. Sci., 25, 416-439.

Fulks, J.R., 1962: On the mechanics of the tornado. NSSP Report No. 4, U.S. Wea. Bur., Washington, D.C., 33 pp.

Jessup, E.A., 1972: Interpretation of chaff trajectories near a severe thunderstorm. Mon. Wea. Rev., 100, 653-661.

Jordinson, R., 1956: Flow in a jet directed normal to the wind. Aeronautics Dept. Paper No. 35, Imperial College, 17 pp.

Keffer, J.F., 1969: The physical nature of the subsonic jet in a cross-stream. Analysis of a jet in a subsonic crosswind, NASA SP-216, National Aeronautics and Space Administration, Washington, D.C., 19-36.

Kropfli, R.A. and L.J. Miller, 1975: Thunderstorm flow pattern in three dimensions. Mon. Wea. Rev. 103, 1, 70-71

Lemon, L.R., 1974: Thunderstorm wake vortex structure and aerodynamic origin. NOAA Tech. Memorandum ERL NSSL-71, National Severe Storms Laboratory, Norman, Oklahoma, 17-43.

Margason, R.J., 1969: Analytic description of the jet-wake cross sections for a jet normal to a subsonic free stream. Analysis of a jet in a subsonic crosswind, NASA SP-216, National Aeronautics and Space Administration, Washington, D.C., 131-140.

Margason, R.J. and R. Fearn, 1969: Jet-wake characteristics and their induced aerodynamic effects on V/STOL aircraft in transition flight. Analysis of a jet in a subsonic crosswind, NASA SP-216, National AEronautics and Space Administration, Washington, D.C., 1-18.

Marwitz, J.D., 1973: Non-hydrostatic pressure in severe thunderstorms. 8th Conference on Severe Local Storms, American Meteor. Soc., 14-17. Unpublished manuscript.

McAllister, J.D., 1968: A momentum theory for the effects of cross flow on incompressible jets. Ph.D. Dissertation, University of Tennessee, Tullahoma, Tennessee, August, 1968.

NASA, 1969: Analysis of a jet in a subsonic crosswind, NASA SP-216, National Aeronautics and Space Administration, Washington, D.C., 247 pp.

Newton, C.W., and H.R. Newton, 1959: Dynamical interactions between large convective clouds and the environment with vertical shear. J. Meteor., 16, 483-496.

Platten, J.L. and J.F. Keffer, 1968: Entrainment in deflected axisymmetric jets at various angles to the stream. University of Toronto,Mechanical Engineering Department TP-6808, June, 1968.

Chapter III

Subcloud vortices of a hailstorm.

I. Introduction

Airflow in the subcloud inflow and updraft region of the 26 May 1972 Cheyenne hailstorm was investigated using two research aircraft. One aircraft performed a horizontal mapping pattern just below cloud base. The second aircraft executed several quasi-vertical arrays of horizontal tracks across the inflow to the updraft from near the surface to the earth up to cloudbase height ten to fifteen kilometers ahead of the precipitation curtain. Figure 8 shows the horizontal projection of the tracks of both aircraft relative to the second hailswath. Aircraft observations were made for 1.5 hours before hail ceased to fall. The first direct measurement of time variation of a subcloud ten kilometer scale cyclonic circulation near cloud base was achieved. Existence of the vortex and a possible mechanism of formation of pairs of contrarotating vortices having pressure deficits of the order of one millibar was reported orally at the 8th Conference on Severe Local Storms (Connell, 1973). The mechanism has been elaborated further in terms of vertical shear of wind velocity and of scaling from wind tunnel observations of jet in a crossflow using a velocity ratio and a turbulence Reynolds number (Connell, 1975). Recently dual-doppler radar data (e.g., Kropfli and Miller, 1975) have shown the existence of contrarotating eddy pairs in the near lee of a cumulonimbus upwind edge. The data seem clearly to confirm

aspects of the hypotheses of Connell (1973) and Lemon (1974.)

This paper presents an analysis of some of the observations of the Cheyenne hailstorm. The vortices and their movement are discussed with reference to the concept of a pair of contrarotating vortices formed in a cumulonimbus in a wind which shears with height.

2. A brief history of the storm.

The thunderstorm apparently formed early in the afternoon in the Laramie Valley, moved eastward across the Laramie Range and downslope at an average velocity of 7 m s^{-1} from 290 deg true. The movement was 40 deg to the right of the mean cloud-layer wind. The storm hailed once west of Cheyenne and produced an extensive swath along the north edge of Cheyenne during the second severe hailfall. The storm apparently split during the second hailstorm, the left and right members moving to the left and right of the wind, respectively. Subsequently, the separate weakened rainstorms drifted with the wind. Figure 9 is a pen sketch of a satellite photograph at 1536 MDT showing the synoptic weather system and the Cheyenne Thunderstorm at about the time of formation of the first hailswath west of the city. The cumulonimbus formed at the edge of the synoptic subsidence in conditions of rising atmospheric pressure. The average early track and the split tracks are superimposed upon the sketch. Figure 8 shows the geometry of the second swath where the storm apparently split.

3. The right-moving member.

Figure 10 shows the windfield at cloudbase of the south member of the split pair for short time intervals centered on 1830, 1835, 1840 and 1843 MDT. A cyclonic circulation appears to have had a diameter of about 20 km and to have moved with a mean velocity of 6 m s^{-1} from 285 deg true. This was very closely the same velocity with which the storm moved from LAR to CYS. Figure 11 contains profiles of wind speed and direction at the nearest rawinsonde station, GVR, 90 km to the southeast for the approximate times 0730, 1030, 1400, and 1700 MDT. The average wind direction in the cloud layer was about 250 deg true; thus the unsplit storm and the south member after the split moved on paths 35 to 40 deg to the right of the wind. Figure 8 shows winds near cloudbase on the inflow edge of the south member to have come from about 150 deg. The inflow entered the storm, which was right-moving, at an angle of 100 deg from the right of the cloud-layer wind.

The cyclonic circulation of the south member dissipated at about 1850 MDT concurrent with updraft weakening. The storm drifted with the wind as observed from the aircraft and from Limon radar which just reached the storm at the limit of the radarscope range.

4. The left-moving member.

At about 1825 MDT the aircraft began measurement of the pair. As can be seen by reference to Figure 8, the (weak) updrafts at cloudbase showed no appreciable horizontal circulation or, at

most, a cyclonic circulation with a diameter greater than 100 km. According to the model of a strong crossflow around the thunderstorm, an anticyclonic circulation should have existed with the left member prior to the split and during its movement to the left of the wind.

Evidence for left movement and for anticyclonic circulation is circumstantial. The primary indication of left movement is that the last part of the hail swath deviates strongly to the left at an angle from 215 deg true or 35 deg to the left of the cloud-layer wind. This is consistent with a split whose motion was symmetric with respect to the direction of the wind.

The second aircraft moved slightly closer to the north storm and executed a set of vertically stacked legs in front at heights of 1800, 1940, 2260 and 2860 m MSL. Ground level was at about 1600 m MSL. Figure 12 (a) shows the height and length of the tracks, and Figures 12 (b), (c), (d) and (e) contain maps of the track and winds at each of the heights, respectively. Anti-cyclonic shear or circulation appears weakly at 2860 and 1800 m, perhaps as remnants of a dissipating left member of a contrarotating pair. The storm was drifting with the wind. The diameter of the anticyclonic region was 10 and 20 km at the two heights. All indications are that the inflow came from the west and southwest. Additional evidence from vertical motion, potential temperature and water vapor mixing ratio will be presented later.

5. Additional features of the right-hand member.

A visual vault was seen most clearly from the cloudbase aircraft approaching the storm from the location labeled 1825 in Figure 10 (a). A sketch of the side view of the storm from that location is presented in Figure 13. The vertical extent of the vault was estimated to be 0.2 to 0.4 km, and it was about 0.5 to 1 km wide. It extended for about 8 km horizontally parallel to the rain curtain. On the first pass under the cloudbase the aircraft flew to the east of the vault and measured two updraft maxima on opposite sides of the cyclonic circulation. On the return leg the track curved under the valut and over the forward-sweeping rain curtain. Turbulence was not observed as the aircraft passed from the updraft to the vault region where there was a downdraft maximum of about 8 m s^{-1}. The vault vanished later at about the same time as the cyclonic circulation dissipated. Apparently dry wind from some upper level descended across the precipitation in the cloud to create a locally higher cloud base or a vault. The vault air was part of the cyclonic circulation.

6. Vorticity and pressure defect.

The cyclonic circulation at cloud base had a calculated mean velocity of 0.4×10^{-3} s^{-1} at 1839 MDT. A linear decrease of vorticity at this rate would result in the demise of the circulation after about thirty minutes, as was observed. The anticyclonic shear on the left member of the storm had a calculated value of mean vorticity of 1.8×10^{-3} s^{-1}.

Using the cyclostropic relation a rough estimate of the pressure defect required to support the observed or inferred circulations may be calculated. For the cyclonic circulation the maximum defect would have had an average value of 0.2 mb. The anticyclonic circulation would have had a central pressure reduction of about 0.5 mb.

7. A hypothesis concerning wind shear and dynamic effect of crossflow on a cumulonimbus.

The 1653 MDT GVR sounding measured a magnitude shear of cloud layer environmental wind of 3×10^{-3} s^{-1} between 3 km (cloud base) and 6.5 km MSL. Above 6.5 km the mean shear was weakly negative. It would appear that shear at the upper part of the cloud was not needed to make it a severe hailstorm. Considering the wind relative to the cloud, the shear produced its direct dynamical effect in the layer from about 1 km to 3.5 km above cloud base. It is suggested that the essential mechanism for growth into a severe hailstorm was developed from the collision between the updraft near the back of the cloud and the winds of maximum speed.

Some of the wind was forced down through cloud base to exit in the vault adjacent to the precipitation on one side and the updraft on the other. The wind was forced around the sides of the updraft and downdraft, as was some of the updraft, forming a pair of contrarotating eddies about half the diameter of the parent storm. Since the eddies formed and appeared to remain as a pair stationary with respect to the moving storm, the

turbulence Reynolds number corresponding to the process must have been somewhere around the range 1500 to 3000 (McAllister, 1968; Connell, 1975). An estimate of the Reynolds number for the Cheyenne storm is calculated as follows:

$$Re_T = vD/K_T = 10 \text{ m s}^{-1} \times 20 \text{ km}/100 \text{ m}^2\text{s}^{-1}$$

$$Re_T = 2000.$$

Such vortices can occur quite close to the upwind side of the storm in a fashion analogous to other fluid-stream obstacles to a crossflow. The radar data by Kropfli and Miller (1975) show this.

A hypothesis for a relation between the vortex pair, the direction of the low-level inflow and the deviation of the track of a thunderstorm from the direction of the mean cloud-layer wind is presented in a separate note (Connell, 1975). Perhaps the process of splitting by left and right deviation is sometimes due to the existence of two lateral and opposing wind directions in the source air of the storm concurrent with the existence of a pair of contrarotating vortices in the updraft.

FIGURES

LEGENDS

Figure 8. Map projection of the flight paths relative to the hailswath at Cheyenne. Wind velocities are indicated.

Figure 9. A sketch of the ESSA 9 visual photograph of the western U.S. showing the Cheyenne Thunderstorm at 1536 MDT as a closed hatched line. The mean track of the storm from LAR to CYS is indicated by a double solid line. The probable tracks for the split pair after CYS are indicated by single solid lines. The synoptic-scale cyclone clouds are centered on northern Montana.

Figure 10. Thirty-second average winds at cloudbase of the south member at four successive times. The rectangles locate best-estimate centers of the circulation. It's mean velocity is shown in Figure 10 (d)

Figure 11. GVR wind soundings at about 0730(···), 1030(--), 1700(__).

Figure 12. Tracks and measured wind velocities for the aircraft which flew in a vertical plane ahead of the left member of the storm. (a) The tracks shown in the plane of the tracks. (b), (c), (d) and (e) horizontal maps of track and winds at 1800 m, 2260m & 2860m MSL respectively.

Figure 13. A sketch of a view of the south member of the thunderstorm from the southwest showing a visible vault.

Figure 14. Estimated streamlines and isotachs (knots) at 1830 to 1840 MDT at cloudbase of the south member of the thunderstorm pair. Regions of observed updraft and downdraft maxima are indicated by U and D respectively.

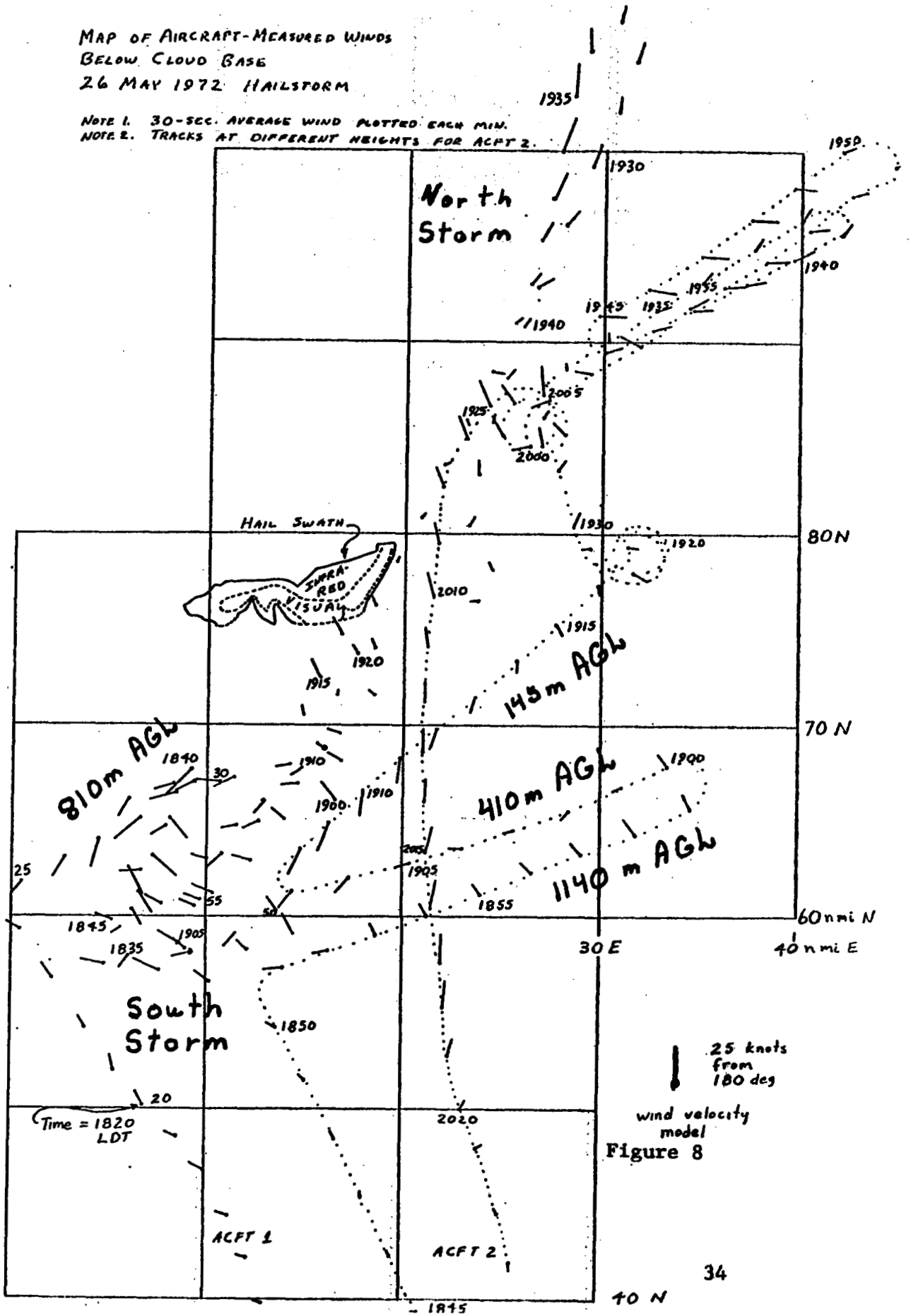
MAP OF AIRCRAFT-MEASURED WINDS
BELOW CLOUD BASE
26 MAY 1972 HAILSTORM
NOTE 1. 30-SEC. AVERAGE WIND PLOTTED EACH MIN.
NOTE 2. TRACKS AT DIFFERENT HEIGHTS FOR ACFT 2.
North Storm
South Storm
HAIL SWATH
INFRA-RED
VISUAL
810m AGL
145m AGL
410m AGL
1140 m AGL
1935
1930
1950
1940
1945
1955
1925
2005
2000
1930
1920
2010
1915
1920
1915
1840
30
1910
1910
1900
1900
25
2005
1905
55
50
1855
1845
1835
1905
1850
20
2020
Time = 1820 LDT
ACFT 1
ACFT 2
1845
80N
70 N
60nmi N
30 E
40 nmi E
40 N
25 knots from 180 deg
wind velocity model

Figure 8

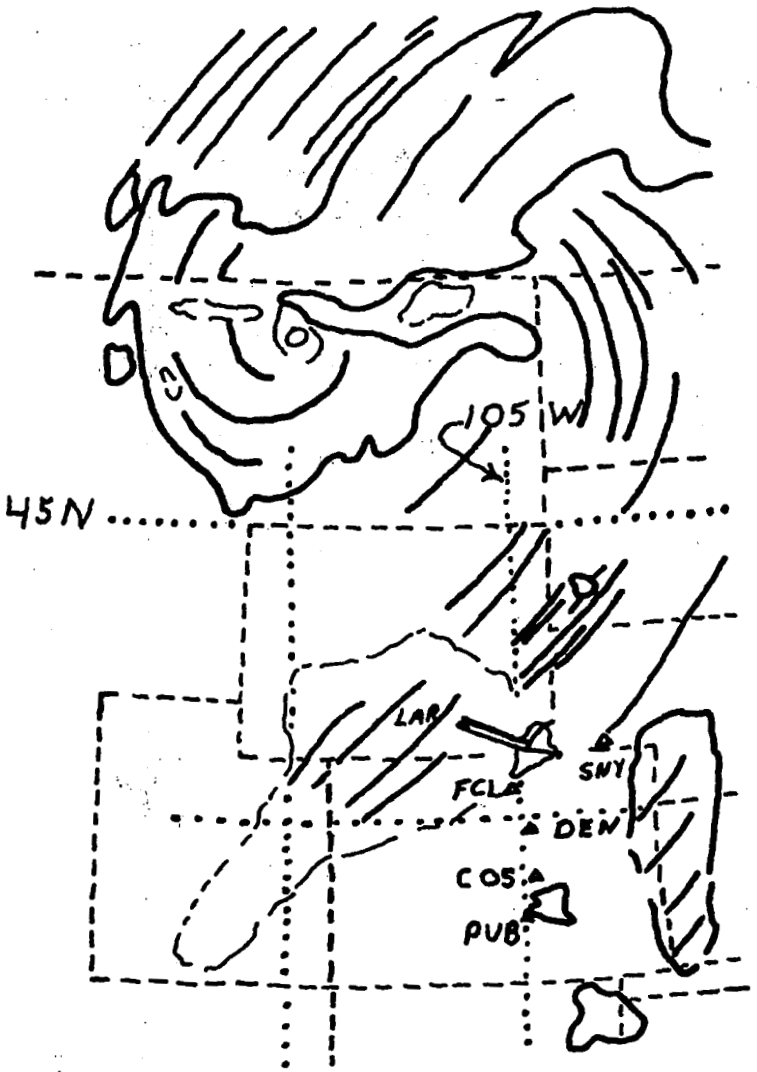

Figure 9

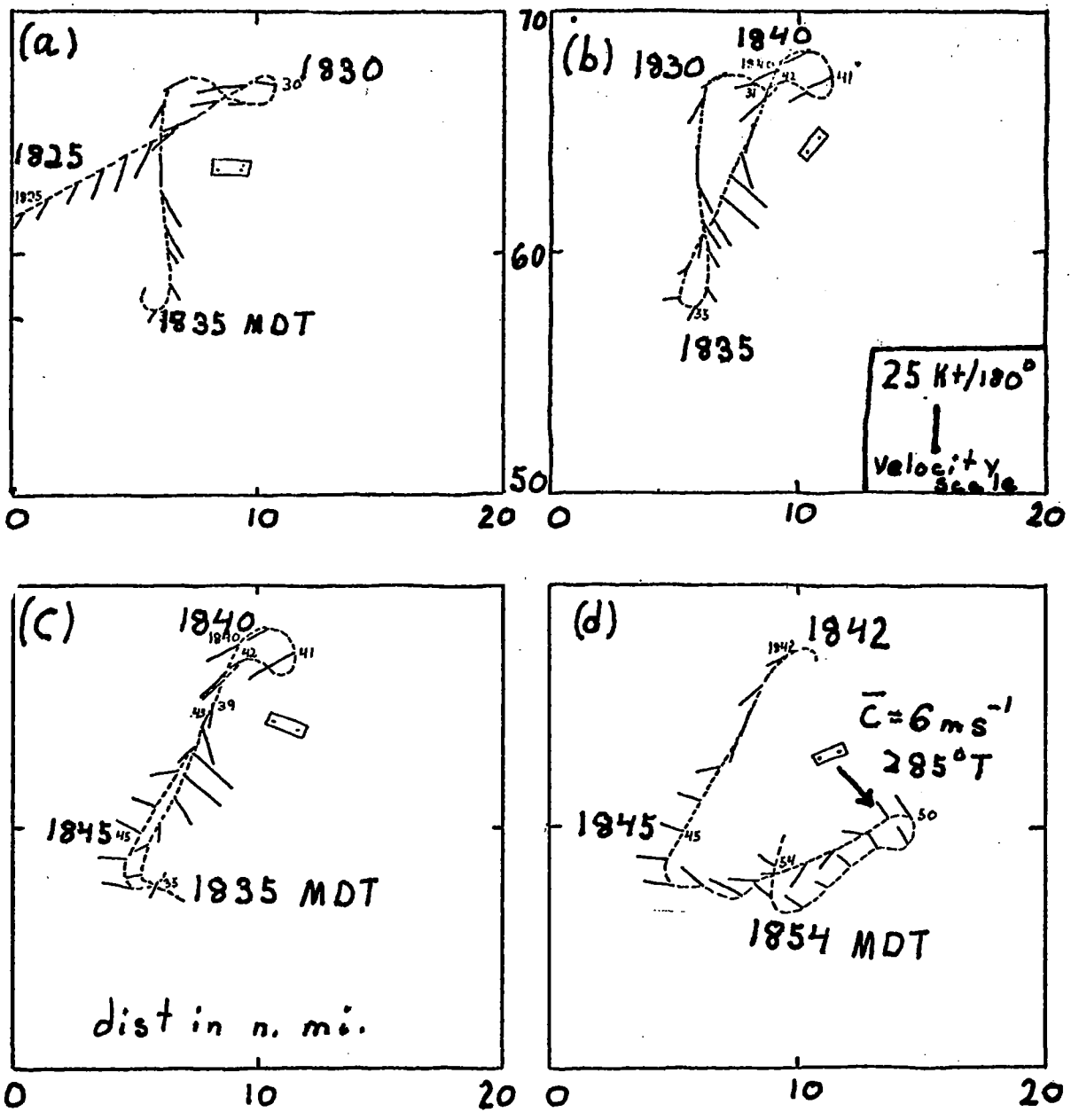
(a)
1830
1825
1835 MDT
(b)
1840
1830
1835
25 Kt/180°
Velocity Scale
70
60
50
0
10
20
(c)
1840
1845
1835 MDT
dist in n. mi.
(d)
1842
$\bar{C}$=6 ms^{-1}
285°T
1845
1854 MDT

Figure 10

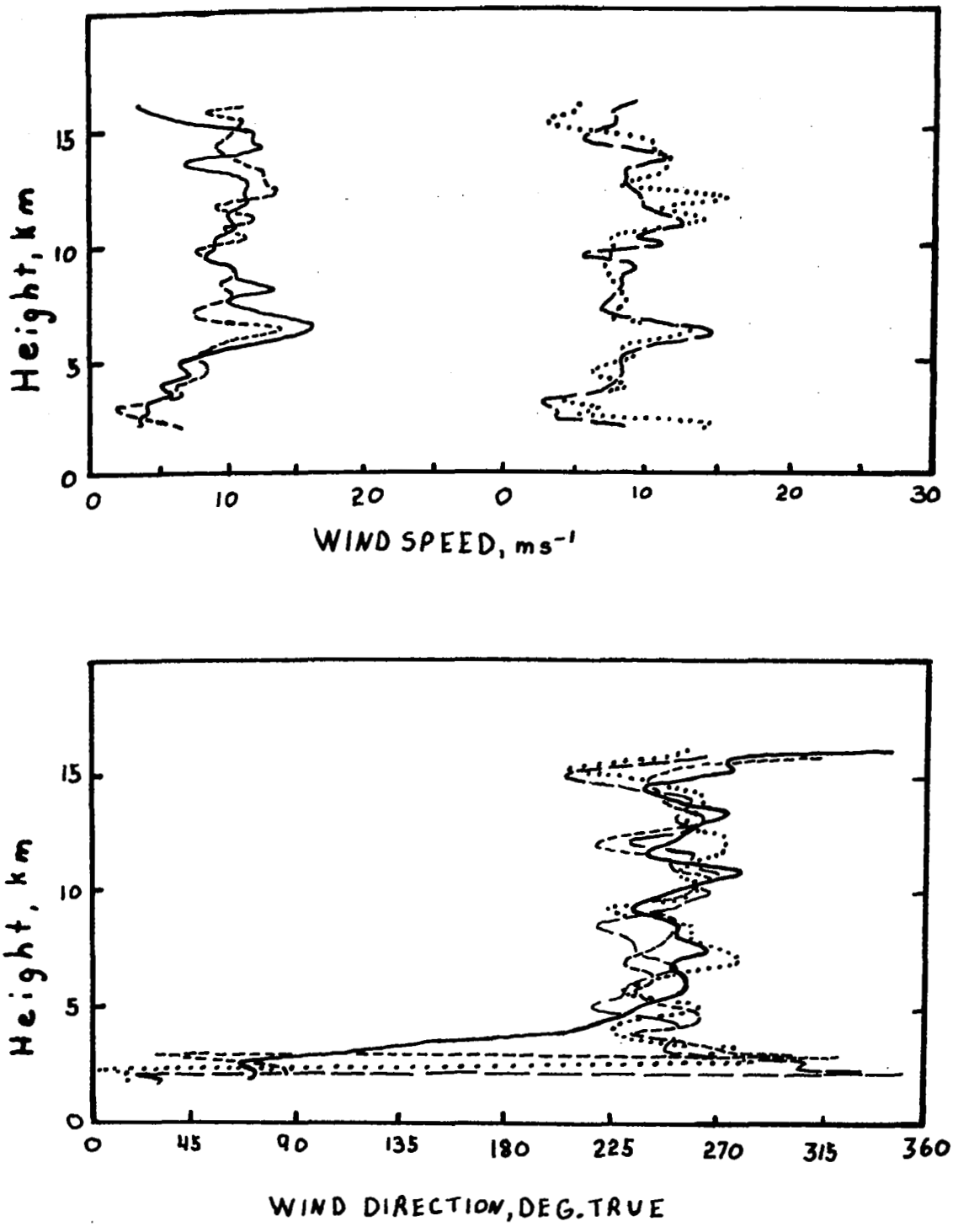
Height, km
15
10
5
0
0
10
20
0
10
20
30
WIND SPEED, ms⁻¹
Height, km
15
10
5
0
0
45
90
135
180
225
270
315
360
WIND DIRECTION, DEG. TRUE

Figure 11

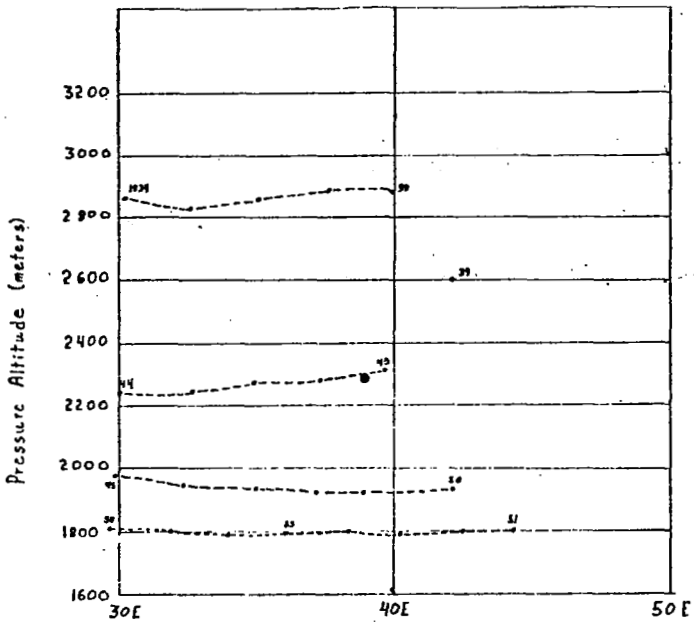

a) Projection of vertical position of aircraft 2 n.m.

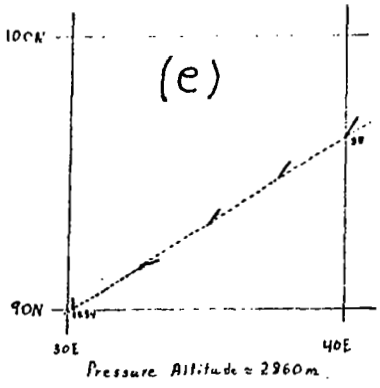

Pressure Altitude ≈ 2960 m.

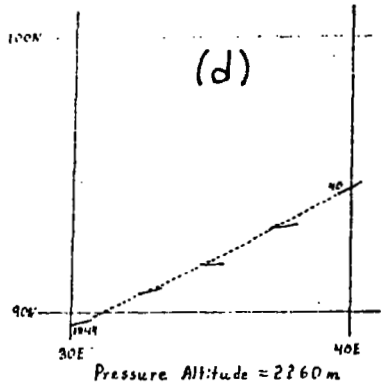

Pressure Altitude ≈ 2260 m.

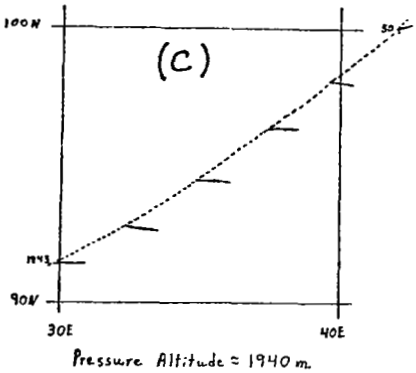

Pressure Altitude ≈ 1940 m.

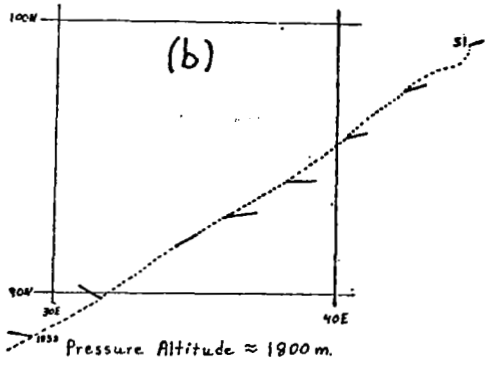

Pressure Altitude ≈ 1900 m.

Plots of horizontal winds for each level of the Altitude Ladder

25 knots from 190 degrees

Figure 12

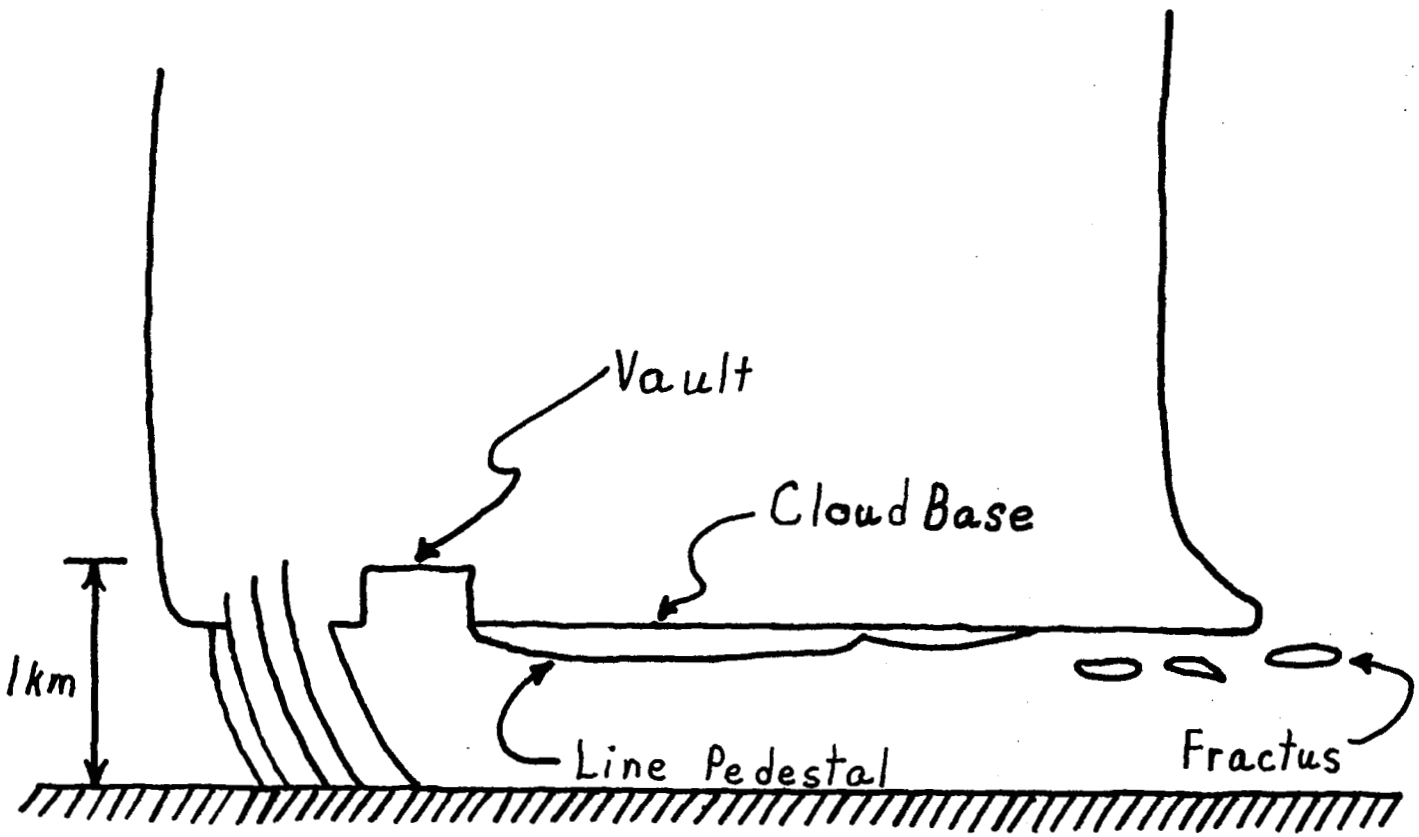

Figure 13

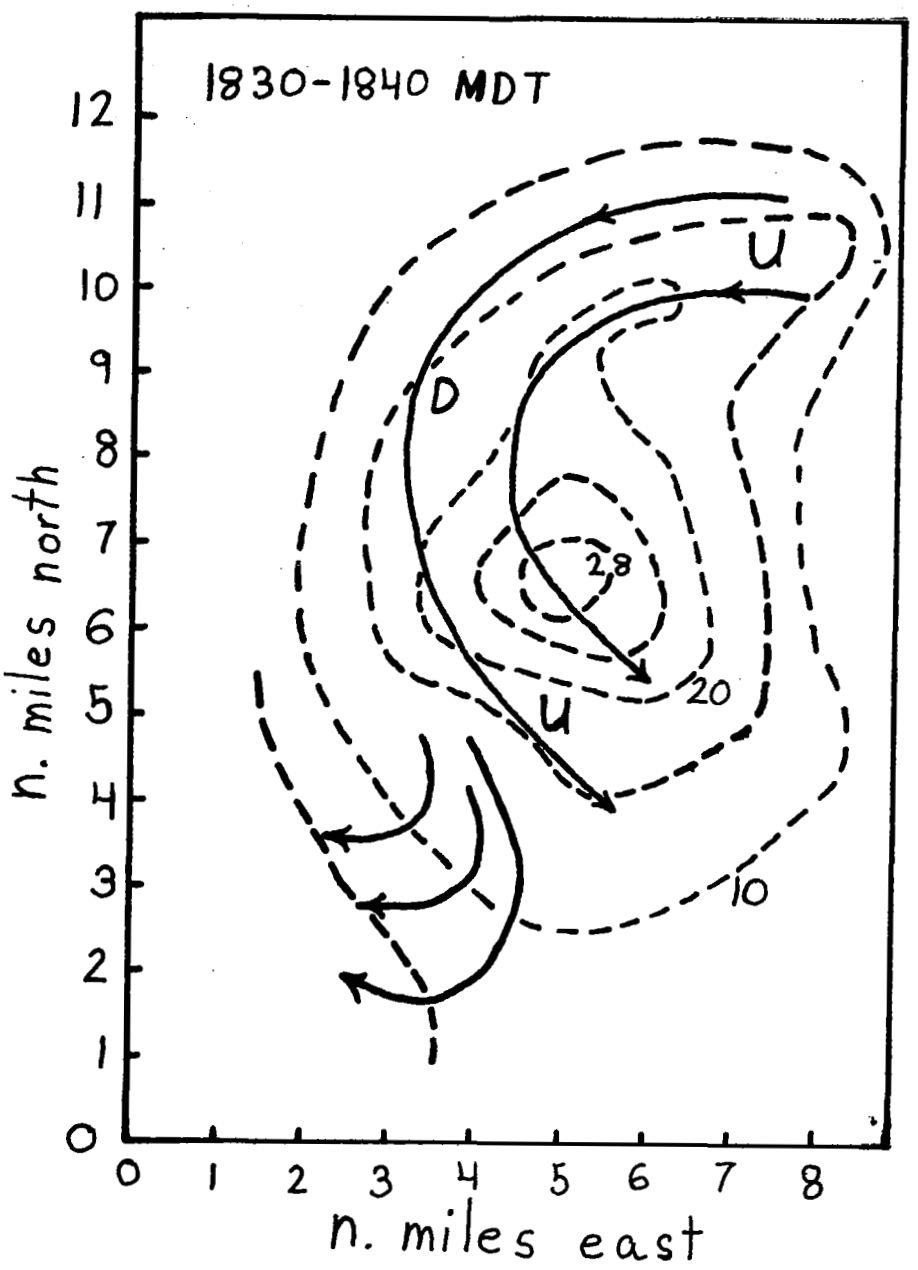
1830-1840 MDT
U
D
U
28
20
10
n. miles north
n. miles east
0
1
2
3
4
5
6
7
8
9
10
11
12

Figure 14

REFERENCES

Connell, J., 1973: Observed inflow-updraft structure related to thunderstorm precipitation and dynamics. 8th Conf. on Severe Local Storms, American Meteor. Soc., Boston, 18-24.

_____, 1975a: A nonthermal mechanism for forcing cumulonimbus updrafts. Submitted to the J. App. Meteor.

Kropfli, R.A. and L.J. Miller, 1975: Thunderstorm flow pattern in three dimensions. Mon. Wea. Rev., 103, 1, 70-71.

Lemon, L.R., 1974: Thunderstorm wake vortex structure and aerodynamic origin. NOAA Tech. Memorandum ERL NSSL-71, National Severe Storms Laboratory, Norman, Oklahoma, 17-43.

McAllister, J.D., 1968: A momentum theory for the effects of crossflow on incompressible turbulent jets. Ph.D. Dissertation, University of Tennessee, Tullahoma, August 1968, 210 pp.

Chapter IV.

A tornadic thunderstorm case study

I. Introduction

The second tornado in a sequence from a rapidly developing Cb line was observed throughout its life cycle from the ground and from the air on 6 July 1972 in Northeast Colorado. Some measurements of temperature, water vapor, and three-dimensional motion of the subcloud tornado-active region of the parent storm were made by two research aircraft.* This paper presents a preliminary composite and interpretation of data which shows (1) tornado subrotations in size or, better, superrotations in intensity which may be "suction vortices" (Fujita, 1971) and (2) interaction of motions on the mesoscale, cloud scale, "cell" scale, tornado scale and "subrotation" scale.

2. Cloud line and vertical soundings.

The cloud line started in a small area northwest of Sterling, Colorado (see the map of PPI radar echoes in Figure 15). The echo grew southeastward at speeds varying from 10 to 35 m s^{-1}. The second tornado occurred at the south or leading region of the developing line under the updraft cloud and in the clear air several miles from the edge of the precipitation (Figure 15c).

---

* From the National Center for Atmospheric Research under the auspices of the National Hail Research experiment.

A ground survey indicated that tornadoes occurred sequentially at the locations marked with triangles on Figure 15.

The spatial variations of environmental wind, water vapor, and temperature are shown in the soundings in Figure 16 as a function of time for the region of tornadoes 1, 2, and 3. Several features stand out: (1) The cloud layer winds were nearly uniform in direction with height (280-310 deg) but with a strong suggestion of gravity waves, especially upwind (KMB, Figure 16d) of the Cb line late in the day. (2) At the storm initiation region the low-level winds were from 80 deg and had a local peak of speed from 120 deg at about 2 km above the ground at the time of cloud-line initiation (STE, Figure 16 c,d). (3) Apparent middle-level high-speed wind subsidence occurred upwind of Sterling (KBM and GVR Figure 16 b,c). (4) The ground-level water vapor content at STE peaked at nearly 12 g/kg, and the temperature peaked at 30 C at 1400 MDT. Using the 1400 MDT sounding it is estimated that a parcel lifted from the surface would have experienced a +9C local temperature excess at 500 mb. (5) Strong (4 to 7 x 10^{-3} s^{-1}) wind shear existed in middle and high tropospheric levels respectively separated at all stations except STE by a region of nearly zero shear.

3. Tornado life cycle.

The tornado developed from a group of dust devils along an eastmoving shear or surge line at the surface of the earth under the updraft cloud. At 1645 MDT one dust devil began to grow in a pulsing fashion until it was several hundred meters in diameter

at the ground and was visible up to about one fourth of the distance(500 m) cloud base. Some features of the ensuing tornado are shown in Figure 17a (photographs) and Figures 17 b (drawings highlighting features of the corresponding photographs in Figure 17a). The vortex extended rapidly upward thereafter and appeared to "lock" into the center of the northernmost of two updraft pedestal clouds about 2 km in diameter. A rapidly rotating collar cloud formed just below the pedestal. Heavy rain and hail with lightning occurred in the region 2 km to 15 km north of the tornado. Ringlike bumps (instabilities?) and vortex "fingers" recurred on the tornado circumference at various heights. Several times there was little visible connection between the lowest and next lowest kilometer of the tornado (see Figure 17b-8).

The track of the tornado was toward the northeast across or into all environmental inflow and cloud-layer wind directions except during its dying stage when it moved toward the southeast. The upper part of the tornado moved more to the northeast than did its lower part such that it attained an increasingly northward tilt. The tornado dissipated in a weak updraft, leaving a nonrotating dust cloud in the otherwise clear air below the cumulonimbus base, at 1715 MDT. The total lifetime was 20 minutes.

One or two surge or shear lines were connected to the base of the tornado and apparently moved slowly about it in a cyclonic direction. Dust devils were observed to move rapidly along them into the tornado. Small diameter cyclonic vortices

of considerable intensity and 200 meters high frequently developed on the circumference of the tornado. They moved around it cyclonically at about 1 revolution per minute, according to a visual estimate. It appeared that the subscale superrotations started on the southwest side and intensified until they reached the north side where they weakened or sometimes tended to be separated from the larger diameter vortex. The lowest 300 meters of the tornado, containing the superrotations, was often distinct from the rest of the tornado. Occasionally this base region tilted so as to lift off the earth on all but one edge near the side of superrotation development. Sometimes the very bottom 100 meters or less was half the diameter of the adjacent higher-altitude tornadic rotation.

The surge lines and superrotations seem to be good indications that a significant part of the tornado vorticity was organized in the lowest several hundred meters of the atmosphere at the shear between downward southeast moving air and northwest-moving inflow to the updraft.

4. Interaction of scales.

A composite of features of the thunderstorm showing the variety of scales is presented schematically in Figure 18. A list of features from mesoscale to tornado superrotation size and ranging in time scales from hours to minutes is presented in Table 1.

Table 1

Flow features of the storm on five length scales.

A. Mesoscale (20-100 km Dia.)

1. Midtropospheric subsidence or downward intrusion upwind of Cb.
2. Gravity waves especially upwind of Cb.
3. Sequence of tornadoes at intervals Δs= 20 km Δt= 40 min. for 120 km toward 155 deg true.
4. Weak jetlike wind at 2 km AGL.

B. Cloud scale (10-20 km Dia)

1. Horizontal cyclonic circulation at z = 1.7 km AGL (approx. 0.3 km below cloud base). Vorticity = 10^{-3} s^{-1}.
2. Zone of horizontal shear on south edge of cloud at z = 1.7 km AGL.

C. Cell scale (1-5 km Dia.)

1. Cyclonic circulation or shear zone (4 km dia) at 1 km AGL in updraft.
2. Strong downdraft at 1 km AGL west and southwest of tornado containing cyclonic motion of dry air.
3. Strong updraft at 1 km AGL south, east and northeast of tornado in both southeast inflow and northwest outflow to cloud.
4. Surge line at and near tornado at ground level.

(Table 1 Continued)

D. Tornado scale (0.2-1 km Dia.)

   1. Surge line at tornado

   2. Rotating tornado column

E. Dust plume and dust devil scale (20-200 m).

   1. Extra-tornadic boundary layer plumes and dust devils, especially on surge lines.

   2. Superrotations within the tornado

   3. Various satellite and possible "return" vortices closing vortex-line circuits.

Briefly, the storm line development and propagation seem to have been associated with an upwind, midtropospheric, sharp subsidence occurring on the mesoscale late in the day at the edge of the moist air zone south and east of Sterling, Colorado (see Figure 16, GVR and KMB soundings).

Single tornadoes developed at intervals of about 20 km for at least 120 km along the line. A preliminary estimated value of the average time intervals between tornadoes is 40 minutes. Cloud-scale cyclonic convergence was observed on the south end of the line at 1.7 km AGL or about 0.3 km below cloud base (Figure 19a) at the time of tornado number 2.

Several features of the observed second tornado in the series were in the one-to-five kilometer size range, which is here called the cell scale. At 1 km AGL, or 1 km below cloud base, either a cyclonic shear zone or one of a pair of circulations was observed moving or extending from the southeast edge of the tornado region in the direction of the line of propagation of the storm (Figures 19a,b). That cyclonic flow was also a strong updraft. On the southwest and west side, at 2-3 km from the tornado, the airflow was a strong downdraft which was relatively dry and cool (Figure 19a). This is suggestive of an upper source for a surface surge line, where the source wind sheared against the southerly and easterly inflow-updraft air. Photographs and visual observations indicated one or two dust lines extending from the tornado in the first

few hundred meters above the ground for horizontal distances up to several kilometers generally in the west, south, and slightly southeast sectors (Figures 17b-4-6-9 and 13). The tornado seemed to remain in this zone near the ground and to move northeasterly, although directions of the cloudline growth, cloud layer environmental winds, and inflow winds were nearly orthogonal to this direction.

The average speed of movement of the tornado, $\bar{c}$, was about 7 m s^{-1} over an 8 km path. A tractor raced it at late middle life measuring $c = 10$ m s^{-1}. The upper part of the tornado moved more northward as though it were in a cloud-scale cyclonic rotation.

The base of the tornado was about 400 m in diameter. Dust devils and dust plumes up to 30 to 100 m diameter (0.20 to 1 km high) were observed along the surge fronts and were seen by ground observers to be moving rapidly into the tornado. Additionally, cyclonic superrotations were observed forming and revolving around the periphery of the tornado. Their diameters were about 50 m to 100 m and their heights were about 300 m. Figures 6a, 6b and 6c are drawings from photographs which show some space and time variations of the superrotations. The two ground-based photographs were taken about four minutes apart. The lowest 300 m of the tornado

appeared to be the source of vorticity for other altitudes in the tornado. Both local organization and transport of vorticity from below seem to have contributed to the tornadic vortex near cloud base. However, the special properties of the lower atmospheric boundary layer tornado appear to result in considerably greater organization and intensity of its superrotations than any near cloud base. The tops of the superrotations seem to occur distinctly and uniformly. Sometimes apparent extensions of their tops bent outward and downward at a larger radius, producing visible, nearly closed, vortex rings (see left side of Figure 20c). Much of what previously has been thought to be ejecta near the base of a simple vortex may be visible effects of these superrotations.

5. A few quantitive estimates.

Vorticity, ζ, may be estimated on five scales. On the cloud scale at z=1.7 km AGL, $\zeta \doteq 2\omega \doteq 2v/r \doteq 2 \times 15 \text{ m s}^{-1} / 10^4 \text{m} = 3 \times 10^{-3} \text{ s}^{-1}$. On the cell scale at z =1 km AGL, $\zeta \doteq 2v/r \doteq 2 \times 7.5 \text{ m s}^{-1} / 1.5 \times 10^3 \text{m} = 10^{-2} \text{s}^{-1}$. Assuming that the zone of shear along the surge line has a width represented by the largest dust plumes (200 m) and using typical wind speeds, $\zeta = \partial v/\partial n = 20 \text{ m s}^{-1}$. It is possible that such shears on the surge surface exist only near the surface of the earth

where the down air penetrates sharply to meet the inflow (see the wind map Figure 19a). The probable source of surge air (strong down air and weak wind) at z =1 km is about 3 km west and northwest of the position of the tornado at the ground.

On the tornado scale the velocity of rotation estimated by one aircraft pilot was 40 m s^{-1}. Damage to a barn and wind effects on a farm interpreted according to Fujita (1971b) suggest a similar speed. From visual estimates and photographs of the tornado, its base diameter was about 400 m. Therefore, its vorticity was about $2\ v/r = 2 \times 40\ m\ s^{-1}/200\ m = 4 \times 10^{-1}\ s^{-1}$.

The propagation speed of the radar echo (toward 150°) at the tornado time was about 12 m/sec. The cell size vortex measured at z = 1 km AGL appeared to move as an entity at 9 m s^{-1} toward about 150°. In another paper by Connell and Kimbrough titled "Subcloud Vortices of a Hailstorm" it is suggested that lee vortices whose diameters are about half of a thunderstorm diameter are to be expected due to the wind crossflow around the updraft. Some wind and water tunnel results applied to thunderstorms in that paper suggest that these vortices will be stationary relative to, say, the interface of the colliding wind and updraft air streams for turbulent Reynolds number values in the low thousands and will tend toward Von Karman vortex streets at slightly higher Reynolds numbers.

The cell-scale vortices observed in the present study may be of the stationary type relative to a collision interface. A crude estimate of the Reynolds number may be made by considering that the inflow speed is 15 m s^{-1} and the environmental cloud wind at, say, 4 km AGL is about 10 m s^{-1}. Therefore,

$$Re_t \frac{15 \text{ (to } 20) \text{ m s}^{-1} \times 5 \text{ (to } 10) \text{ km}}{30 \text{ (to } 100) \text{ m}^2\text{s}^{-1}} = 750 \text{ to } 6700$$

A value of Re less than 1500 is expected to represent conditions for a stationary vortex pair downwind of the updraft, whereas Re greater than 1500 is for a vortex street which is steady (Von Karman type) for Re less than about 2500 for solids and perhaps greater for air updrafts (McAllister, 1968, p. 33). The cores of the trailing vortices in water tunnel experiments of a jet in a crossflow are surprisingly like tornadoes. The present author, in some qualitative wind tunnel experiments with a rotating jet in a crossflow, found whole-jet rotation to enhance the similarly rotating trailing vortex and to tend to suppress the oppositely rotating vortex.

6. Tentative conclusions.

The 6 July 1972 N.E. Colorado number 2 tornado appears to have been formed when a source of very strong vorticity organization near the surface of the earth was coupled for twenty minutes to a source of vorticity one order of magnitude weaker at higher levels by strong updrafts in the subcloud region. The lower source at a surge line, may have been

associated with upwind mesoscale, mid-level, downward intrusion of air interacting with a cyclonic cloud scale circulation. The upper source may have been a lee vortex due to collision of the thunderstorm updraft with the crossflowing environmental wind. The pair of lowered regions of updraft cloud base (pedestals) may have been a result of two such lee vortices whose slightly lesser central pressure caused the downward extension of cloud base.

Subrotations in size, which are superrotations in cyclonic wind speed and which formed around the circumference of the bottom portion of the tornado, appear to have been a result of boundary layer rotations and inflow processes. Somewhat similar, more diffusely organized vortices near cloud base seem to have been independent of them. The nature of damage at the ground suggests that it was caused by the smaller, circumferential boundary layer superrotations.

FIGURES

Figure 15. Ten-cm-radar PPI contoured images at about 2.5 Km AGL in N.E. Colorado on 6 July 1972: (a) rawinsonde sites and tornado locations, (b) early aborted development, (c) (d), and (e) tornadic thunderstorm at several times.

Figure 16. Vertical atmospheric profiles: (a) temperature, (b) dew point temperature, (c) wind speed and (d) wind direction on 6 July, 1972 at the four stations KMB, GVR, STE, FTM shown in Figure 15 Soundings are shown for approximate MDT times (symbols) 0730 (xxx) 1100 (···), 1400(←→), 1630 (---) and 1800 (——). KMB: Kimball, Neb., GBR: Grover, Colo., STE: Sterling, Colo. FTM: Fort Morgan, Colo.

Figure 17a. Photographs of the life cycle of tornado number two in NE Colorado on 6 July, 1972. Time span is approximately 20 minutes. Exact time of each photograph is not known.

Figure 17b. Tracings of photographs in part (a) highlighting several features. Arrows indicate the horizontal direction from which the photograph was taken, north being at the top of the page.

Figure 18. A schematic composite of features of the tornadic thunderstorm emphasizing interaction of scales. View is from above and from the south. AGL means above ground level.

Figure 19. Composite maps of aircraft derived properties of the subcloud airflow of the parent storm at 1 Km and 1.7 Km AGL for tornado number 2, N.E. Colo. 6 July 1972. (a) Streamlines and tornado location (b) Isotachs & streamlines (c) Water vapor, potential temperature. Up and down airflow indicated by U & D respectively. Plus & minus signs indicate strong and weak drafts. Tornado location at an intermediate time is drawn.

Figure 20. Artist-enhanced tracings of photographs showing tornado superrotations and dust lines. (a) Aerial photographs showing superrotations and 2 possible surge lines. (b) Ground photo showing small diameter superrotations in the lowest few hundred meters and 2 possible surgerelated dust features to the south. (c) Ground photo for same location about 4 min. later. Note tilt and lift of superrotation region and apparent "return" vortex from top of 2 superrotations.

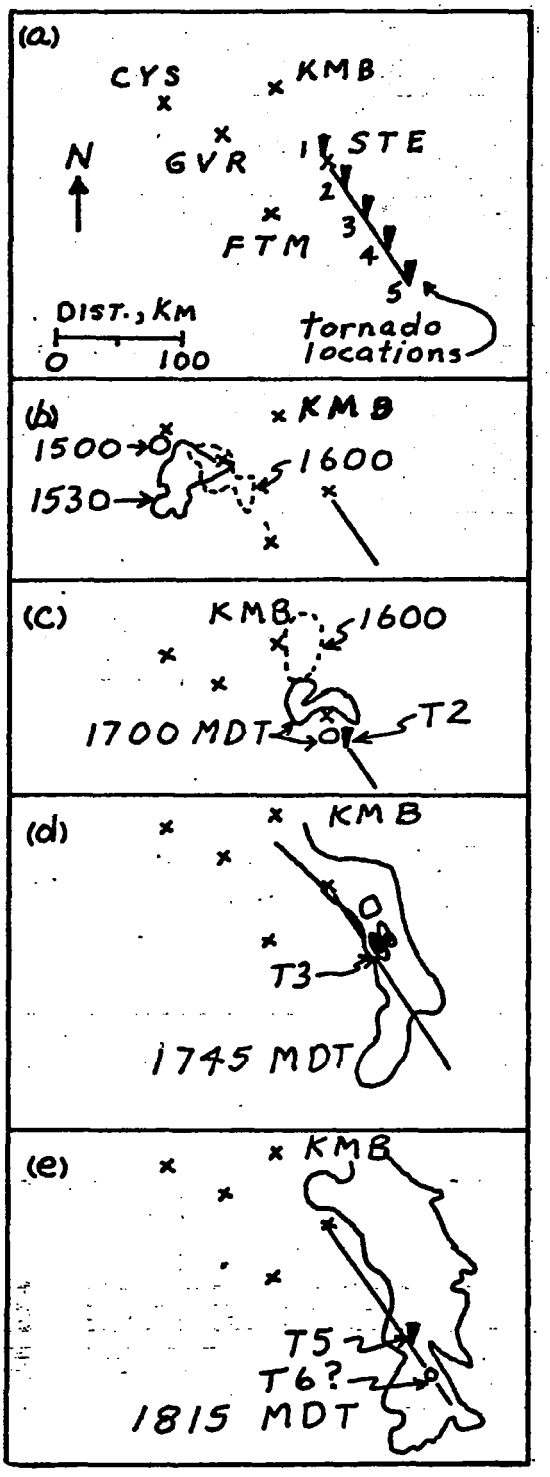
(a)
CYS
KMB
N
GVR
STE
1
2
3
4
5
FTM
DIST., KM
0
100
tornado locations
(b)
KMB
1500
1530
1600
(c)
KMB
1600
1700 MDT
T2
(d)
KMB
T3
1745 MDT
(e)
KMB
T5
T6?
1815 MDT

Figure 15

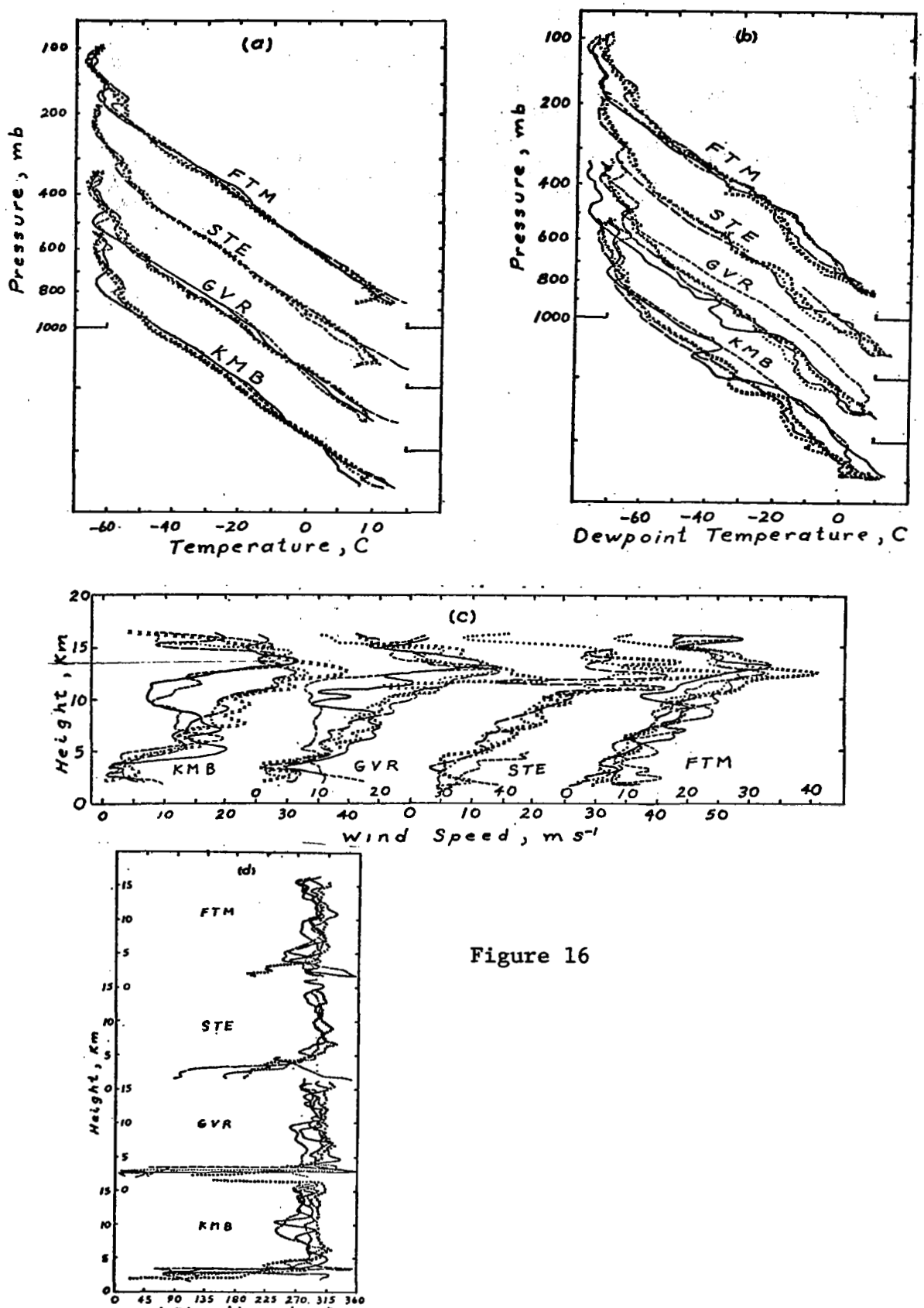
(a)
Pressure, mb
100
200
400
600
800
1000
FTM
STE
GVR
KMB
-60
-40
-20
0
10
Temperature, C
(b)
Pressure, mb
Dewpoint Temperature, C
(c)
Height, Km
Wind Speed, m s-1
(d)
Wind Direction, deg. True
0
45
90
135
180
225
270
315
360

Figure 16

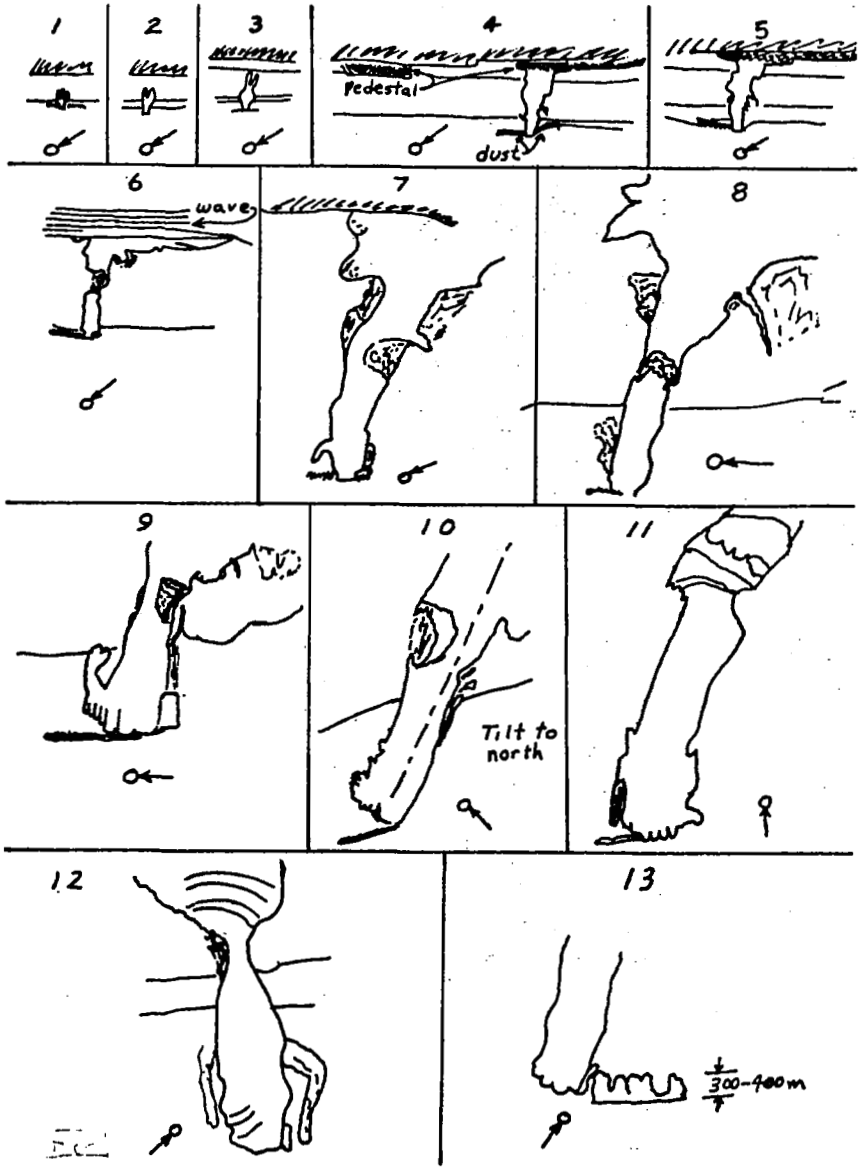

Figure 17a

Figure 17b

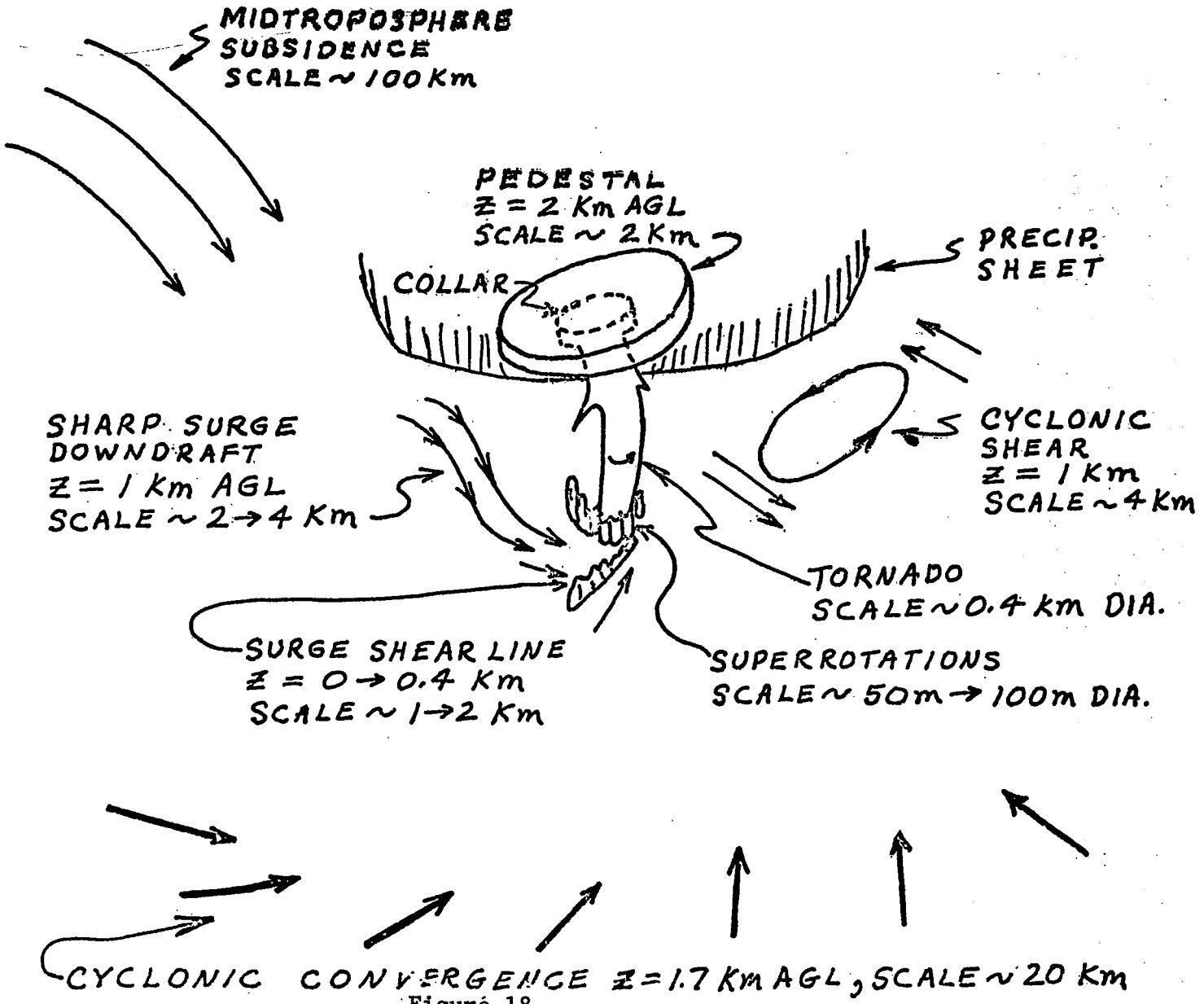
MIDTROPOSPHERE
SUBSIDENCE
SCALE ~ 100 Km
PEDESTAL
Z = 2 Km AGL
SCALE ~ 2 Km
COLLAR
PRECIP.
SHEET
SHARP SURGE
DOWNDRAFT
Z = 1 Km AGL
SCALE ~ 2 → 4 Km
CYCLONIC
SHEAR
Z = 1 Km
SCALE ~ 4 Km
TORNADO
SCALE ~ 0.4 km DIA.
SURGE SHEAR LINE
Z = 0 → 0.4 Km
SCALE ~ 1 → 2 Km
SUPERROTATIONS
SCALE ~ 50m → 100m DIA.
CYCLONIC CONVERGENCE Z = 1.7 Km AGL, SCALE ~ 20 Km

Figure 18

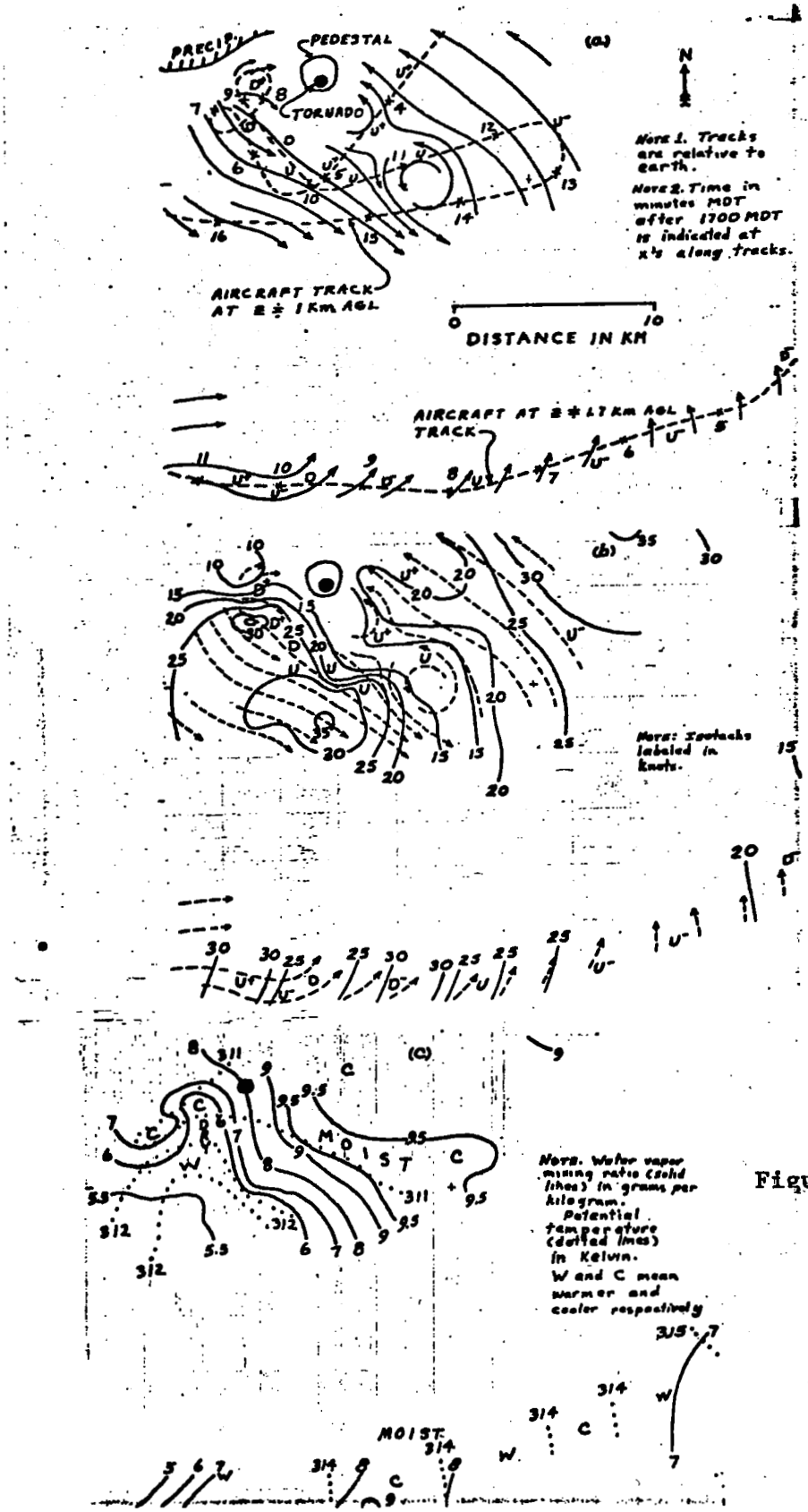
PRECIP.
PEDESTAL
TORNADO
(a)
N
Note 1. Tracks are relative to earth.
Note 2. Time in minutes MDT after 1700 MDT is indicated at x's along tracks.
AIRCRAFT TRACK AT 2 ± 1 Km AGL
0
10
DISTANCE IN KM
AIRCRAFT AT 2 ± 1.1 Km AGL
TRACK
(b)
Note: Isotachs labeled in knots.
(c)
MOIST
Note. Water vapor mixing ratio (solid lines) in grams per kilogram. Potential temperature (dotted lines) in Kelvin. W and C mean warmer and cooler respectively

Figure 19

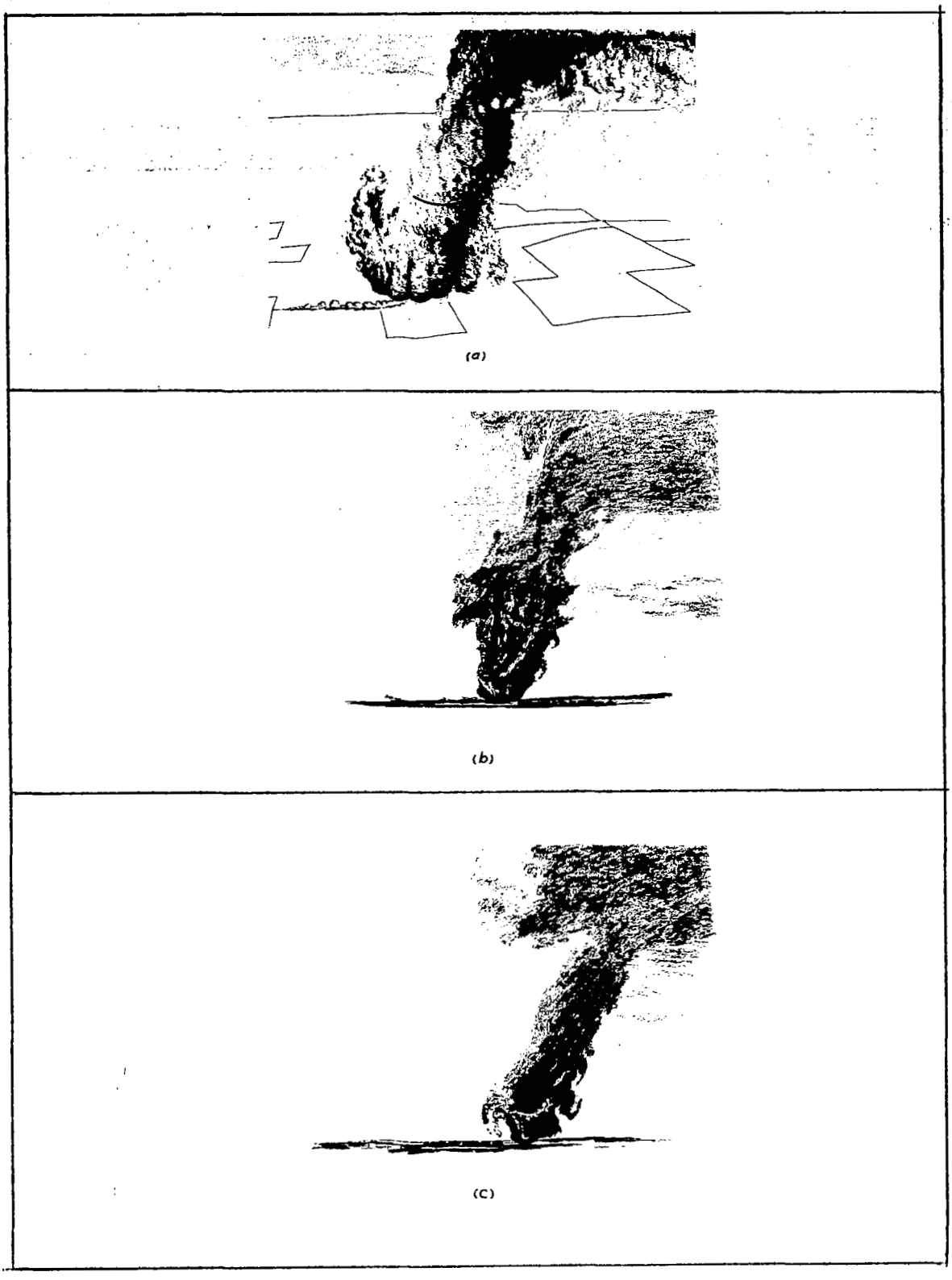

Figure 20

REFERENCES

Connell, J.R. and L. Kimbrough, 1975: Subcloud vortices of a hailstorm Preprints 9th Conf. on Severe Local Storms, Amer. Meteor. Soc., Boston, 79-84.

Fujita, T.T., 1971: Proposed mechanism of suction spots accompanied by tornadoes. Preprints 7th Conf. on Severe Local Storms, Amer. Meteor. Soc., Boston, 208-213.

_____, 1971b: Proposed characterization of tornadoes and hurricanes by area and intensity. S.M.R.P. Research Paper No. 91, The University of Chicago, 42 pp.

McAllister, J.D., 1968: A momentum theory for the effects of cross-flow on incompressible turbulent jets. Ph.D. Dissertation, University of Tennesse, Tullahoma, August, 1968, 210 pp.

Chapter V.

A parameterized model of non-thermal dynamics of a Cb in a crossflow.

The model for a Cb in a crossflow is schematically represented by Figure 21. Figure 21a represents a thunderstorm and Figure 21b shows a jet in crossflow with normal incidence for which useful data is available (Jordinson, 1956).

The jet in crossflow data is parameterized by a set of non-dimensional plots of pressure and pressure geometry as a function of 3-d position following the position scheme indicated in Figure 22.

Jordinson, 1956, has produced the most comprehensive data for a jet in a crossflow, providing jet axis shape, pressure fields at several axial positions, and streamlines along one vertical section for jet to wind speed ratios of four, six and eight. A small amount of data is available for V/W =2. The jet used was a round jet of air issuing orthogonally into a presumed nearly uniform wind. The orifice diameter was 1 inch, the boundary layer was about 0.1 inch high at the orifice. The center of the orifice was 1.5 inch downwind of the leading edge of a false floor which was 1 inch above the actual floor.

The most commonly considered property is the geometry of the axis of the jet. Figure 23 shows the axis shape measured by Jordinson as a dashed line for each speed ratio V/W =8.1, 6.2 and 4.3, where V is the speed of jet air at the orifice and W is the speed of the freestream crosswind. Three

proposed equations for the axis shape are given at the bottom of the figure and are plotted at three values of downwind location. It is seen that the fits have maximum errors of about 30% near the orifice and 25% at x/d =11. The errors are greatest for smallest velocity ratios. Ivanov's equation is the best fit. The equation by Margason and Fearn, 1969, has been developed to allow for non-orthogonal initial angles of the jet. It is shown in Figure 1, chapter 2, along with other figures from Jordinson, 1956. Clearly there is need for much more experimental data for jets in crossflows to gain accuracy and detail. Nevertheless, a first effort can be made to parameterize the jet properties according to the scheme suggested by Figure 22.

Figure 24 shows the separation of leeside vortices, downwind displacement of vortices, their diameter and central pressure as a function of speed ratio V/W. The central pressure deficit of the vortices is highest near the orifice where the crossflow and impulse is the greatest between the jet and the wind (see Figure 24a). The figure also shows a strong increase in maximum pressure defect with decreasing speed ratio. Figure 24b is a semilogarithmic plot of the pressure coefficient $C_{p\ max}$ at an axial distance $\zeta = 2.5\ d$ as a function of V/W. While no data exist to validate

a semilogarithmic linear extrapolation to the lower V/W appropriate for thunderstorms, such extrapolation is shown as a dashed extension of the solid line. Thus at V/W = 2 one might expect more than a doubling of the low pressure deficit in the vortex over that observed at V/W =4. Figure 24c shows the symmetry of the measurements of pressure defect in the jet for left and right vortices. Figure 24d is a plot of the lines of maximum leeside pressure deficit in the (x,z)- plane in relation to the jet axis. One important point is that the minimum pressure is well within the radius of the jet. Another is that the low pressure is closer to the "ground" plane for smaller values of V/W.

A qualitative conclusion is that the pressure effect of a jet in a crossflow on the low level airflow corresponding to thunderstorm inflow-updraft is greatest for smaller values of V/W and thus for typical thunderstorm conditions. This leads one to suppose that the influence of the vortices produced by non-thermal means may be considerable for thunderstorm development. Some additional factors must be parameterized quantitatively to permit description of the influence. The lateral geometry is probably the most significant.

Figure 24e shows that the separation of vortex centers relative to the vortex diameter is decreased at low (and high) values of V/W. Thus thunderstorm conditions of V/W should result in vortices having great lateral separation since they are of large diameter. This provides for greater off-center

effects in thunderstorms such as deviate motion and a symmetric development of the storms whose inflow direction is not parallel or antiparallel to the cloud layer winds in the levels of strong collision in crossflow.

Figure 24f is a plot of downwind displacement of the line of centers of the vortices relative to the jet local axis. Again, it is seen that the diameter of vortices is largest for low V/W near the "ground plane". It is also clear that the absolute downwind displacement for V/W = 4 is less near the origin of the jet. Figure 24g brings this out more clearly in a plot of L/D (instead of L/d) vs V/W (instead of D/d).

The next step is to compare a few parameters from a few observed thunderstorms with those for the jet in a crossflow.

There is precious little data and, therefore, the comparisons of identical parameters is seldom possible. The most useful dual-doppler data is that published by Kropfli and Miller, 1975. A small amount of radar data is also available from other reports, and when used it is identified on the figures. Some aircraft data are available in Chapter 3 and 4 and are not repeated in the present chapter.

Figure 25a defines the parameters in the context of thunderstorm airflow and geometry. This may be compared with Figures 22a and b. Instead of pressure coefficients we have estimates of the vorticity of the left and right vortices. Crudely speaking, there must be an increase in central pressure defect for an increase in vorticity given a constant diameter of all vortices.

Figure 25b shows that unlike the orthogonal jet in a crossflow the vortex pair is less symmetric in intensity. Further, the left or anticyclonic member is immediately obvious only in the upper levels (Z/H>0.6). This may be due to whole cloud cyclonic rotation. Figure 25c shows the X-Z projection of the axes of the vortices in the thunderstorm. Considering the difference between airflow and updraft below cloud base and the wind and jet flow as observed by Jordinson (1956), there is a striking similarity between jet and thunderstorm (Compare 25c with 24d).

Figure 25d shows that the vortices generally increase in diameter with increase in height from D = 4 km to 6 km. Figures 25e and f show that the separation of vortices increases with height from about 1 to 2 vortex diameters or from about 0.75 cloud height to 0.85 cloud height.

The downwind displacement of vortices relative to the upwind side of the interaction zone between airflows increases with height except in the lowest levels (see Figure 25g). This is consistent qualitatively with the results for the jet in a crossflow as plotted in Figure 24g. Figure 25h is a slightly different plot of displacement vs height from that in Figure 25g (L/H instead of L/D vs Z/H).

In summary, there are many similarities between the parameters of a jet in a crossflow and of a thunderstorm even when the available observations do not exist for corresponding initial flow directions, wind shears, and speed ratios.

These parameters, which are discussed in Chapter 2 relative to their influence on thunderstorm development and in Chapters 3 and 4 for specific thunderstorm studies, need to be much more accurately and fully studied in controlled conditions such as with a wind or water tunnel. As field measurement programs can be directed toward adequate, accurate and comprehensive measurements, the more easily obtained laboratory data to be acquired can be better scaled and interpreted.[3]

It is obvious that without more and better data the concepts cannot be built into a detailed and quantitative model. However, the results of the study described in the present report indicate some new ways to interpret mesoscale rawinsonde, radar and satellite data in order to develop a better capability for predicting thunderstorm development and motion.

The main clue is that vector wind shears just above and below (±several kilometers) cloud base may be instrumental in generation of vortex pairs, which in turn affect control of cloud processes which may determine intensity and movement of thunderstorms as suggested in earlier chapters.

The next chapter presents a brief sample of the types of radar and SMS 1 satellite photo analyses which may be incorporated in a developmental program of research aimed at verifying the concept of cloud modification through vector wind shear in small layers on the mesoscale.

FIGURES

Figure 21. Models of Cb and jet in crossflow.

Figure 22a. Parametric model of jet or Cb in a crossflow

Note: (1) $D_L \equiv$ dia. of left vortex

$D_r \equiv$ dia. of right vortex

$D \equiv$ dia. of single vortex or mean of left and right.

(2) The pressure defect of the low pressure centers is measured by

$$C_{p\ min} \equiv \frac{P_{jet} - P_{wind}}{P_{jorifice} - P_{wind}}$$

(3) The mean vorticities $\equiv 2w = v^2/r$, ΔP using cyclostrophic assumption are computed for dual-doppler observations of Cb.

Figure 22b. Top view of vortex features of jet or thunderstorm at an arbitrary height.

Note: $\frac{D_L + D_R}{2} \equiv D$

Figure 23. Shape of jet axis of round jet in crosswind.

Figure 24a. Maximum pressure deficit in wake vortices.

Figure 24b. Maximum pressure deficit as a semilogarithmic function of ratio of jet velocity to wind speed.

Figure 24c. Relation of maximum pressure deficit to velocity ratio at specified distances (in jet diameters) from orifice along jet axis.

Figure 24 d. Lines of maximum Cp deficit in relation to jet axis. (Measurement stations are numbered.)

Figure 24e. Ratio of distance between vortex centers to diameter of vortex as a function of velocity ratio.

Figure 24f. Downwind displacement of the line of centers of the vortices from local jet axis.

Figure 24g. Displacement of the line of vortex centers as a function of the velocity ratios.

Figure 25a. Parametric model of a Cb in a wind shear.

Notes: (1) $D_L \equiv$ dia. of left vortex

Dr$\equiv$ dia. of right vortex

D $\equiv$ dia. of single or mean of L+r

(2) The mean vorticity $\equiv 2w = \frac{v^2}{r}$. and

(3) Δp computed using cyclostrophic assumption computed for dual-doppler observation of cumulonimbi winds.

Figure 24 b. Average vorticity as a function of height.

Figure 25c. Location of vortex centers from dual-doppler data of Kropfli and Miller.

Figure 25d. Average diameter of vortices as a function of height.

Figure 25e. Separation between vortices as a function of height.

Figure 25f. Ratio of separation between vortices to cloud height as a function of height.

Figure 25g. Downwind displacement of vortices relative to

the upwind side of interaction zone between airflows.

Figure 25h. Ratio of downwind displacement of vortices to cloud height.

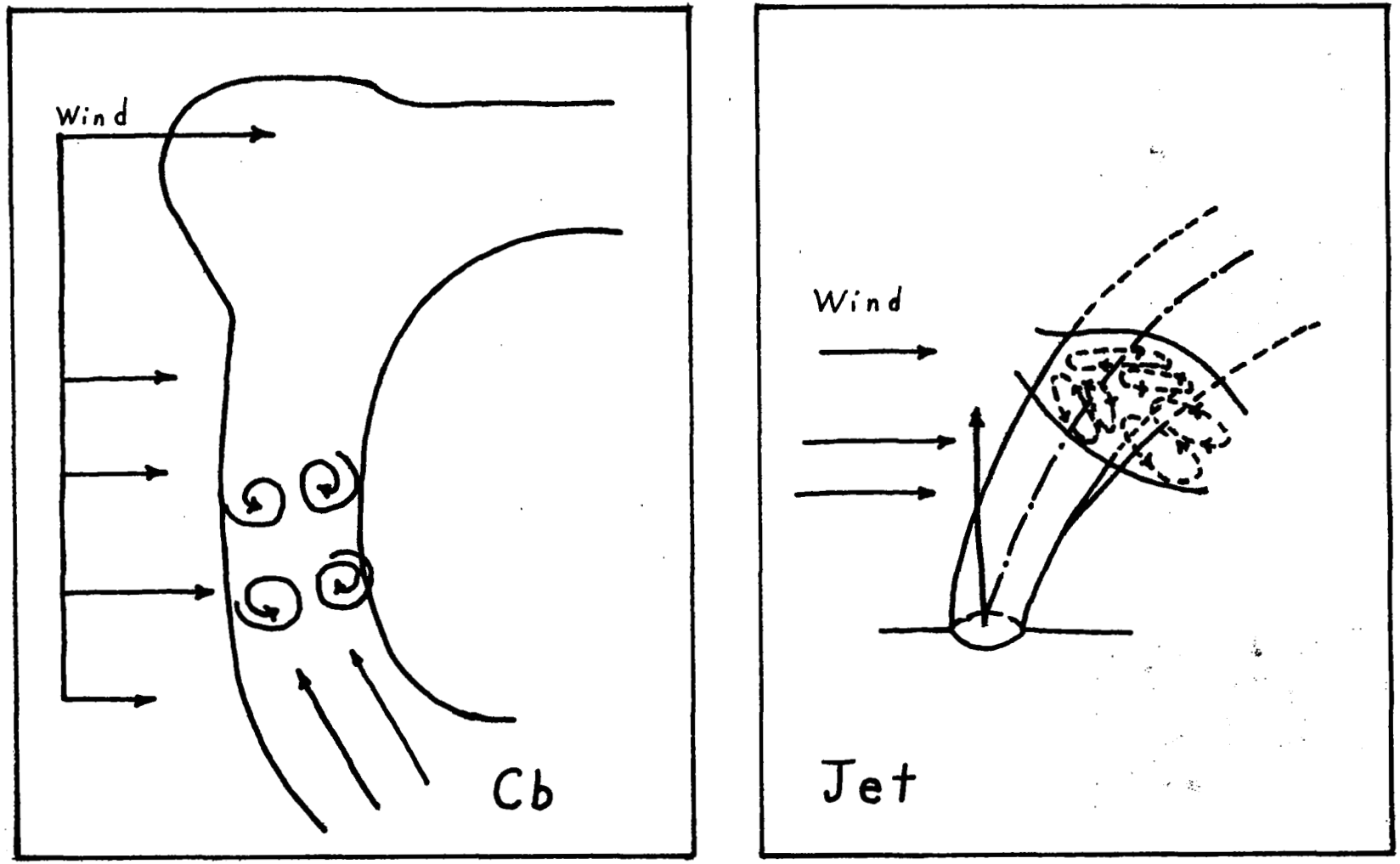

Figure 21

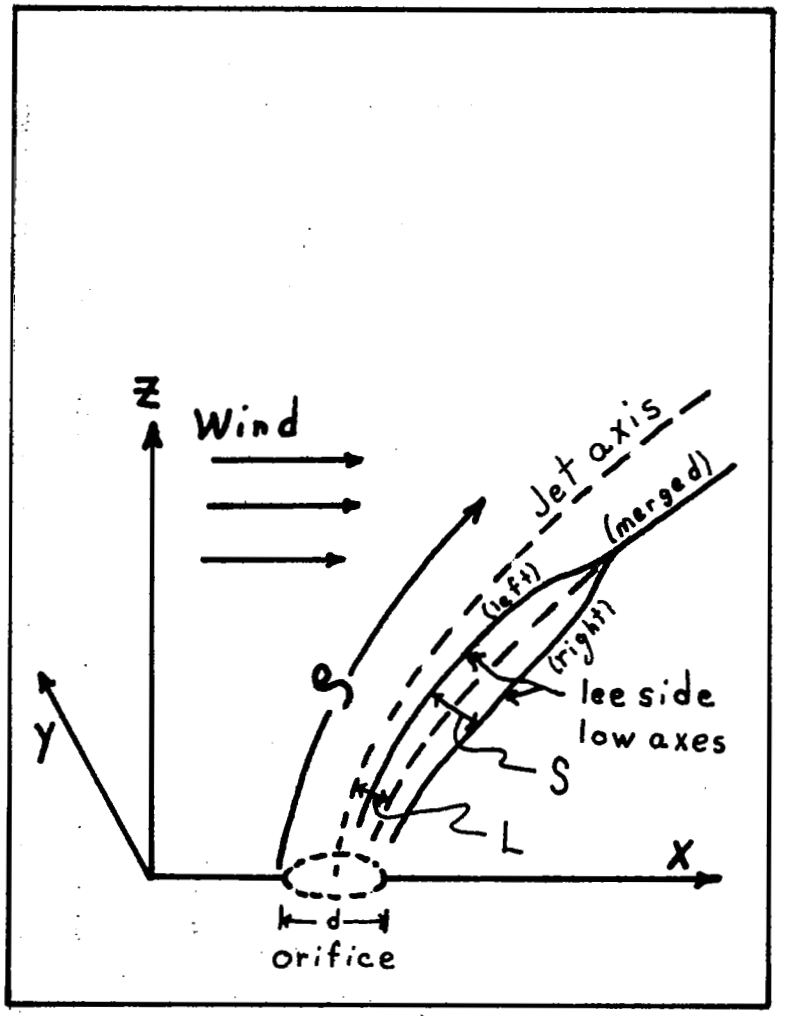

Figure 22a

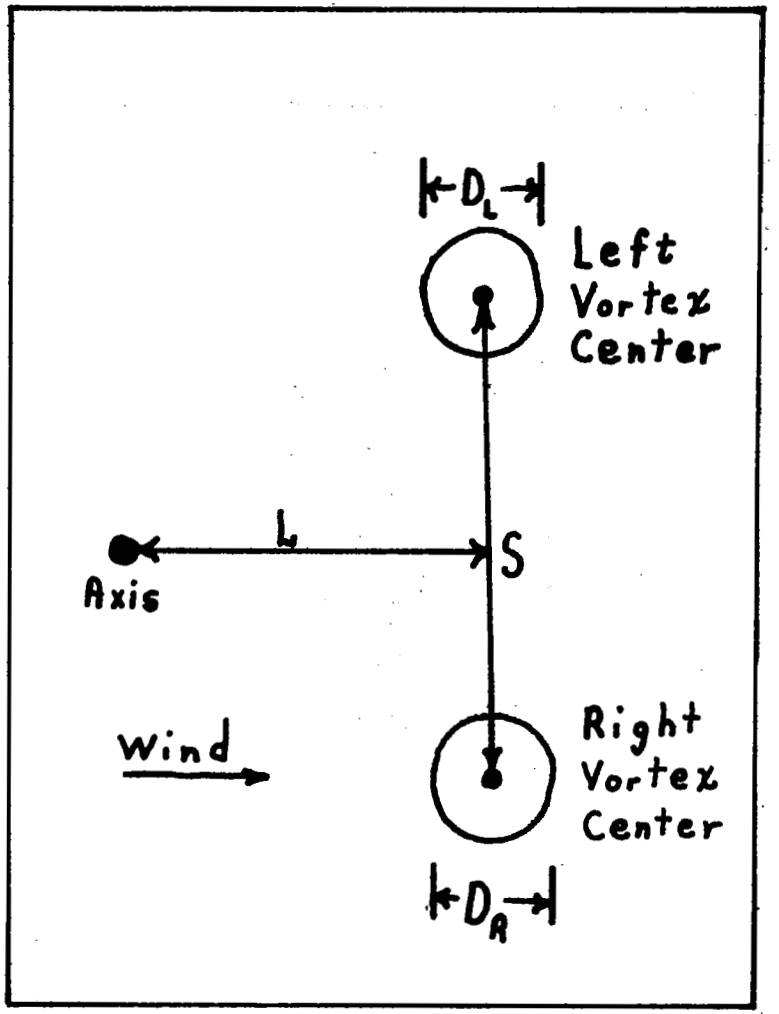

Figure 22b

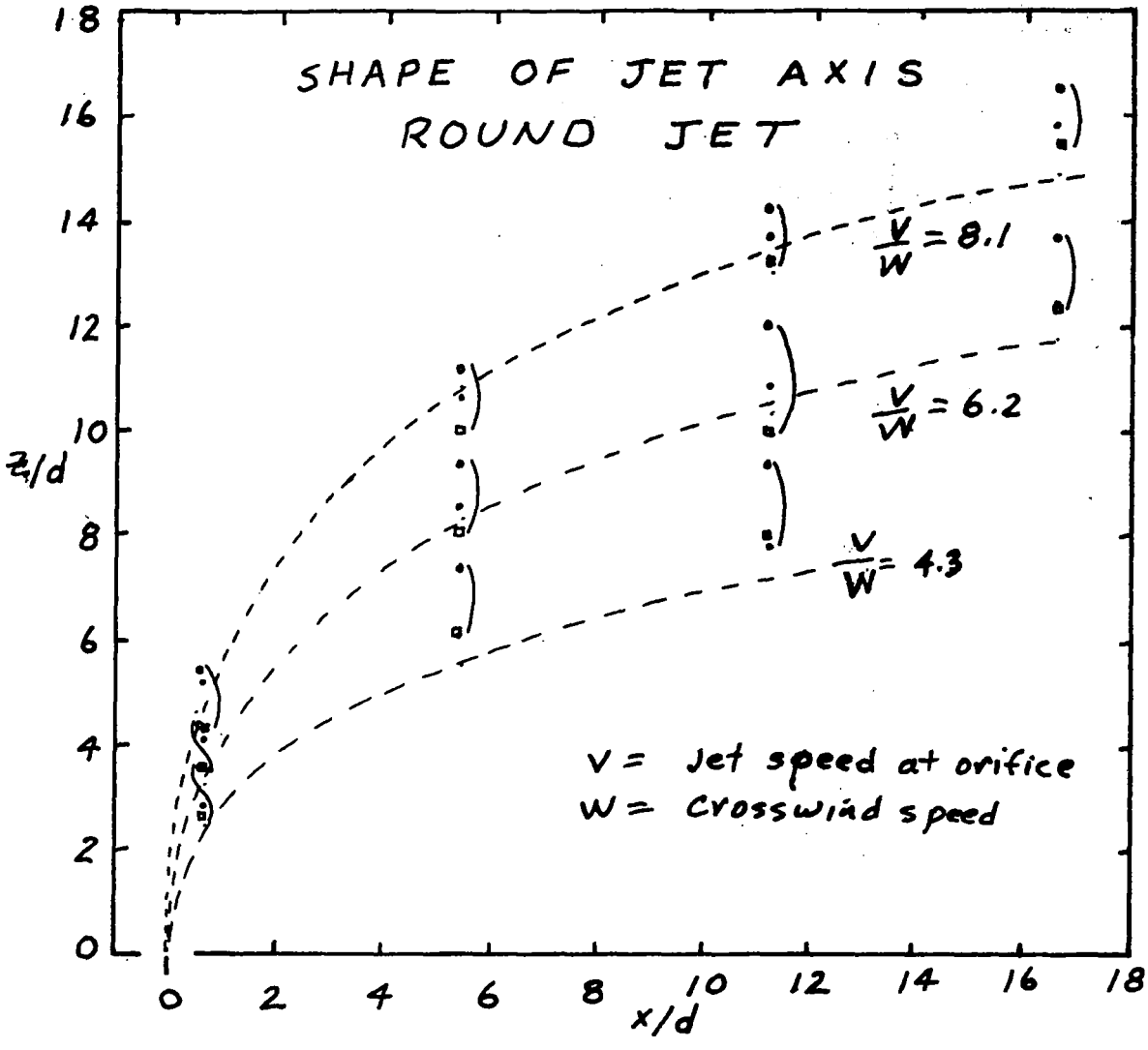

Jordinson (1956) ---

Margason and Fearn (1969) o

Ivanov (1952) •

Shandorov (1957) □

$$\frac{x}{d} = \frac{1}{4}\left(\frac{W}{V}\right)^2\left(\frac{z}{d}\right)^3$$ Margason and Fearn

$$\frac{x}{d} = \left(\frac{W^2}{V^2}\right)^{1.3}\left(\frac{z}{d}\right)^3$$ Ivanov

$$\frac{x}{d} = \frac{W^2}{V^2}\left(\frac{z}{d}\right)^{2.55}$$ Shandorov

Figure 23

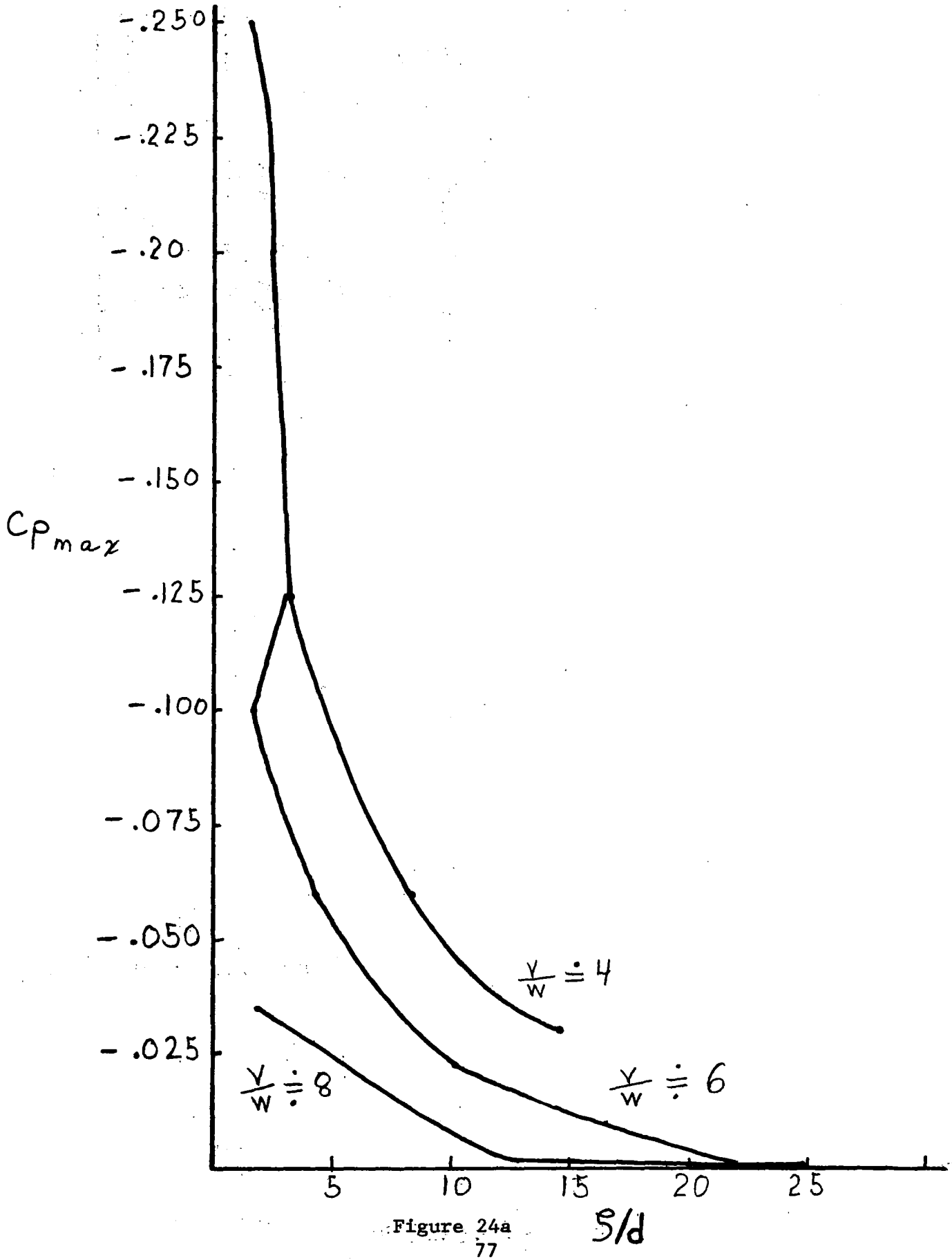
-.250
-.225
-.20
-.175
-.150
$C_{P_{max}}$
-.125
-.100
-.075
-.050
-.025
$\frac{Y}{W} \doteq 4$
$\frac{Y}{W} \doteq 6$
$\frac{Y}{W} \doteq 8$
5
10
15
20
25
S/d

Figure 24a

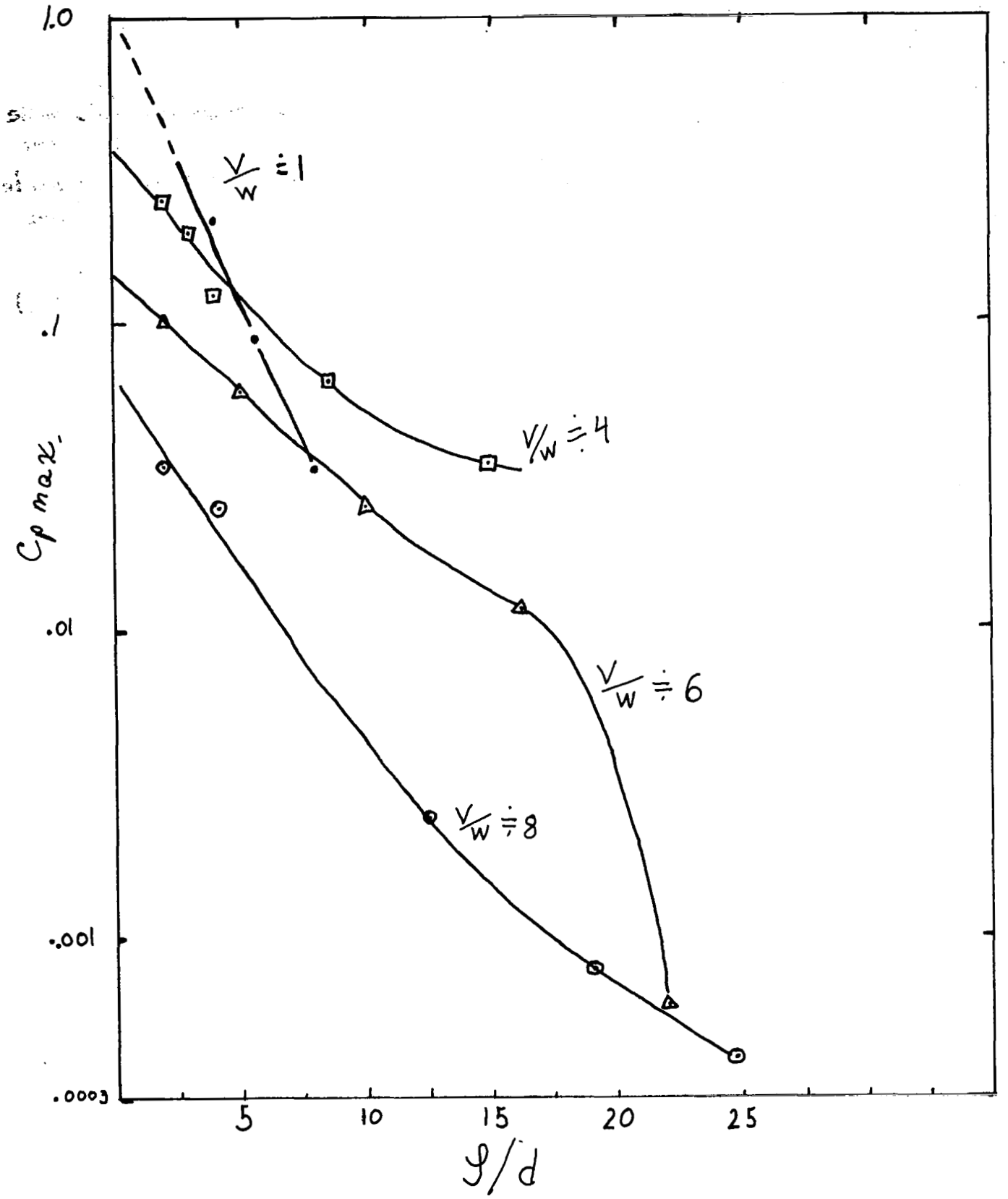

Figure 24b

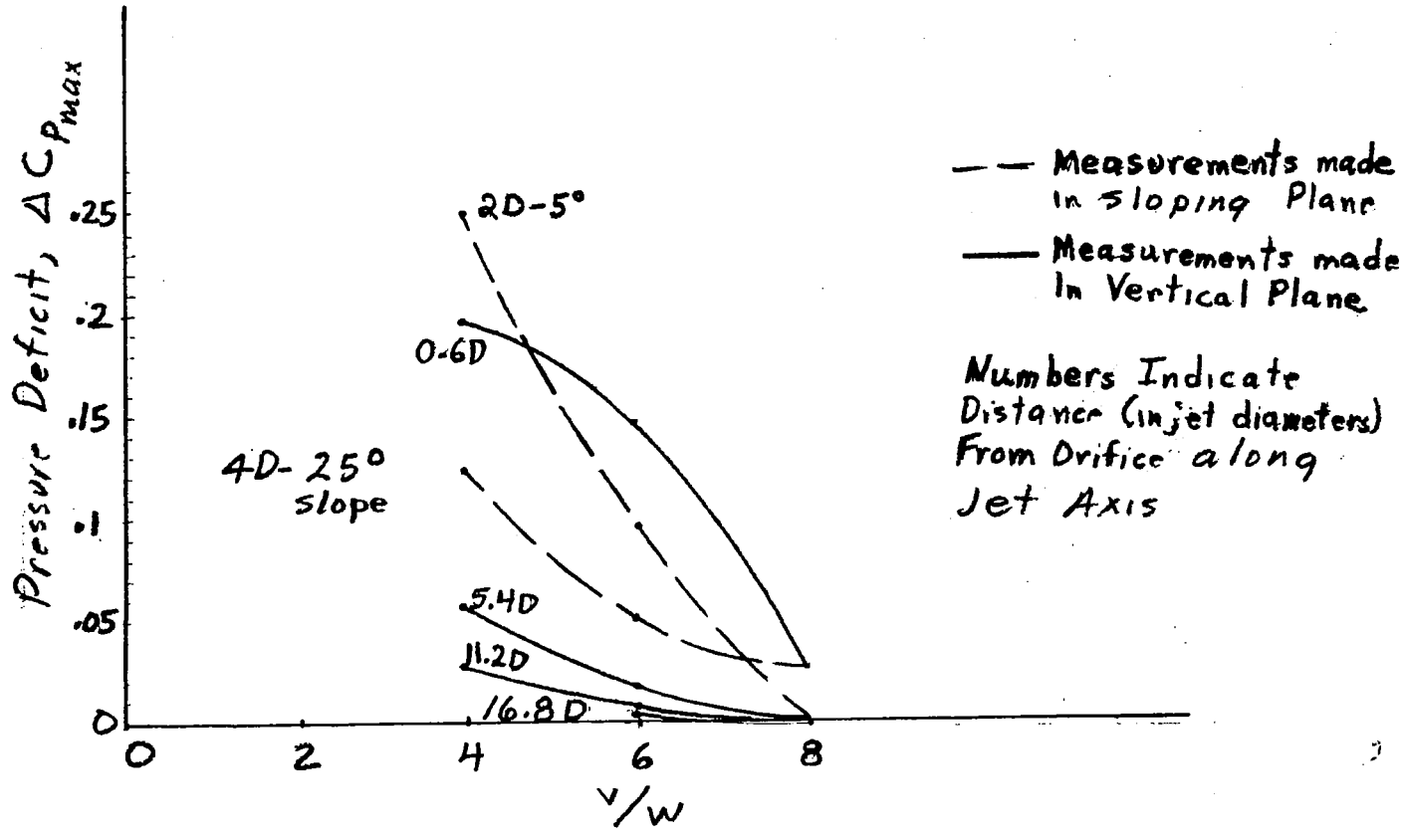
Pressure Deficit, $\Delta C_{p_{max}}$
.25
.2
.15
.1
.05
0
0
2
4
6
8
V/W
2D-5°
0.6D
4D-25° slope
5.4D
11.2D
16.8D
— — Measurements made in sloping Plane
—— Measurements made in Vertical Plane
Numbers Indicate Distance (in jet diameters) From Orifice along Jet Axis

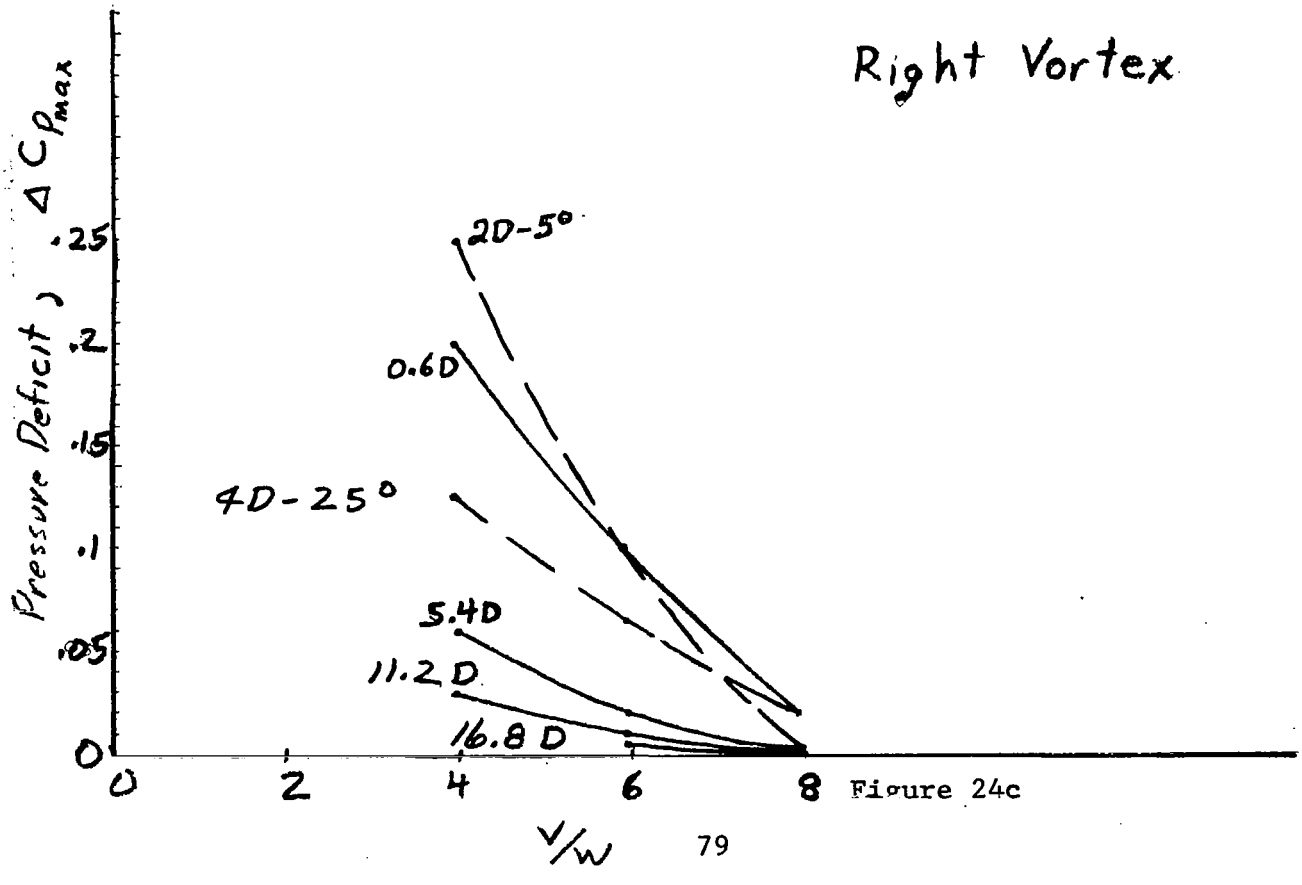
Right Vortex
Pressure Deficit, $\Delta C_{p_{max}}$
.25
.2
.15
.1
.05
0
0
2
4
6
8
V/W
2D-5°
0.6D
4D-25°
5.4D
11.2D
16.8D

Figure 24c

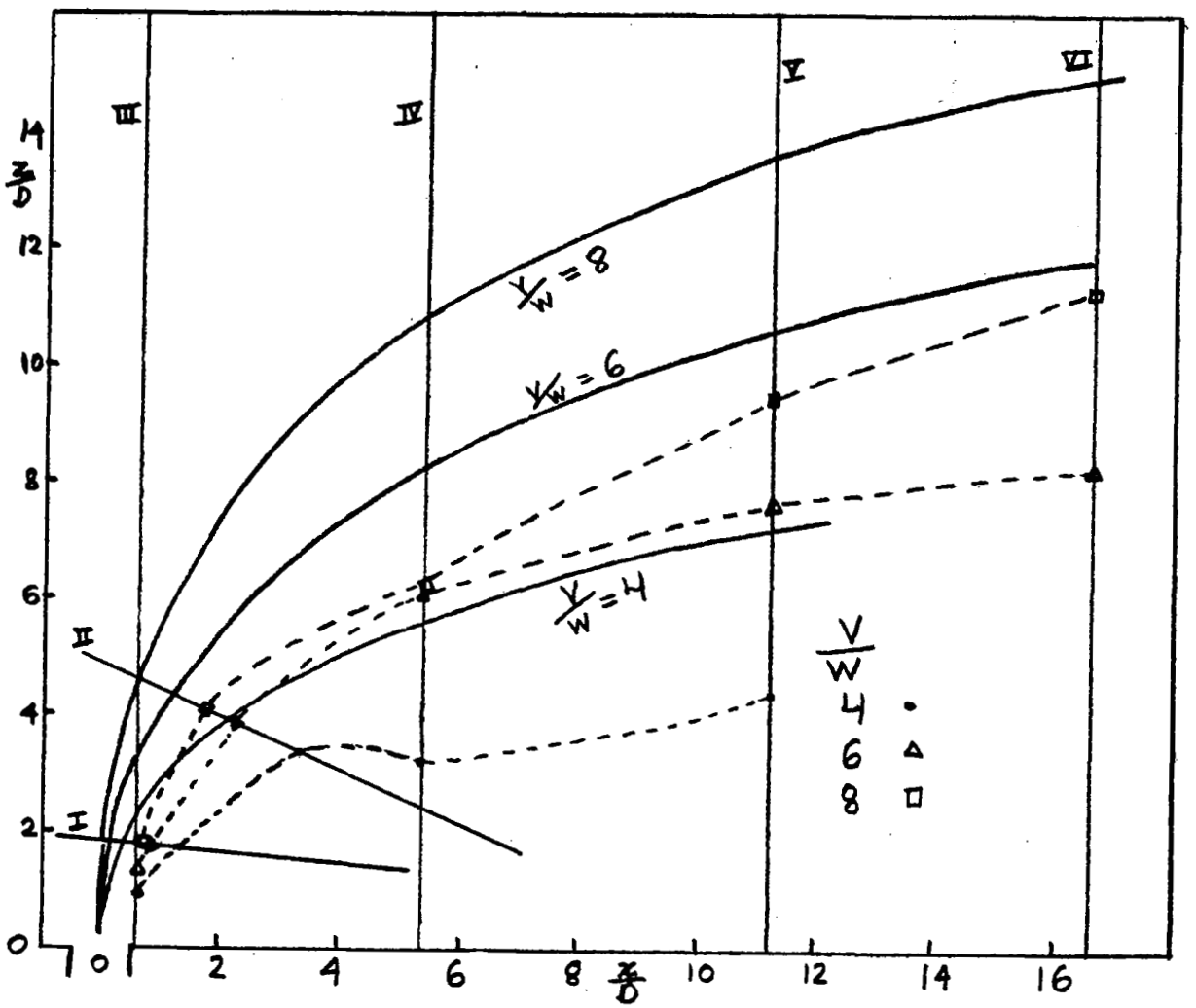

Lines of maximum Cp deficit
In Relation to Jet Axis

Figure 24d

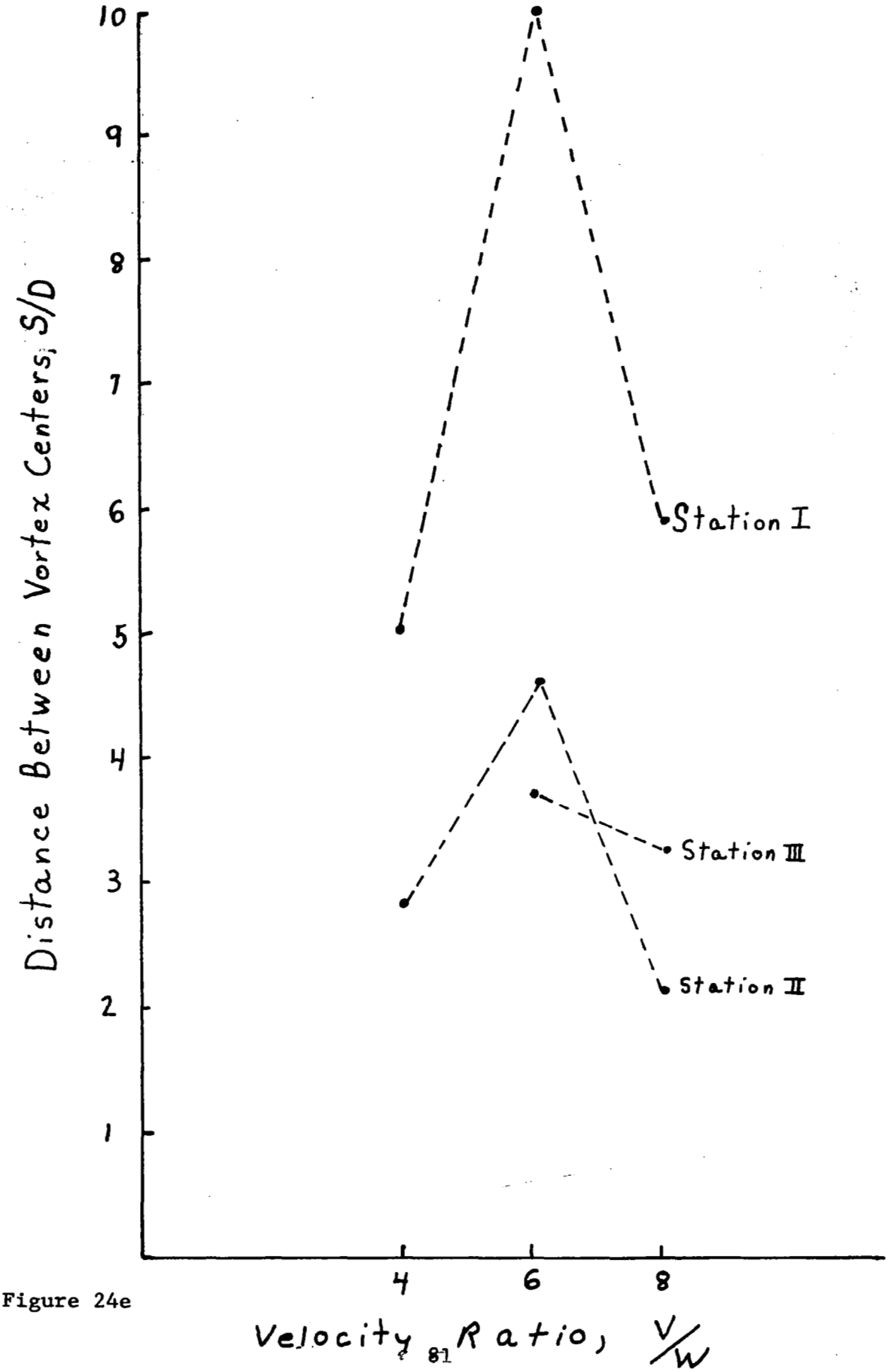
Distance Between Vortex Centers, S/D
10
9
8
7
6
5
4
3
2
1
Station I
Station III
Station II
4
6
8
Velocity Ratio, V/W

Figure 24e

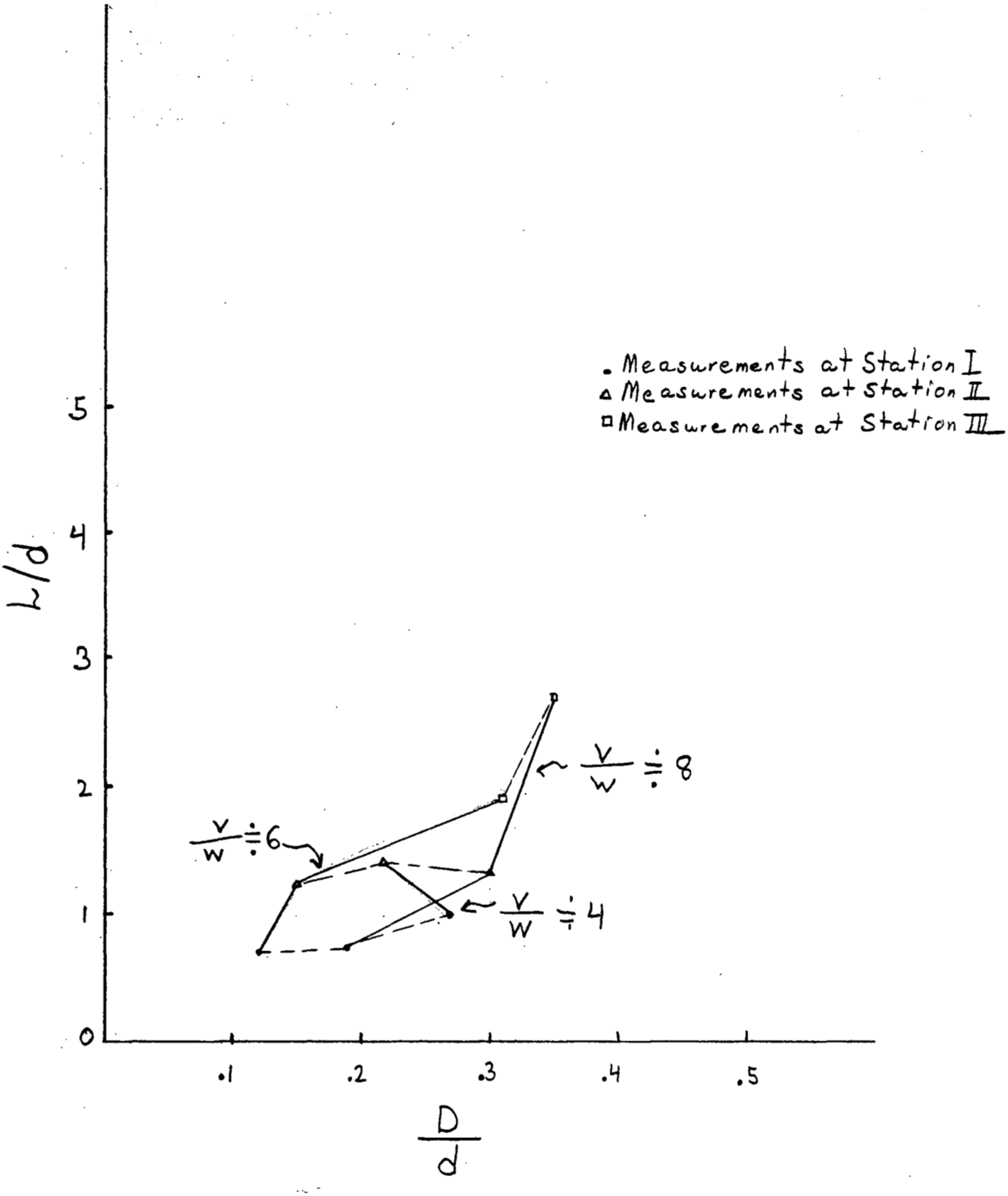
• Measurements at Station I
△ Measurements at Station II
□ Measurements at Station III
L/d
0
1
2
3
4
5
.1
.2
.3
.4
.5
D/d
V/W ≒ 8
V/W ≒ 6
V/W ≒ 4

Figure 24f

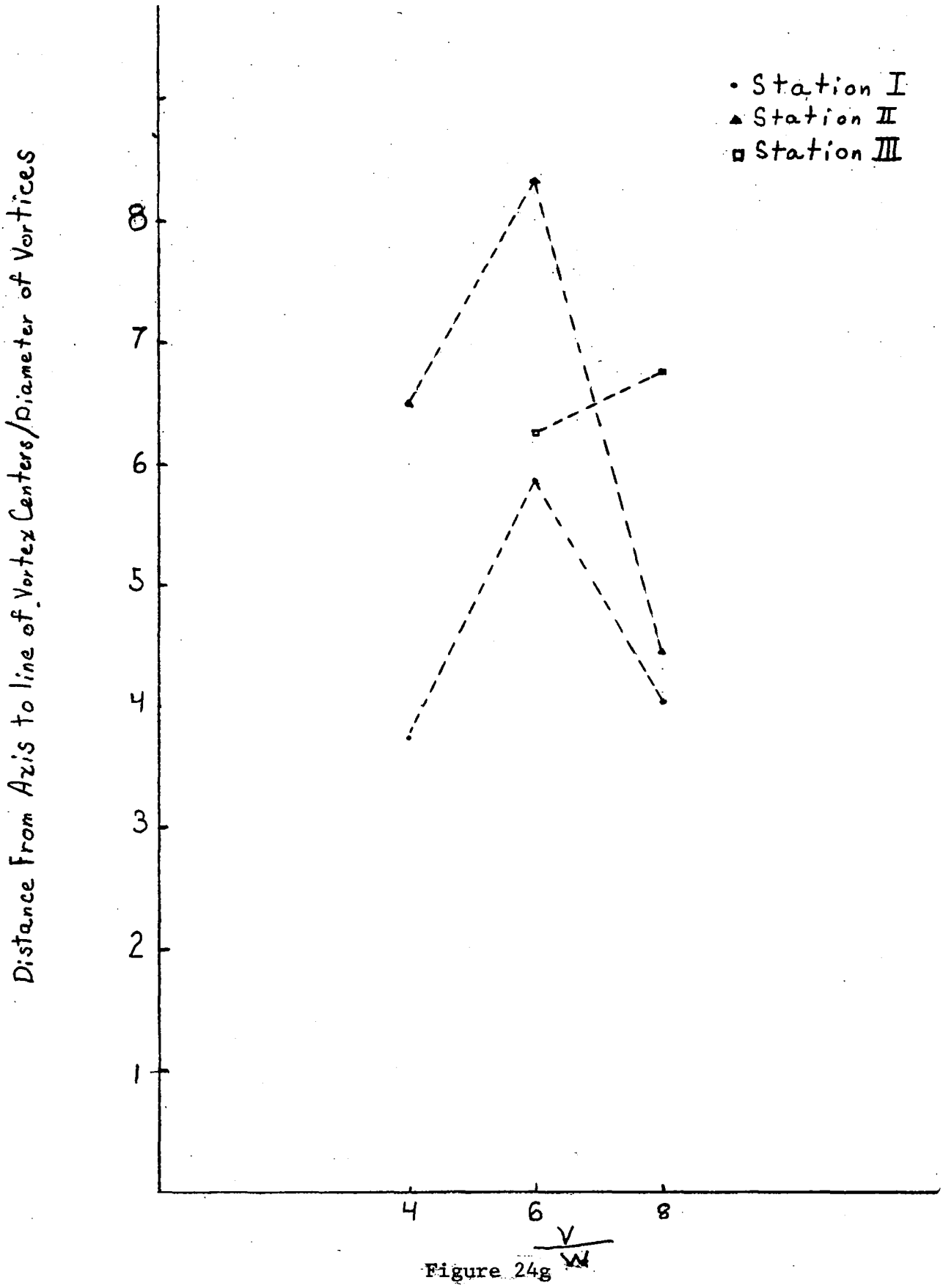
Distance From Axis to line of Vortex Centers/Diameter of Vortices
• Station I
▲ Station II
□ Station III
8
7
6
5
4
3
2
1
4
6
8
V/W

Figure 24g

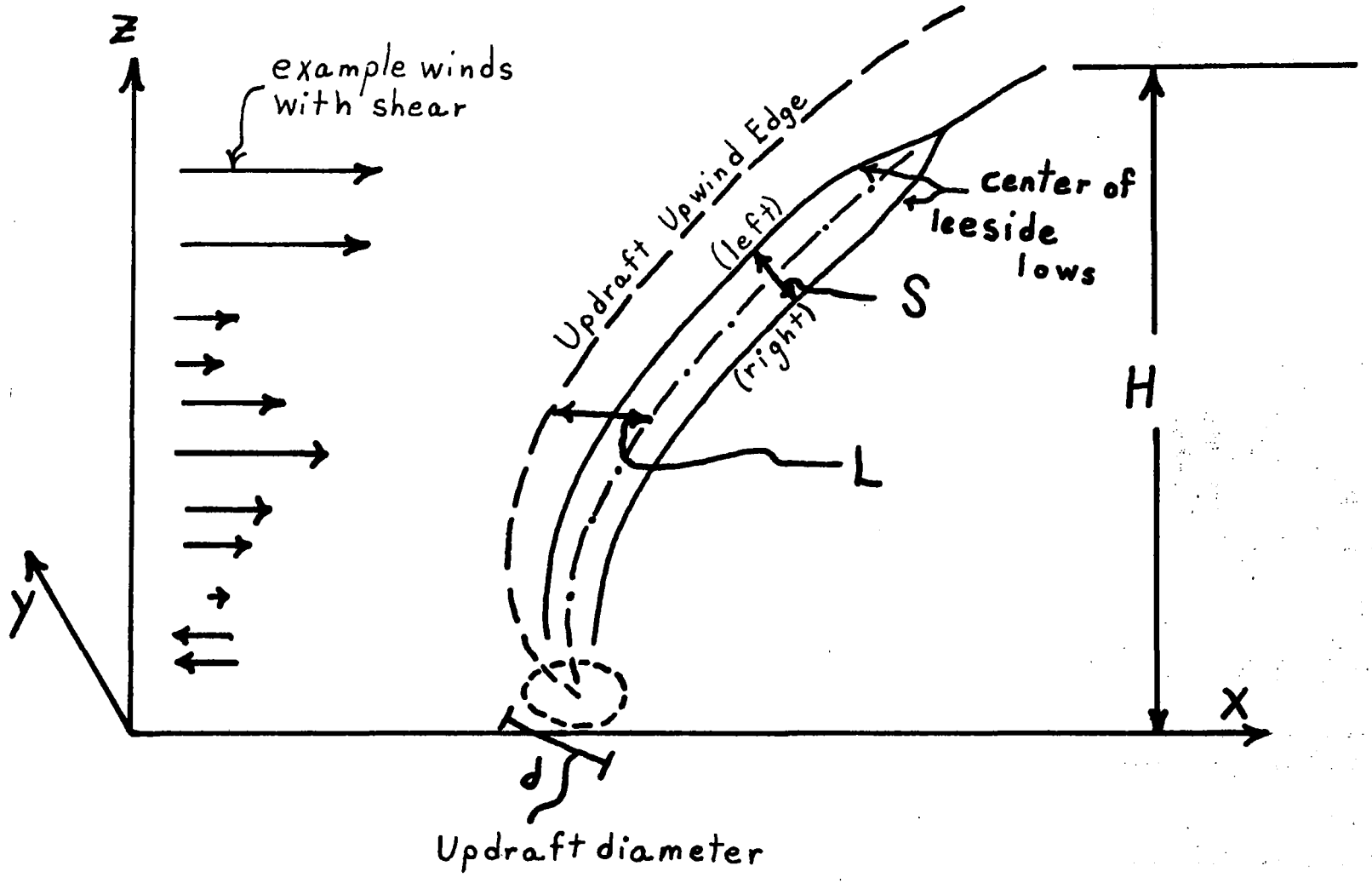
z
example winds
with shear
Updraft Upwind Edge
(left)
(right)
center of
leeside
lows
S
H
L
y
x
d
Updraft diameter

Figure 25a

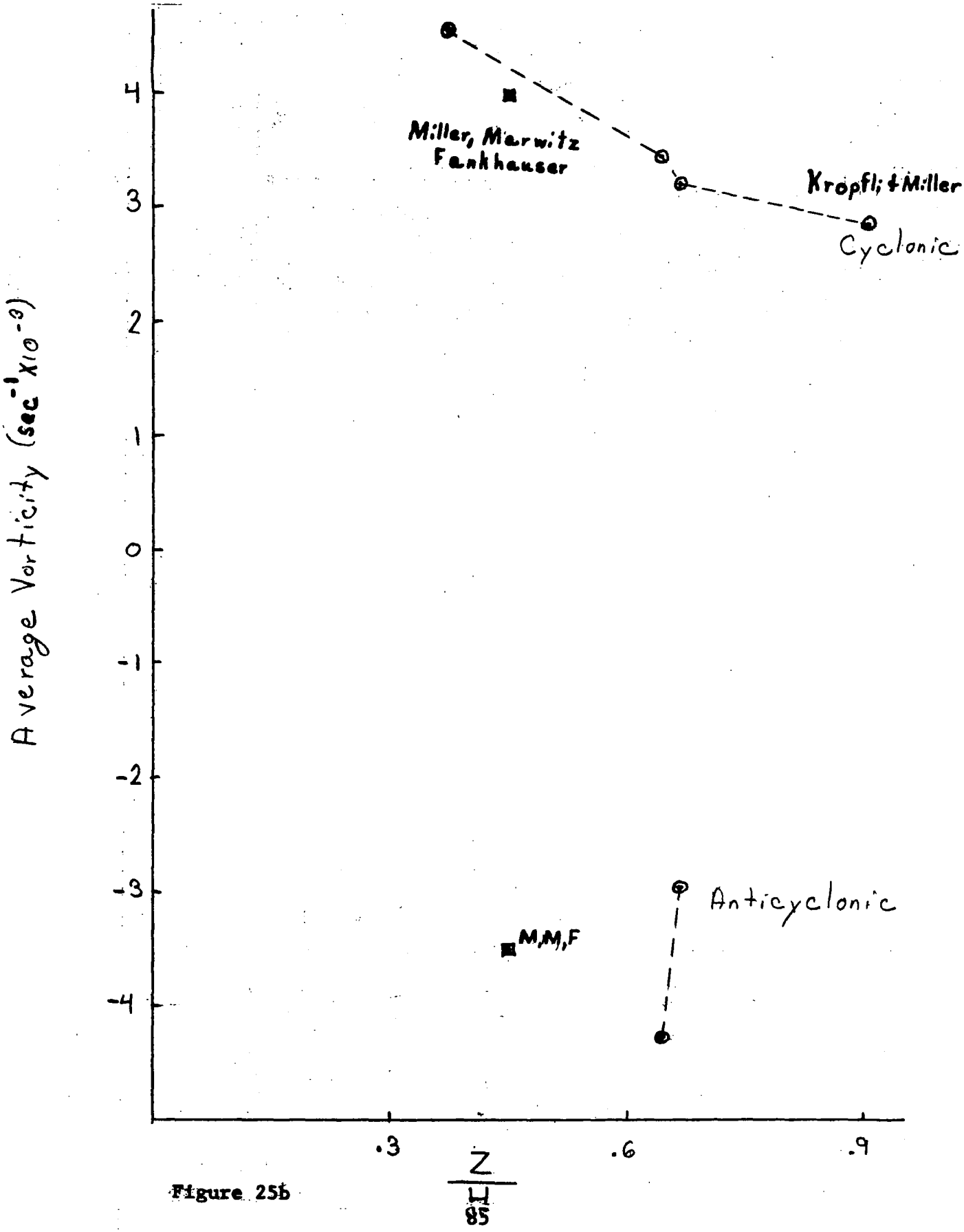
Average Vorticity ($sec^{-1} \times 10^{-9}$)
4
3
2
1
0
-1
-2
-3
-4
Miller, Marwitz
Fankhauser
Kropfli & Miller
Cyclonic
Anticyclonic
M,M,F
.3
.6
.9
Z/H
85

Figure 25b

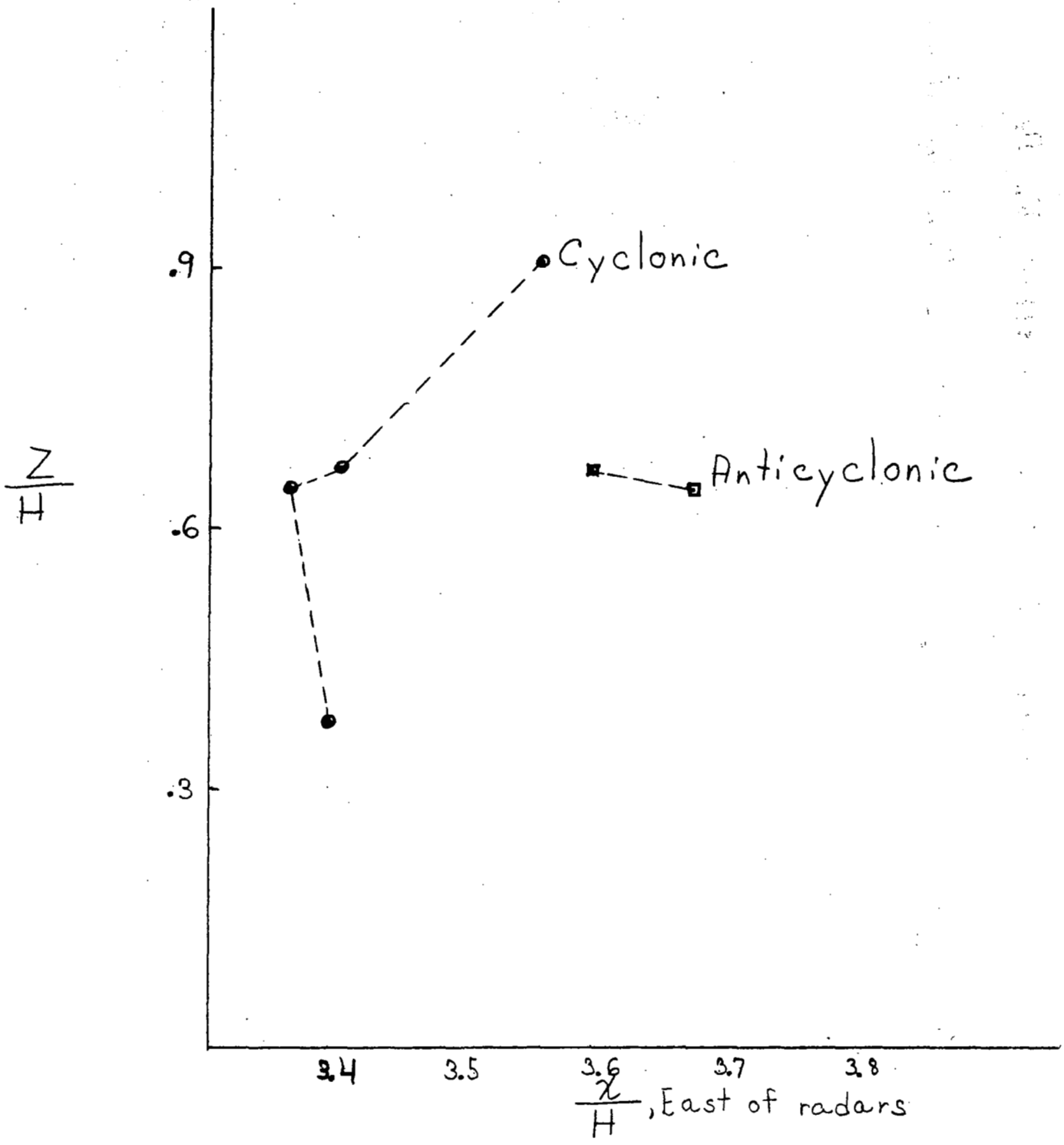

Kropfli and Miller - Location of Vortex Centers

Figure 25c

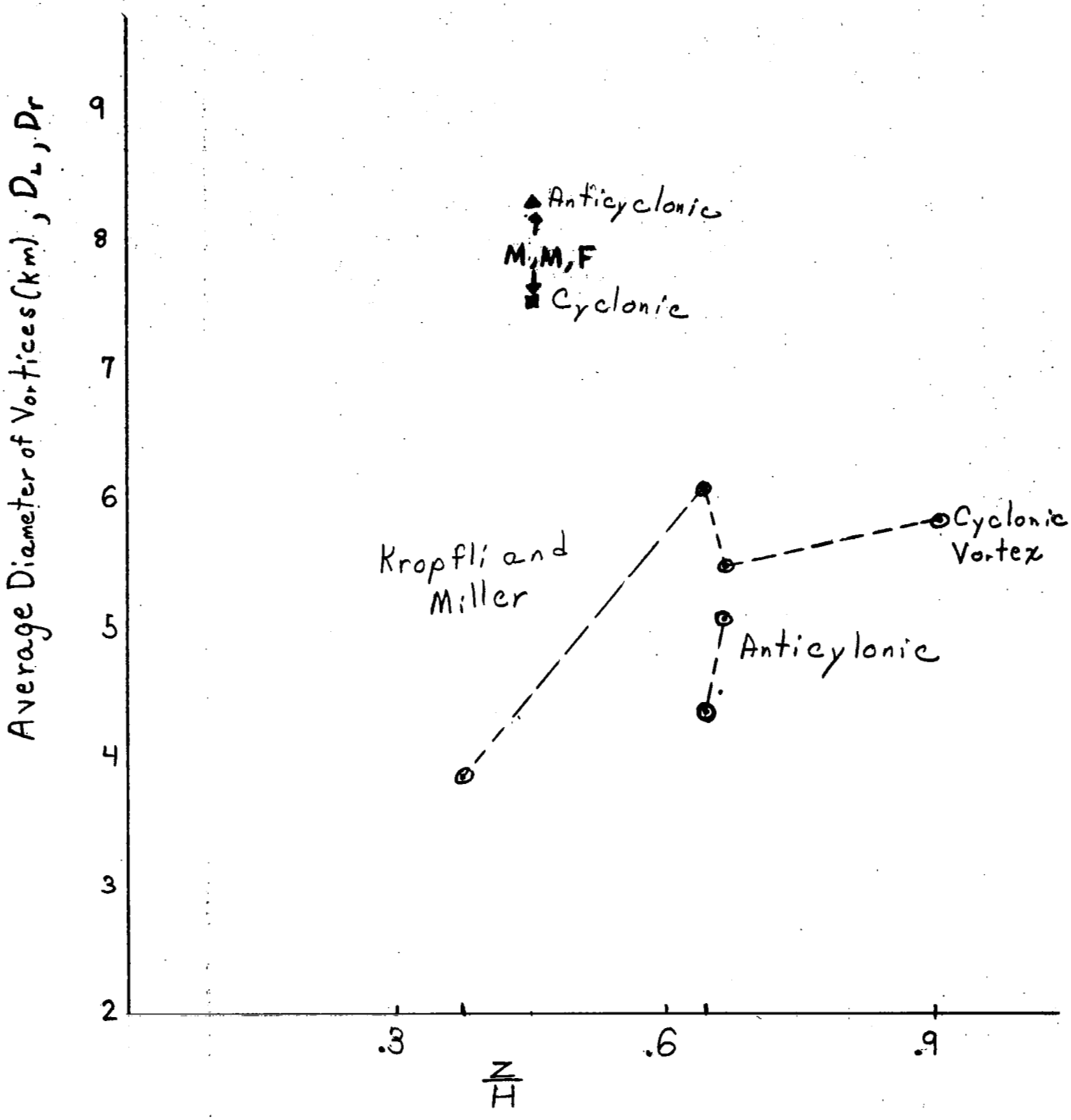
Average Diameter of Vortices (km), D_L, D_r
9
8
7
6
5
4
3
2
Anticyclonic
M, M, F
Cyclonic
Kropfli and Miller
Cyclonic Vortex
Anticylonic
.3
.6
.9
$\frac{Z}{H}$

Figure 25d

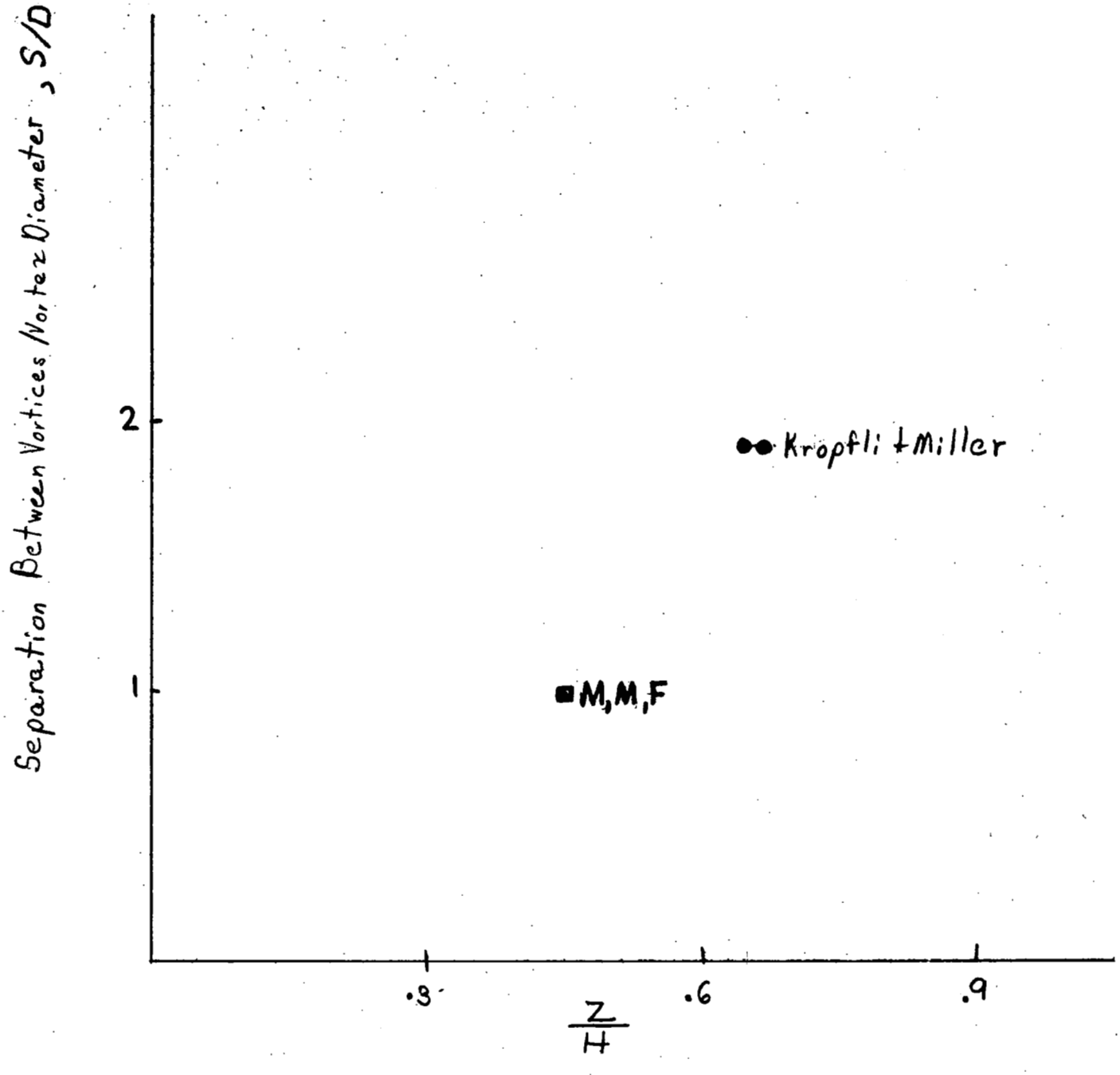
Separation Between Vortices Vortex Diameter , S/D
2
1
Kropfli & Miller
M,M,F
.3
.6
.9
Z/H

Figure 25e

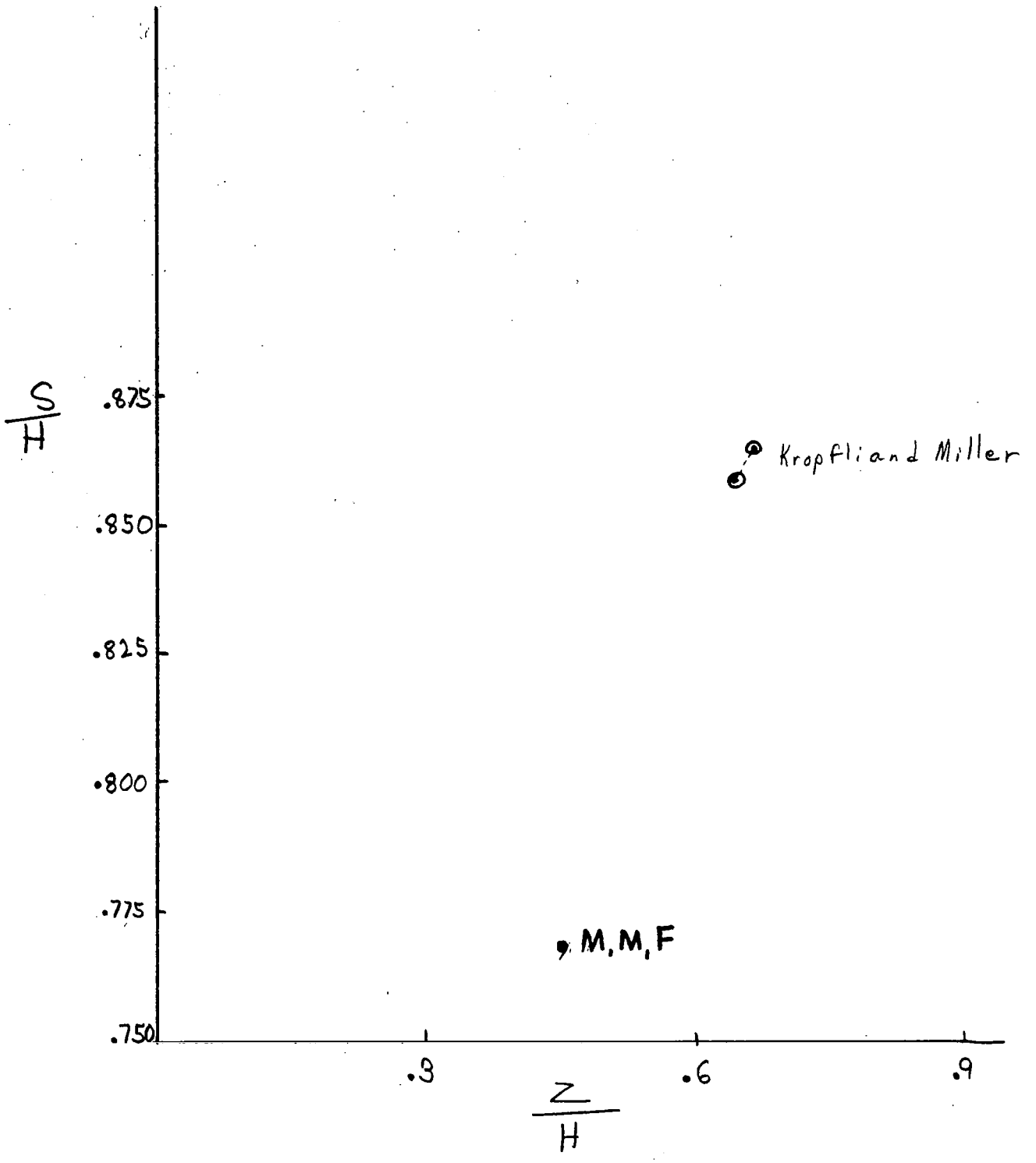

Figure 25f

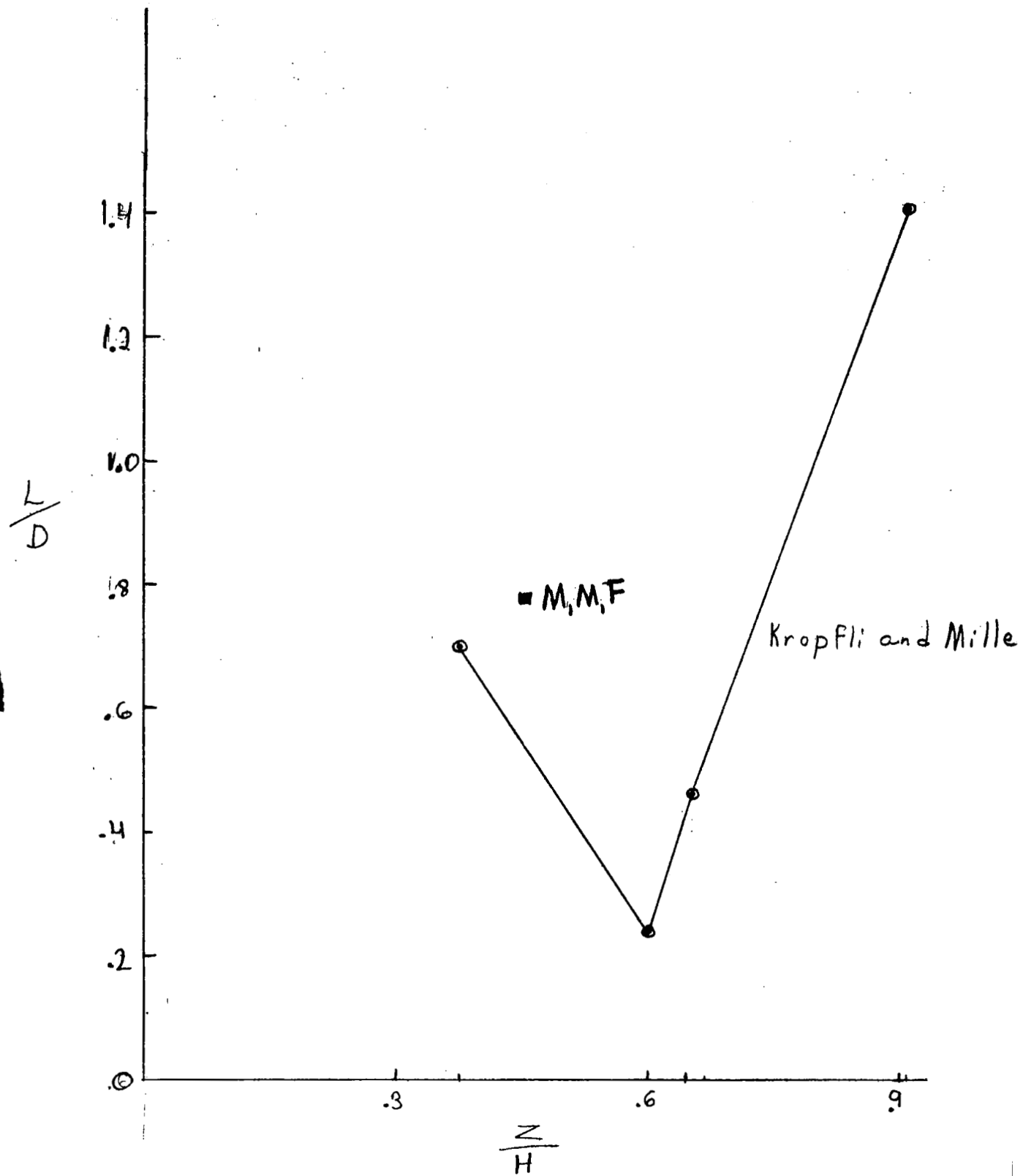

Figure 25g

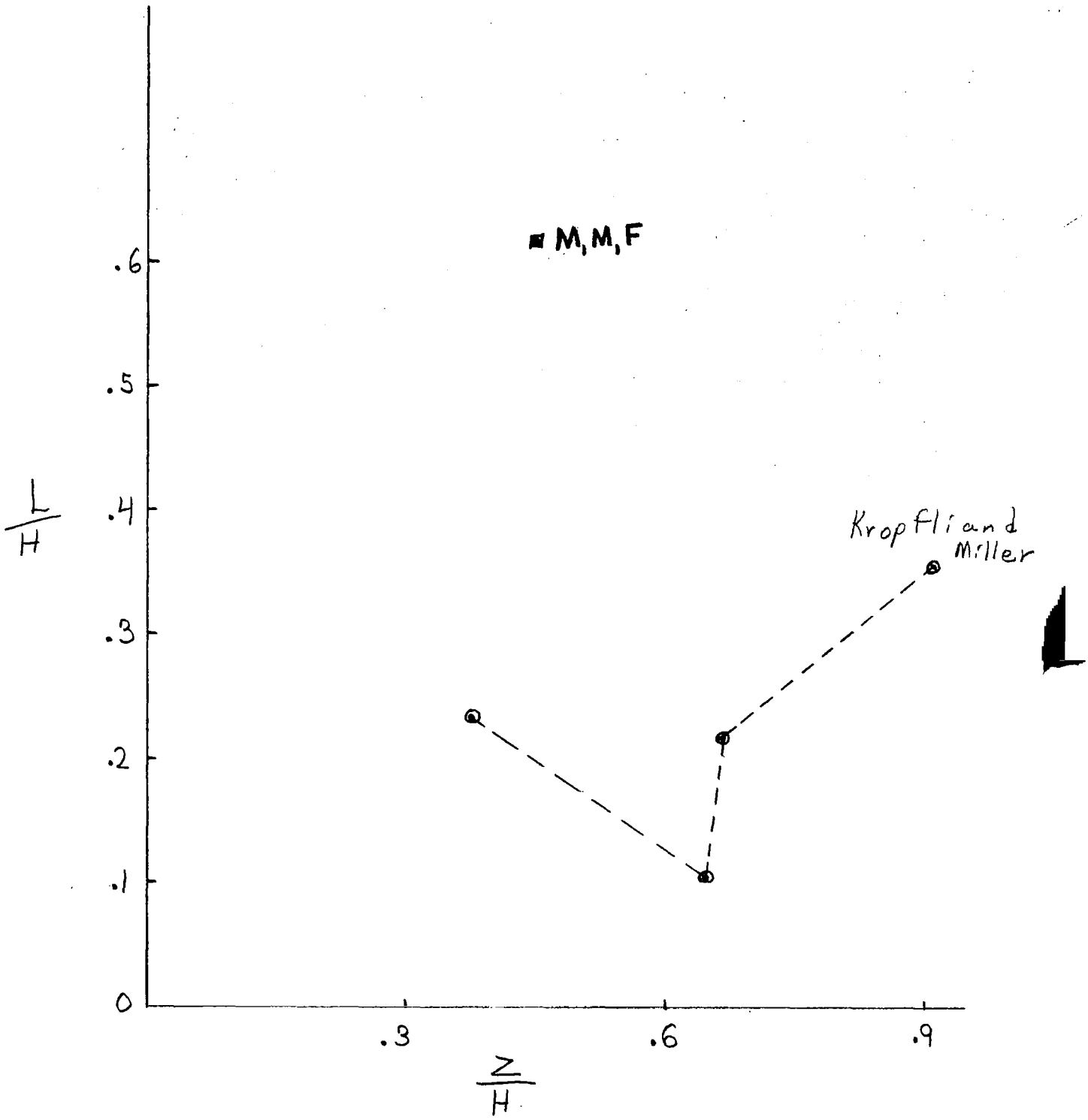

Figure 25h

REFERENCES

Ivanov, Yu. V., 1952: "Equations for trajectories of jets with acute blast," Sovetskoe Kotloturbostroenic, 8.

Jordinson, R., 1956: Flow in a jet directed normal to the wind. Aeronautics Dept. Paper No. 35, Imperial College, 17 pp.

Kropfli, R.A. and L.J. Miller, 1975: Thunderstorm flow pattern in three dimensions. Mon. Wea. Rev., 103, 1, 70-71.

Margason, R.J., and R. Fearn, 1969: Jet-wake characteristics and their induced aerodynamics effects on V/STOL aircraft in transition flight. Analysis of a jet in a subsonic crosswind, NASA SP-216, National Aeronautics and Space Administration, Washington, D.C., 1-18.

Miller, L.J., J.D. Marwitz, and J.C. Fankhauser, 1975: Kinematic Structure of a Colorado Thunderstorm, Preprints, 16th Radar Meteorology Conf. American Meteor. Soc., Boston, 128-133.

Shandorov, G.S., 1957: "Flow from a channel into stationary and moving media." Zh. Tekhn. Fiz., 37, 1.

Chapter VI.

Applications of AVE data to development of a capability for predicting thunderstorm motion and intensity.

The non-thermal mechanism of a cumulonimbus in a wind shear is expected to be most significant for the more intense storms. The first available AVE data for intensive storms is for AVE IV. The best test of the hypothesis outlined first in Chapter 2 is expected to come from analysis of detailed vertical profiles of wind and from tracks of storms as determined by radar or by visual tracking. The concept of formation of leeside low pressure centers by winds in collision may be used two ways. First a model may be rather fully developed from direct measurements of a properly formed jet in a crossflow and adjusted with the available direct measurements of thunderstorm flow and motion. The model may then be used to estimate, by kinematic or dynamic means, the deviate motion and updraft forcing to be expected. The model is then to be tested against many field observations in which storm track and intensity and environmental shear can be measured. A high success rate in prediction verifies the model. This may be done empirically (e.g., by noting a proportional difference between predicted and observed storm properties).

The second method of using the model concept is to simply note that vector wind shear in small layers is given as the critical factor in determining the existence of pairs of leeside low pressure centers. It is also held to be important in

which center dominates in producing deviate motion and updraft control. A complete model is not required since a direct prediction is not made. Instead, the wind shear, atmospheric stability and storm motion and intensity deviation are to be correlated in a multivariate scheme using mesoscale maps of these properties and perhaps others for thin layers of the atmosphere.

In chapter 5 it was pointed out that present data do not permit a very complete realistic model of the non-thermal mechanism. Until laboratory experiments can be made to provide data for the whole model, the direct prediction approach is impossible. Consequently, the multivariate correlation using mesoscale data is to be used in producing the best possible prediction capability.

Figure 26 shows the tracks of thunderstorms near Kansas City (MKC Radar) on day 113, 1975 (AVE IV) for the period 1930 Z to 2239 Z. The northern tracks come from WNW while the southernmost track comes from WSW to W. The detailed analysis must be related to wind, temperature and water vapor fields which are not yet available for AVE IV. Consequently further analysis and development of the prediction scheme cannot be done at this time. However, the SMS 1 satellite data are available for the same time period at 30-minute intervals. Figure 27 shows a map of the U.S. as reviewed from SMS 1. Anvils for storms at 2100 Z, day 113, 1975, are shown sketched in near station MKC. The

photographs show indications of a non-uniform wind field at cloud heights including anvil heights. Interestingly, the storm whose tracks moved most to the right had initial anvils which extended most to the left (the north storms). This suggests that their low-level inflow came from the right and penetrated to high levels with some of its original direction of momentum. More detailed analysis of the satellite data will perhaps be warranted when the radiosonde data become available.

The satellite data shown also in Figure 28 verify the observations discussed by Allison, et al., 1974, concerning clear areas initiating thunderstorms. The radiosonde and surface thermal data can be related to the clearness and possibly the air mass movement implied by cloud areas and other early day cloud features near the storms as additional input to the prediction schemes which should be developed in a continuation study to this preliminary six-month study.

The next and final chapter briefly states the main conclusions of the present report and recommends several possible continuation studies.

FIGURES

LEGENDS

Figure 26. MKC Radar Tracks of severe storm cells (1 deg. beam elevation). 1930 to 2239Z, day 113.

Figure 27. Map of storm region as viewed from SMS 1, day 113, 1975. Locations of storm and radar MKC are shown.

Figure 28. Tracings from SMS1 visual photos. See fig. 27 for map.

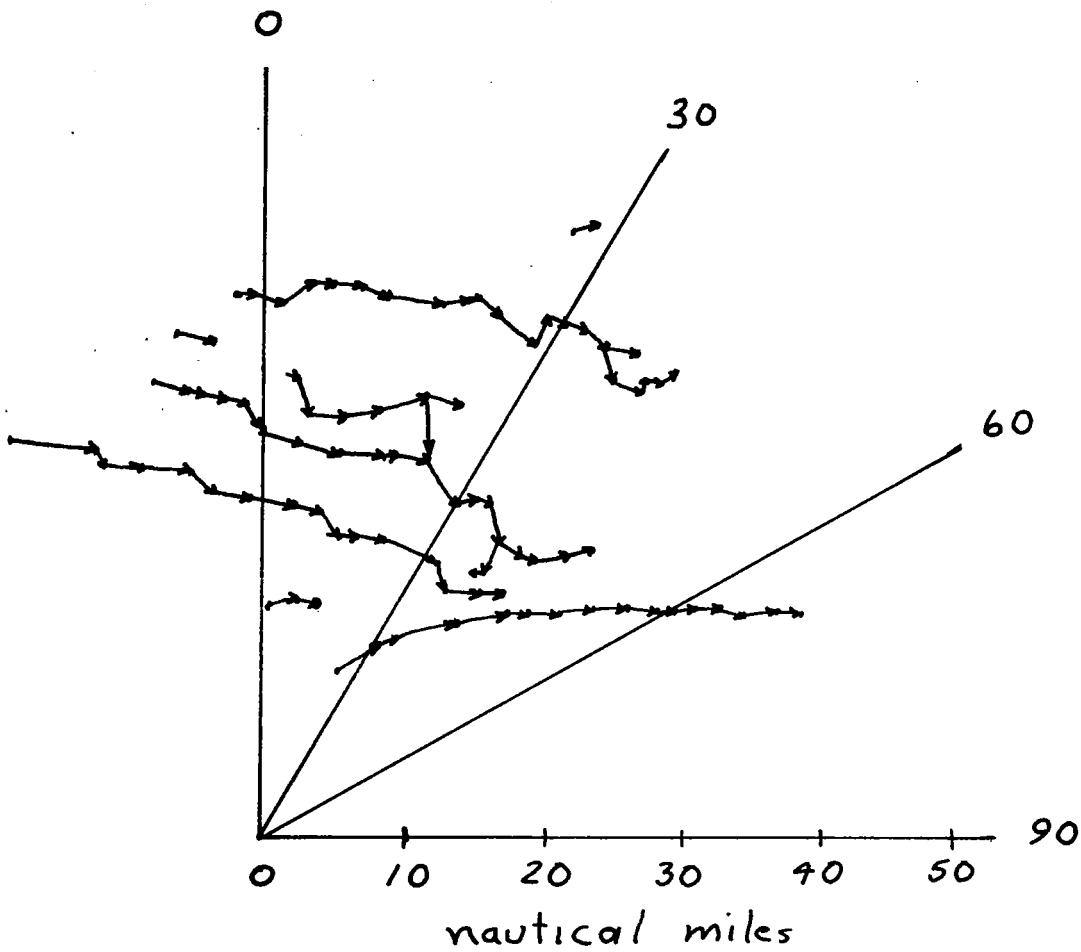

Figure 26

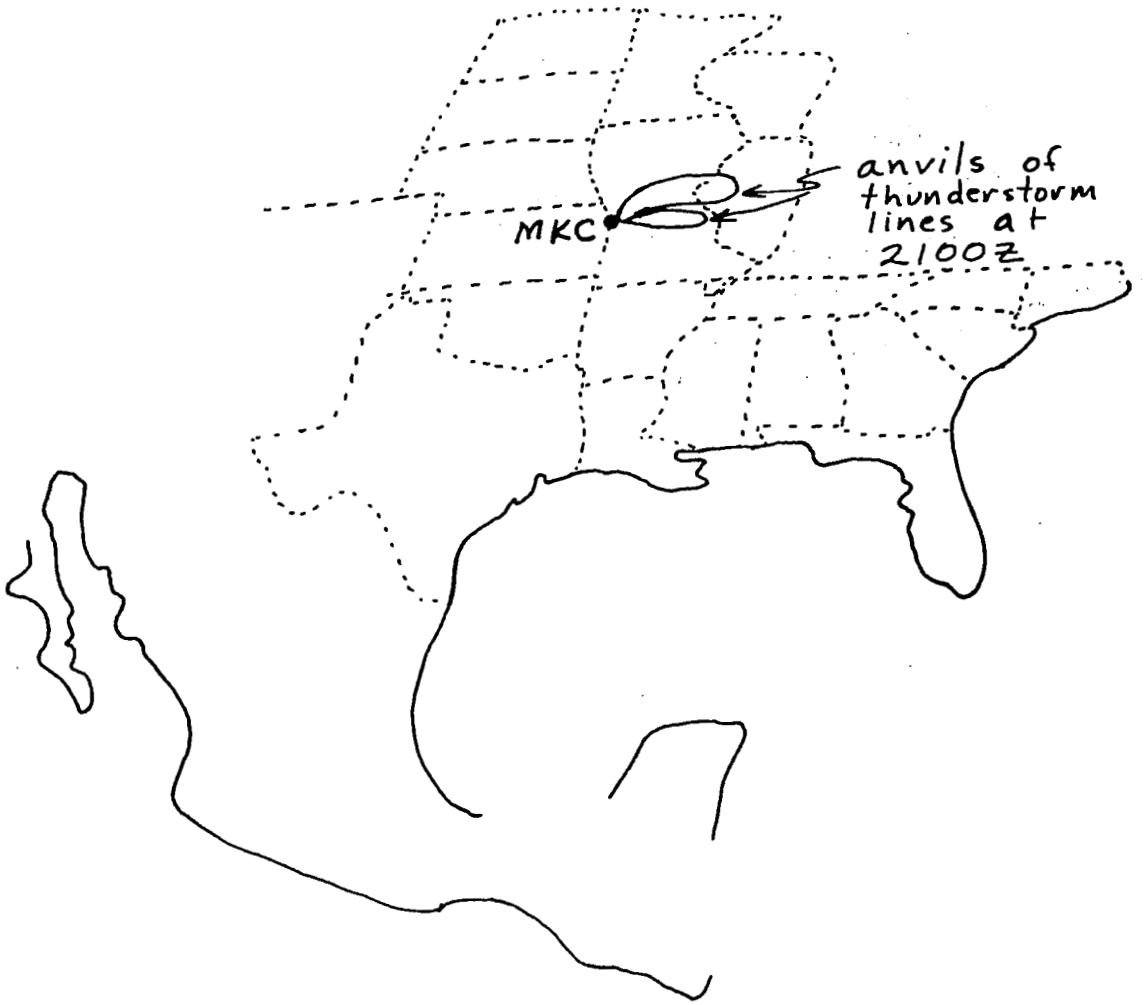

Figure 27

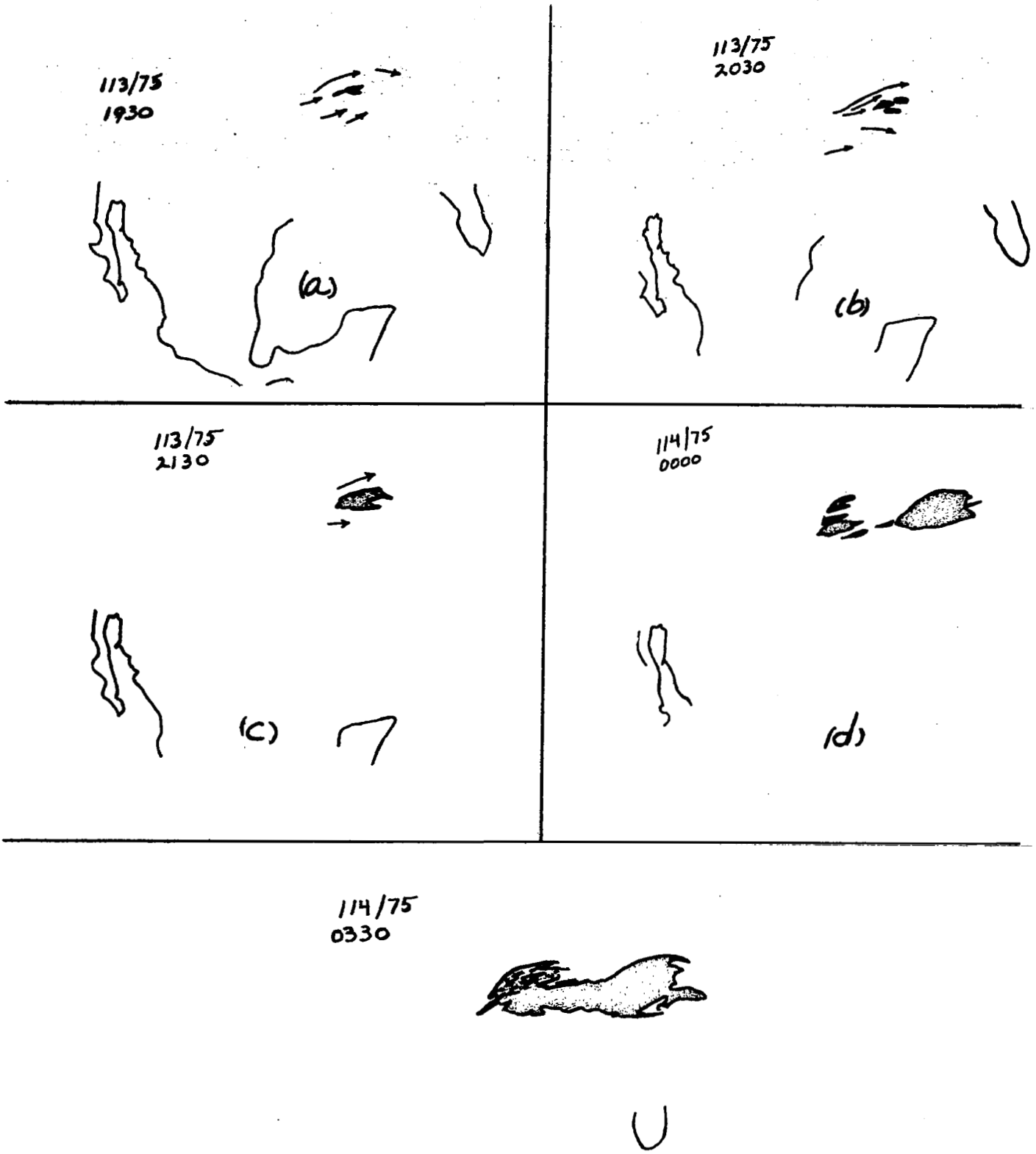
113/75
1930
(a)
113/75
2030
(b)
113/75
2130
(c)
114/75
0000
(d)
114/75
0330
(e)

Figure 28

REFERENCES

Allison, L.J., A. Arking, W.R. Bandeen, W.E. Shenk, and R. Wexler, 1974: Meteorological Satellite Accomplishments, Preprint X-910-74-327, Goddard Space Flight Center, Greenbelt, Maryland.

Chapter VII.

Conclusions and recommendations.

The conclusions which bear upon the non-thermal mechanism of thunderstorm development are in four categories. First, the concept of the mechanism is developed in Chapter 2 from observations in wind and water tunnels of a jet in a crossflow. Second, examples of leeside vortices in the subcloud inflow to thunderstorms are given using data taken with research aircraft. Thirdly, dual-doppler observations of thunderstorms produce added detail about vortex pairs which is compared with additional analysis of wind tunnel data. Finally, a first look at radar and satellite data for thunderstorms of the AVE IV experiment provides indications of the need and possibilities for success in applying the concept developed to analysis and stratification of mesoscale data. The purpose is to develop a practical tool for prediction of thunderstorm movement and development.

Briefly, it is concluded that thunderstorms, and perhaps weaker convective clouds, contain the mechanism for generation of contra-rotating vortex pairs within themselves at and above the region of strong collision between cloud winds and ambient environment winds. The scale of the vortices is about half that of the spread width of the cloud updraft-downdraft region.

The vortices may exist very close to the upwind side of the cloud or they may trail as a downwind street depending upon the magnitude of a turbulence Reynolds number. If whole cloud rotation occurs (it is usually cyclonic) then the member of the smaller scale vortex pair having the opposite rotation is apparently suppressed or weakened.

The vortices have lowered central pressure and may induce upward motion in the air below them. Thus depending upon the direction of the subcloud inflow-updraft relative to the vortex pair, advance lifting may occur at specific locations. As a result, the cloud is preferentially formed causing sequential development and propagation or movement of the storm differing from the case without vosrtex pairs. If some conditions of change of Reynolds number or dual direction of inflow occur, the storm may split.

The region of strong collision will occur wherever there is a great shear in the local wind. Thus one would expect vortex pair generation from slightly below cloud base to a few kilometers above cloud base. Similarly one might expect generation near cloud top and jet stream levels or in some cases throughout the vertical extent of the cloud.

An analytical model with direct predictive capabilities could be developed from wind or water tunnel simulation of thunderstorm conditions. It would be more difficult, yet possible, to achieve the essence of the process by 3-dimensional numerical simulation; but it has the advantage of permitting

eventual incorporation of thermal effects. Neither of these simulation schemes has been adequately utilized as of the time of the present report. Consequently the only quick, viable approach to incorporating the vortex pair mechanism into thunderstorm development predictions is by indirect means of mesoscale analysis of mesoscale atmospheric parameters in their layers and to perform a multivariate correlation analysis related to storm motion and intensity.

It is recommended that

(1) A multivariate correlation analysis between storm intensity and motion and mesoscale winds, wind shears and stability be performed. The purpose is to develop a best prediction of storm development using mesoscale parameters with greater vertical resolution than heretofore and with more selectivity in layers of importance in the problem;

(2) A carefully devised water tunnel experiment be performed to provide a more comprehensive set of data for modeling the vortex pair mechanism for thunderstorm geometries and kinematics;

(3) A 3-d numerical simulation be made of a simple round jet in a crossflow to be compared against the few available observations. Favorable simulation would lead to extension of the simulation method to thunderstorms and, very importantly, also to the problems of vertical takeoff and landing aircraft (VTOL).

Acknowledgement

Miss Lillian Kimbrough, graduate research assistant on the project, refined the preliminary compilation for Chapter 3, did the data reduction for Chapters 5 and 6 and proofed the final draft. Mrs. Barbara Connell donated her services to draft, in final form, many of the Figures for this report. The rest of the figures were drafted by Miss Kimbrough.

Mrs. Marie Henderson typed the several drafts of the report.

Quite importantly, Mr. Kelly Hill, was of considerable help in proofing.

Finally, appreciation is expressed to NASA-MSFC for the opportunity to complete the portion of thunderstorm study reported herein.

*U.S. GOVERNMENT PRINTING OFFICE: 1976 - 635-275/58